

A DIFFERENT PERSPECTIVE OF CIRCULATORY BIOMARKERS IN NEURODEGENERATIVE DISEASES:
focus on serum high molecular weight fraction

1 2  9 0
UNIVERSIDADE D
COIMBRA

1 2  9 0

UNIVERSIDADE D
COIMBRA

Miguel Maria Varandas Anão Rosado

**A DIFFERENT PERSPECTIVE OF CIRCULATORY
BIOMARKERS IN NEURODEGENERATIVE DISEASES:
FOCUS ON SERUM HIGH MOLECULAR WEIGHT FRACTION**

VOLUME 1

Dissertação no âmbito do Mestrado em Biotecnologia Farmacêutica orientada pelo
Doutor Bruno José Fernandes Oliveira Manadas e pelo Professor Doutor Luís Pereira de
Almeida e apresentada à Faculdade de Farmácia da Universidade de Coimbra

Setembro de 2019

1 2 9 0



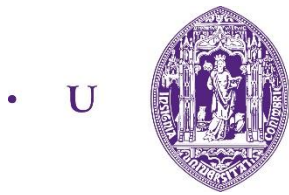
UNIVERSIDADE D
COIMBRA

Miguel Maria Varandas Anão Rosado

**A DIFFERENT PERSPECTIVE OF CIRCULATORY
BIOMARKERS IN NEURODEGENERATIVE DISEASES:
FOCUS ON SERUM HIGH MOLECULAR WEIGHT FRACTION**

VOLUME 1

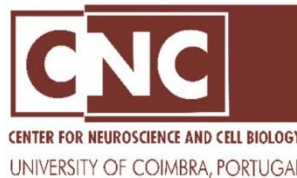
Dissertação no âmbito do Mestrado em Biotecnologia Farmacêutica orientada pelo Doutor Bruno José Fernandes Oliveira Manadas e pelo Professor Doutor Luís Pereira de Almeida e apresentada à Faculdade de Farmácia da Universidade de Coimbra



• U • C •

FFUC FACULDADE DE FARMÁCIA
UNIVERSIDADE DE COIMBRA

**Center For Neuroscience and Cell
Biology**



**Fundação para a Ciência e a
Tecnologia**



**European Regional Development Fund: COMPETE
2020**



This work was financed by the European Regional Development Fund (ERDF) through the COMPETE 2020 - Operational Programme for Competitiveness and Internationalisation and Portuguese national funds via FCT – Fundação para a Ciência e a Tecnologia, I.P., OE FCT/MCTES (PIDDAC) under projects: POCI-01-0145-FEDER-029311, POCI-01-0145-FEDER-007440 (strategic project UID/NEU/04539/2019), POCI-01-0145-FEDER-016428 (ref.: SAICTPAC/0010/2015), and POCI-01-0145-FEDER-016795 (ref.: PTDC/NEU-SCC/7051/2014); POCI-01-0145-FEDER-029311 (ref.: PTDC/BTM-TEC/29311/2017); POCI-01-0145-FEDER-30943 (ref.: PTDC/MEC-PSQ/30943/2017); PTDC/MED-NEU/27946/2017 Beyond Beta Amyloid; and by The National Mass Spectrometry Network (RNEM) under the contract POCI-01-0145-FEDER-402-022125 (ref.: ROTEIRO/0028/2013).

Agradecimentos

A realização da presente dissertação foi uma longa jornada da qual fizeram parte inúmeros desafios, incertezas, percalços, alegrias, mas sobretudo, um grande esforço por parte de uma grande equipa. Desejo exprimir os meus agradecimentos a todos aqueles que, de alguma forma, permitiram que o alcance deste meu objetivo fosse possível. Em primeiro expresso o meu maior apreço e agradecimento ao Bruno, que me escolheu acolher-me no seio de uma equipa de investigação fantástica. Obrigada pelo apoio, motivação, simpatia, e pelo conhecimento transmitido. Contudo, o contributo de toda a restante equipa foi basilar neste processo.

Assim, agradeço à Vera, por toda a disponibilidade e esclarecimento de dúvidas sempre que as houve. Ao camarada Rafael, pela ajuda e partilha de conhecimentos durante o último ano, mas especialmente nesta reta final. Gostava igualmente de agradecer à Inês, à Cátia, à Margarida, à Mariana e ao João por todo o espírito de entreajuda, pela simpatia com que me trataram, assim como pelo seu profissionalismo e boa disposição. À Sandra deixo ainda um enorme agradecimento por me ter sempre guiado ao longo do ano em praticamente todos os aspetos. Foram todos incansáveis e espero poder continuar a aprender e partilhar estas experiências convosco, independentemente do que o destino académico tiver planeado para mim.

Aos meus amigos de longa data, Frutas, Cardoso, Zana e Gambutas deixo um enorme agradecimento, porque ainda que nesta fase as circunstâncias da vida não nos permitam partilhar grandes momentos, os que já estão escritos na memória ditam que ainda muitos nos aguardam e sei que, passem anos ou décadas, a festa do nosso reencontro será igualmente grandiosa. À Sara, minha namorada, agradeço por aturares o meu mau feitio e sempre me apoiares mesmo quando a vida nos vira de pernas para o ar. Sem ti, decididamente que não teria conseguido!

Por fim, agradeço a toda a minha família, com especial gratidão para com os meus pais, Fernando e Cecília, assim como para com o meu irmão, Fernando, que sempre aqui estiveram para me apoiar e que, apesar de tudo, sempre em mim confiaram e elevaram as minhas capacidades. Termino mais uma etapa do meu percurso académico com o sentimento de dever cumprido, especialmente por saber que não poderia ter tido melhor preparação, nem melhor companhia!

Abstract

Several attempts have failed to identify high confidence biomarkers of neurodegenerative diseases, which would be determinant in developing early diagnostic methods for those disorders, including Alzheimer's and Parkinson's disease (AD and PD), thereby improving patient prognosis.

Blood (and its fractions, namely serum), being an easily accessible biofluid that both percolates throughout and maintains intricate contact with virtually every tissue in the human body, is of great interest in the search for potential disease biomarkers. More recently, the blood protein content has been implicated as a potentially rich source of biomarkers, since most of the cellular proteome could theoretically be represented in this fluid either in the form of intact proteins or fragments resulting from their degradation. Nonetheless, their detection through mass spectrometry (MS), during comprehensive proteome analysis, is severely hindered by the presence of highly abundant species like albumin and 20 other proteins that make up about 99% of the blood protein mass. Thus, sample complexity challenges the sensitivity of modern detection methods.

Therefore, to circumvent the problem of the extremely wide protein dynamic range of the blood (10^{12}), it is suggested herein the development of a fractionation method for serum sample preparation for downstream MS analysis. One fraction is to be specifically investigated: the high molecular weight (above 300 kDa) sub-proteome. The objective is the discovery of potentially altered protein complexes and degradation mechanisms. The final aim is for this blood fraction to serve as a source of new potential circulating biomarkers of neurodegenerative diseases, particularly for AD and PD.

Resumo

Várias tentativas têm falhado em identificar biomarcadores de alta confiança para doenças neurodegenerativas, o que seria determinante no desenvolvimento de métodos de diagnóstico precoce para esses distúrbios, incluindo a doença de Alzheimer e Parkinson, melhorando assim o prognóstico dos pacientes.

O sangue (e suas frações como o soro), sendo um biofluido de fácil acesso que penetra por todo o corpo e mantém contato contínuo com praticamente todos os tecidos do corpo humano, é de grande interesse na busca de possíveis biomarcadores de doenças. Mais recentemente, o conteúdo proteico do sangue tem sido implicado como uma fonte potencialmente rica de biomarcadores, uma vez que a maior parte do proteoma celular pode teoricamente ser representado neste fluido sob forma de proteínas intactas ou fragmentos resultantes da sua degradação. No entanto, a sua detecção por espectrometria de massa, ao longo de uma análise abrangente do proteoma, é severamente prejudicada pela presença de espécies altamente abundantes como a albumina e outras 20 proteínas que representam cerca de 99% da massa de proteica do sangue. Assim, a complexidade da amostra desafia a sensibilidade dos métodos modernos de detecção.

Portanto, para contornar o problema do intervalo dinâmico de concentrações proteicas extremamente amplo do sangue (10^{12}), sugere-se aqui o desenvolvimento de um método de fracionamento para a preparação de amostras de soro para subsequente análise por espectrometria de massa. Uma fração deve ser especificamente investigada: o subproteoma de alto peso molecular (acima de 300 kDa). O objetivo é a descoberta de complexos proteicos e mecanismos de degradação potencialmente alterados. O objetivo final é que essa fração sanguínea sirva como fonte de novos potenciais biomarcadores circulantes de doenças neurodegenerativas, particularmente para a doença de Alzheimer e Parkinson.

List of Abbreviations

•OH	Hydroxyl radical	FDA	Food and Drug Administration	NO	Nitric oxide
AD	Alzheimer's disease	FDR	False Discovery Rate	NSAIDs	Non-steroidal anti-inflammatory drugs
AICD	APP intracellular domain	GFAP	Glial fibrillary acidic protein	PAMPs	Pathogen-associated molecular patterns
APH	Anterior pharynx defective	GVD	Granulovacuolar degeneration	PBMCs	Peripheral blood mononuclear cells
APOE	Apolipoprotein E	HMW	High molecular weight	PBS	Phosphate Buffer Saline
APP	Amyloid precursor protein	HPLC	High performance liquid chromatography	PD	Parkinson's disease
Aβ	β -Amyloid	HSV1	Herpes simplex virus type 1	PEN-2	Presenilin enhancer-2
ATP13A2	ATPase type 13A2	IAA	Iodoacetamide	PET	Positron emission tomography
BACE1	β -secretase β -site APP cleaving enzyme-1	IDA	Information-dependent acquisition	PS1	Presenilin 1
BBB	Blood brain barrier	IgG3	Immunoglobulin G3	PS2	Presenilin 2
CAA	Cerebral amyloid angiopathy	iNOS	Inducible nitric oxide synthase	PTMs	Post-translation modifications
CD33	Cluster of differentiation 33	LBs	Lewys bodies	RNS	Reactive nitrogen species
CD36	Cluster of differentiation 36	LCMS	Liquid chromatography mass spectrometry	ROS	Reactive oxygen species
CFH	Complement factor H	LMW	Low molecular weight	RPLC	Reverse-phase liquid chromatography
CID	Collision-induced dissociation	LMWF	Low molecular weight fraction	RT	Retention time
CNS	Central nervous system	LNs	Lewy neurites	SDS	Sodium dodecyl sulphate
CSF	Cerebrospinal fluid	LRRK2	Leucine-rich repeat kinase 2	SNpc	Substantia nigra pars compacta
CUF	Centrifugal ultrafiltration	MCI	Mild cognitive impairment	SNPs	Single nucleotide polymorphisms
Da	Daltons	MMTS	Methyl methanethiosulfonate	SPECT	Single-photon emission computed tomography
DALYs	Disability-Adjusted Life Years	MPTP	1-methyl-4-phenyl-1,2,3,6-tetrahydropyridine	β-HCH	β -Hexachlorocyclohexane
DAMPs	Danger-associated molecular patterns	MRI	Magnetic resonance imaging	SWATH	Sequential Window Acquisition of All Theoretical Mass Spectra
DAT	Dopamine transporter	MS	Mass spectrometry	TCEP	Tris(carboxyethyl) phosphine
DDA	Data-dependent acquisition	MS/MS	Tandem MS	TEAB	Triethylammonium bicarbonate
DIA	Data-independent acquisition	mTOR	Mammalian target of rapamycin	TLR	Toll-like receptor
DMV	Dorsal motor nucleus	MWCO	Molecular weight cut off	TNF-α	Tumor necrosis factor- α
DTT	Dithiothreitol	NCT	Nicastrin	TOF	Time-of-flight
ELISA	Enzyme-linked immunosorbent assay	NDs	Neurodegenerative Diseases	TREM2	Triggering receptor expressed on myeloid cells 2
EMA	European Medicines Agency	NFL	Neurofilament light	UPDRS	Unified Parkinson's Disease Rating Scale
ENS	Enteric nervous system	NFTs	Neurofibrillary tangles	WHO	World Health Organization
ESI	Electrospray ionization	NMWC	Nominal molecular weight cut-off	XIC	Extracted-ion chromatogram
FAD	Familial AD				

Table of Contents

Agradecimientos-----	1
Abstract -----	2
Resumo-----	3
List of Abbreviations-----	4
I. Introduction -----	9
I.1 Neurodegenerative Diseases-----	9
I.1.1 Alzheimer’s Disease -----	11
I.1.1.1 Hallmarks of AD -----	15
I.1.1.2 Hypotheses for AD Pathology -----	22
I.1.2 Parkinson’s Disease-----	36
I.1.2.1 Hallmarks of PD-----	39
I.1.2.2 Hypotheses for PD Pathology-----	43
I.2 Biomarker Discovery in Neurodegenerative Diseases-----	47
I.2.1 Established and Potential AD Biomarkers-----	49
I.2.2 Established and Potential PD Biomarkers -----	50
I.2.3 Blood as a Potential Biomarker Source: Pros, Cons, and Fractionation-----	52
I.3 Bottom-Up Proteomics Approaches -----	55
I.3.1 The Mass Spectrometer: Functioning and General Layout-----	56
I.3.1.1 High-Performance Liquid Chromatography -----	56
I.3.1.2 Electrospray Ionization -----	57

1.3.1.3 Quadrupole Time-of-Flight Mass Analyzer -----	58
1.3.2 Sample Preparation for Mass Spectrometry -----	59
1.3.3 Tandem Mass Spectrometry -----	60
1.3.4 Data Acquisition Methods: DDA and DIA -----	60
1.3.4.1 Sequential Window Acquisition of All Theoretical Mass Spectra -----	61
2. Objectives -----	63
3. Experimental Procedures -----	65
3.1 Workflow Optimization -----	65
3.1.1 Protein Quantification of Fractionated Serum -----	65
3.1.1.1 Centrifugal Ultrafiltration -----	65
3.1.1.2 Bicinchoninic acid assay quantification -----	65
3.1.2 Low Molecular Weight Fractionation -----	65
3.1.2.1 Internal Standard Protein: Fractionation -----	65
3.1.2.2 Internal Standard Protein: Single VS Double Digestion -----	66
3.1.2.3 Internal Standard Protein: Different MWCO Filters -----	66
3.1.3 HMW Fractionation -----	67
3.1.3.1 Internal Standard Protein -----	67
3.2 Differential Proteomics of AD and PD Samples -----	67
3.2.1 Samples -----	67
3.2.2 High Molecular Weight Fractionations -----	67
3.2.3 Protein Precipitation -----	68
3.2.4 Solubilization, Denaturation, and Alkylation -----	68

3.2.5 Short GeLC	69
3.2.6 Gel Processing.....	69
3.2.6.1 Lane Cutting and De-staining.....	69
3.2.6.2 In-Gel Digestion.....	70
3.2.6.3 Peptide Extraction	70
3.2.7 Peptide Clean-Up	70
3.3 SWATH Acquisition and Data Analysis.....	71
3.4 Bioinformatics Tools	74
3.5 Ethics Committee Approval.....	75
4. Results and Discussion	77
4.1 Patient Information.....	77
4.2 Protein Identification Library.....	77
4.3 Differential Proteomics Analysis.....	84
4.4 Cohort Discrimination Using Altered Proteins.....	90
5. General Conclusions	95
6. References	96
7. Supplementary Data	121
7.1 Protein Quantification Results of Fractionated Serum	121
7.2 Identification of LMW Internal Standard Protein in Fractionated Serum and Buffer	122
7.3 Single vs Double Digestion of LMW Internal Standard Protein	125
7.4 Low Molecular Weight Protein Identifications Using Different MWCO Filters ..	128

7.5 Additional Tables ----- 130

I. Introduction

I.1 Neurodegenerative Diseases

Neurodegeneration refers to the gradually progressive and irreversible loss of select neuron populations which are either anatomically or physiologically associated (1-4). It is a common event affecting numerous heterogeneous disorders of the Central Nervous System (CNS) such as AD (5) and PD (6), the two most prevalent neurodegenerative diseases (NDs) (7). Neurons (Figure I.1) are brain cells that process information (8) through electric excitability and synaptic communication with other neurons/cell types. Although their survival is sustained by other brain cell populations (such as glial and endothelial cells) (8) (Figure I.1), they are directly implicated in both sensory and motor functions, therefore being ultimately responsible for regulation and control over the entire organism. Given their pivotal role and their uniqueness (in the sense that, in general, neurons are post-mitotic cells), it is safe to assume that mass degeneration of even only discriminate populations of susceptible neurons will result in dramatic perturbations on the systemic level. An example of the magnitude of these perturbations is the progressive (and debilitating) cognitive decline observed in AD and PD patients (5, 6).

Aside from nerve cell loss in particular brain regions, NDs also share another main phenotype: the formation (and accumulation) of insoluble intra- and/or extracellular proteinaceous aggregates (4, 7, 9, 10). The aggregation of β -Amyloid (A β) peptide into extracellular senile plaques (SPs) and of hyperphosphorylated tau protein into intracellular neurofibrillary tangles (NFTs) (Figure I.2 A and B), and the aggregation of α -synuclein into intracellular Lewy bodies (LBs) and Lewy neurites (LNs) (Figure I.2 C), are representative cases of this abnormal protein clumping in AD and PD, respectively (7).

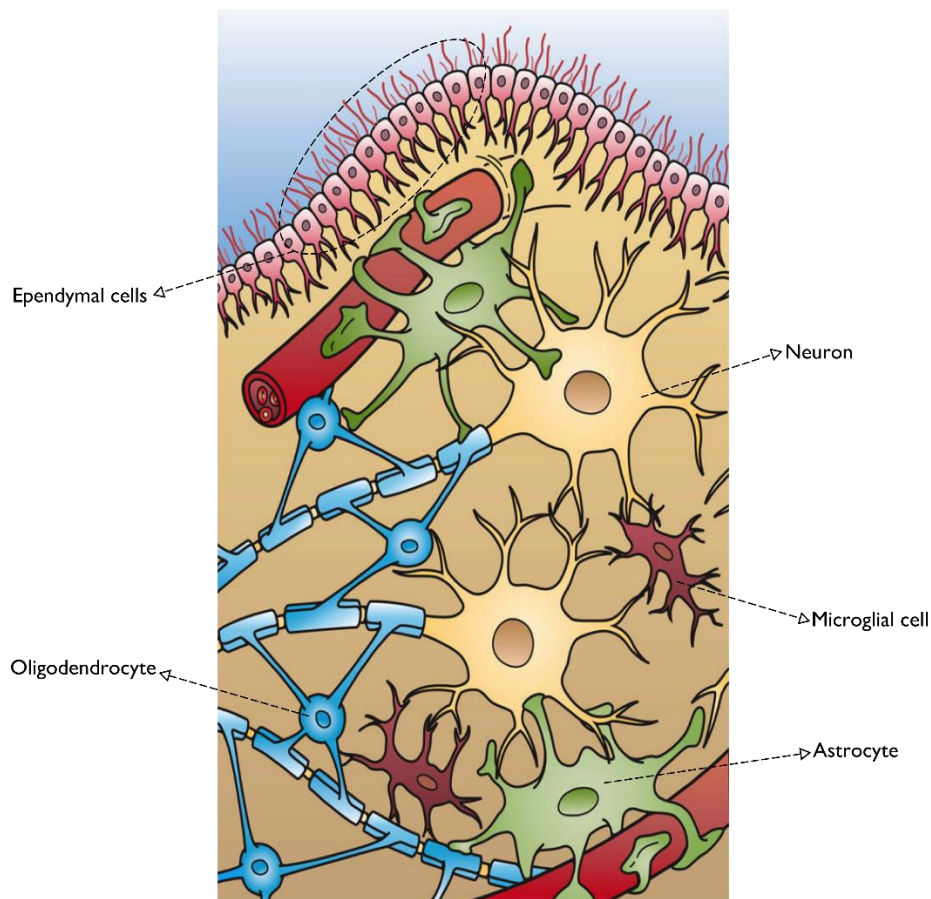


Figure 1.1 Various cell populations in the brain. Not only neurons, but also glial and ependymal cells are illustrated. Adapted from (11).

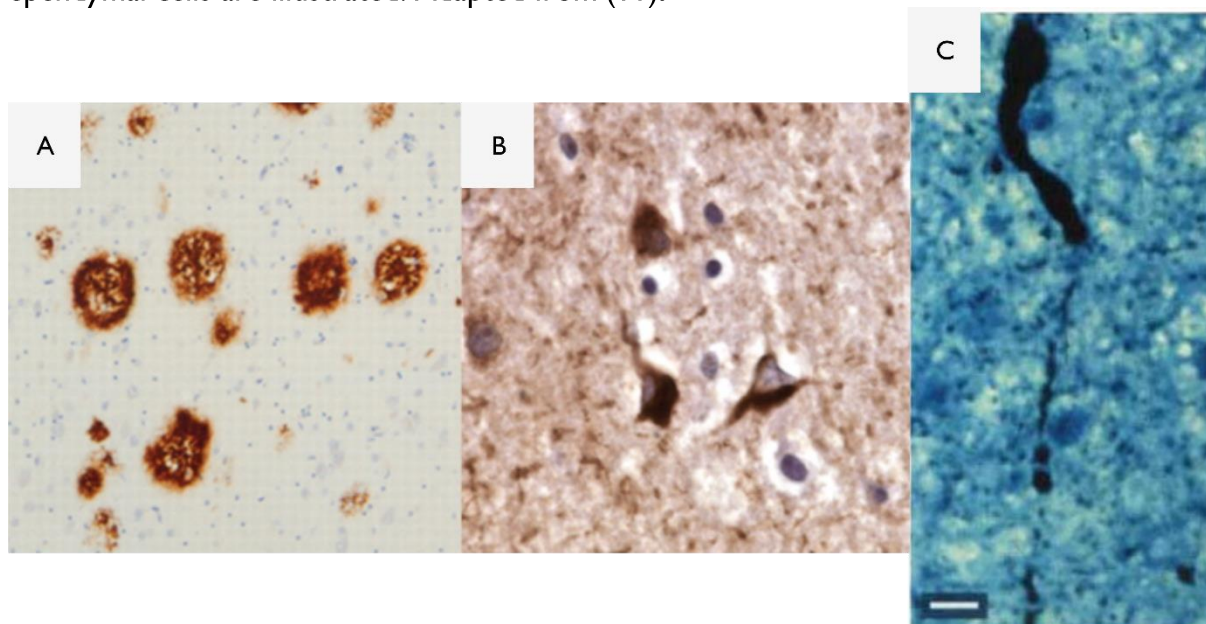


Figure 1.2 Protein aggregates commonly found in AD and PD. Immunohistochemistry directed against A β (A) and tau (B) reveal SPs and NFTs in photomicrographs, respectively. LNs revealed from immunohistochemistry directed against α -synuclein (C) in neuronal processes from the substantia nigra of a sporadic PD patient. Scale bar in (C) is 10 μ m. (A) and (B) are adapted from (12), and (C) is adapted from (7).

Besides the multiple risk factors involved in each of these diseases (discussed in subsequent chapters), a paramount aspect of NDs (which is reflected in their progressive profile) is the effect of aging on neurodegeneration (13). According to the World Health Organization (WHO) the average global life expectancy at birth in 2016 was 72.0 years and a recent publication involving 18 high-income countries revealed a clear trend of increasing life expectancy between 1990 and 2015 (14). In 2010, total European costs for dementia (of which AD is the main contributor) were about 105.2 billion €PPP (Purchasing Power Parity) (15, 16). In addition, according to the World Alzheimer Report 2018 (17), global dementia costs in 2018 were about 1 trillion US\$ (with 50 million people afflicted all over the world), a value that is expected to reach 2 trillion US\$ by 2030. Thus, increasing life expectancy, ageing as the main risk factor for NDs, and the already enormous cost of brain disease worldwide collectively indicate that, in a not so distant future, the social and economic burden of NDs will be completely unsustainable, justifying the need to invest more scientific resources in research that might help either revert or at least reduce the progressive pace of neurodegeneration in these disorders.

1.1.1 Alzheimer's Disease

AD is the most common ND and the major causative agent of dementia, mainly in people over 65 years of age (18-22). Clinically speaking it is characterized by a slow and gradual progression of language, memory and cognitive decay (19). Due to this slow pace of disease development, another definition has been established, known as Mild Cognitive Impairment (MCI), which aims to designate the stage of cognitive impairment that frequently precedes the transition from cognitive changes in normal aging to those normally observed in dementia (23). Usual symptoms exhibited by distressed patients include apathy, restlessness, anxiety, depression, hallucinations, delirium, motor activity abnormality, irritability, sleep disorders, eating disorders, euphoria and disinhibition (19), which still today complicate clinical diagnosis due to heterogeneity among patients and overlap with other neurological disorders (24). Even more so is AD diagnosis complex in earlier stages of disease, since neuropathological changes in the brain may start to accumulate 10 to 15 years prior to the first clear indications of clinical impairment (25). Thus, unequivocal diagnosis of AD is only presently achieved by autopsy (and examination of the brain) after death (25).

At the beginning of the 20th-century clinical psychiatrist and neuroanatomist Alois Alzheimer (Figure 1.3) made the 1st anatomical observations of what one day would be

classified as the disease named after him, (AD). The subject was a 51-year-old woman, admitted at the Frankfurt insane asylum, showing complex symptoms such as complete disorientation, auditory hallucinations, and memory and speech impairment, which did not allow for an objective classification of her ailment. After almost 5 years of sickness she died and a *post-mortem* observation of specimens from her brain tissue was elaborated. Significant histological alterations were discovered, among them localized neurodegeneration and the first-ever remarks of what we today call SPs and NFTs. Later that century, Alzheimer made similar observations on another subject with a peculiar difference: only plaques, but not tangles, were present in the slide preparations of this subject's brain tissue. In 1998 results from reinvestigation of the latter case with modern neurohistochemical techniques were published (Figure 1.4), indicating both cases were merely different stages of the same disease (26-28).

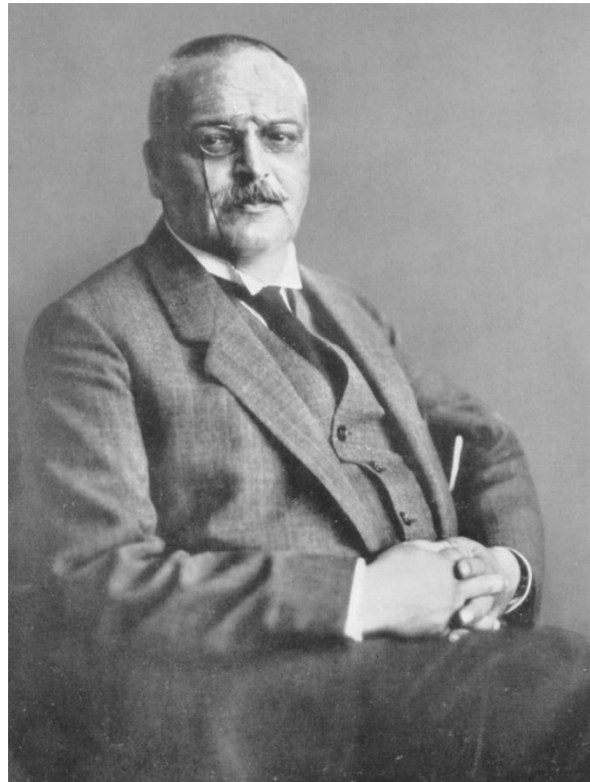


Figure 1.3 Alois Alzheimer roughly around 1909 (27)

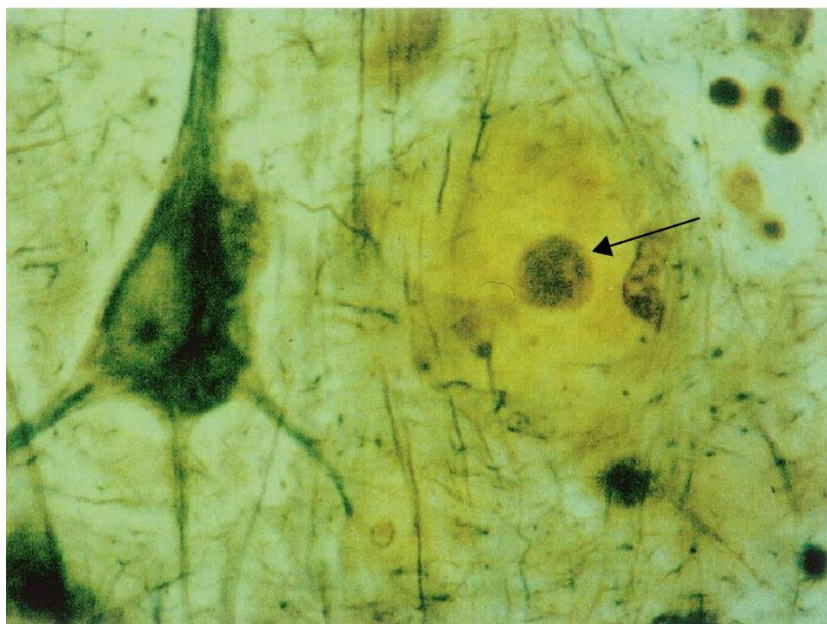


Figure 1.4 Classical staining of SPs from the cerebral cortex of the AD patient observed by Alois Alzheimer in 1911. A pyramidal neuron is clearly seen (left) as well as a dense-core plaque (indicated by black arrow). No neurofibrillary changes are observable. Image magnified x500. (28)

As stated before, the burden of dementia on society is predicted to increase dramatically in the next few decades and it is anticipated that 152 million people worldwide will be affected by some form of dementia, presumably most of them AD, in 2050 (17). In fact, the effects of aging population, due to increased life expectancy, are already being felt and a study published earlier this year concluded that, between 1990 and 2016, the global number of deaths, Disability-Adjusted Life Years (DALYs – Definition according to the WHO: “The sum of years of potential life lost due to premature mortality and the years of productive life lost due to disability”), and prevalence (proportion of a population affected by a medical condition) of AD (and other dementias) have increased 148%, 121%, and 117%, respectively. Additionally, these disorders were the 3rd largest contributor to global neurological DALYs, with an average of 9 to 12.1 years (29). Regarding these statistics, it is critical to objectively characterize the pathophysiology of AD, in order to pre-emptively design therapeutic solutions to the imminent (and potentially catastrophic) burden of dementia on society. Thus, in the next chapters a comprehensive review of both the main hallmarks and explanatory theories for AD pathogenesis is presented.

Through clinical observation, AD cases can be classified according to the age of onset of disease: before 60 years of age, it is considered early-onset, whereas after 60 years of age it is considered late-onset (the latter comprising the vast majority of instances). In either class, lesions hallmarked for AD share equal distribution pattern in the brain (30).

Another classification scheme is based on the presumed etiology of AD and separates patients into sporadic AD and autosomal dominant familial AD (FAD) (30, 31). Sporadic AD cases comprise about 95% of all AD cases (32) and most of late onset cases (30), of which the main genetic risk factor is apolipoprotein E (APOE), more precisely the $\epsilon 4$ allele (APOE4) (32). This allele increases the risk of developing AD or cerebral amyloid angiopathy (CAA) and, specifically for AD, individuals bearing one or two copies respectively have a 3- to 4-fold and 8- to 12-fold increased risk of developing the disorder, as compared to others bearing the most common genotype (homozygotic for APOE $\epsilon 3$ allele) (31, 33, 34). According to the literature, the connection between AD and APOE genotype is supported by research that indicates this protein is implicated in the modulation of A β , with the APOE4 allele being linked to amplified A β plaque pathology and mitigated A β clearance, among other features (31, 32, 34). Additionally, APOE4 is known to modulate A β -induced effects on inflammatory receptor signalling. Aside from its role in A β -related processes, APOE4 is also known to aggravate tau-mediated neurodegeneration and neuroinflammation (33). Although APOE genotype seems to be the most relevant risk factor to sporadic AD, there are multiple influencing aspects at hand, both genetic and environmental (32). The triggering receptor expressed on myeloid cells 2 (TREM2) is linked to APOE function, and polymorphisms of this protein also influence risk of AD by the means of dysregulated microglial inflammatory responses (31, 33). Many other genetic variants linked to late-onset AD (in numerous ethnic groups) have been studied and identified, albeit most of them are still awaiting functional validation (34).

On the other hand, FAD and early-onset AD largely overlap (30). FAD is caused by mutations in genes relative to proteins involved in A β production (enhancing its accumulation), namely amyloid precursor protein (APP), presenilin 1 (PS1), and presenilin 2 (PS2) (30-33). Yet, most of these mutations do not directly affect A β production, but instead increase its propensity to aggregate or constrain its degradation, vehemently influencing disease onset but not progression (31), i.e., disease starts at an earlier age but progresses from then on at a similar pace than sporadic AD. For instance, AD-associated PS1 mutations tend to reduce γ -secretase activity, which in turn results in an imbalance of the A β 42/A β 40 ratio, leading to increased aggregation. Of note, in both sporadic AD and FAD there is evidence that suggests C-terminal fragment products of APP processing (like APP intracellular domain - AICD) are toxic, being closely related to the pathogenesis of disease when accumulated (33).

Another “genetically predisposed population” are people afflicted by Down's syndrome, showing the earliest onset (at about 40 years of age), as in this pathology there is trisomy of chromosome 21, which contains the APP gene, resulting in a significant surplus of APP (about 1.5 times the regular amount in the brain) and therefore accelerated accumulation of A β , eventually leading to the precocious onset of AD (31, 33, 35).

1.1.1.1 Hallmarks of AD

From a clinical perspective, hallmarks of AD (some of which have already been discussed above) include continuous and increasing deterioration of memory, judgment, decision making, orientation to physical surroundings, and language (7). From a neuropathological viewpoint, Serrano-Pozo *et al* (12) have described the hallmarks of AD as being separated into two categories: “positive” and “negative” lesions. Positive lesions consist of otherwise undetectable or poorly detectable features (that are clearly visible in the brain tissue of afflicted patients, for instance, upon appropriate elaboration of proper staining procedures (12)) and comprise A β peptide related lesions (such as SPs and CAA), hyperphosphorylated tau related lesions (like NFTs, neuropil threads, and dystrophic neurites), and glial responses (including astrogliosis and microglial cell activation). Moreover, there are other more localized (but also distinctive) lesions in the hippocampal formation, namely Hirano bodies and granulovacuolar degeneration. Negative lesions consist of the absence of regularly observed brain/cellular features (which are normally detected under non-pathological circumstances) and comprise loss of neurons, neuropil, and synaptic elements. Of all of these, the most relevant and invariant attributes of AD seem to be SPs, NFTs, and neuronal (7) and synaptic loss (36). To clarify: neuropil threads are nerve cell processes dispersed in the neuropil, discriminated by their argyrophilic (affinity for silver) staining profile (37).

The amyloidogenic pathway engaged in the proteolytic processing of a large type I transmembrane protein (38), known as APP, through its consecutive cleavage with β - and then γ -secretases at secretory or endocytic compartments (18), results (predominantly) in a 42 or 40 amino acid long peptide branded A β (A β 42 and A β 40, respectively). In AD stricken patients, this peptide is very prone to aggregation, either in the form of insoluble β -sheet pleated amyloid fibrils or its intermediate, synaptotoxic soluble oligomers. SPs are extracellular deposits of aggregated proteins in the brain parenchyma, mostly consisting of A β peptide (32), which can be classified as diffuse or dense-core (according to their staining profile) and are frequently found in the cerebral cortex of individuals bearing AD.

Dense-core plaques are defined by their condensed core (hence the name) and are frequently associated to synaptic loss, glial responses, and dystrophic neurites (which in turn are essentially any neuron process, be it dendrite or axon, evidently affected by A β pathology). Unlike the latter, diffuse plaques present an amorphous morphology with unclear boundaries, observable in cognitively intact elderly people, therefore not being associated with those pathological features of AD. Both A β types are present in SPs, but due to a higher insolubility/hydrophobicity, rate of fibrillization, and a consequent increased tendency to aggregate, A β 42 is more plentiful in these lesions (12, 33). Of note, although A β 's role under physiological conditions has not yet been ascertained, it is suspected to be associated with synaptic activity modulation and signaling (12, 39). Additionally, in spite of the fact that temporal extent and acuteness of dementia/cognitive decline in AD does not correlate (or poorly correlates) with amyloid burden (which includes SPs) (12, 32), some disease staging models have been proposed (37, 40). Braak and Braak described the A β deposition distribution pattern in 3 stages (37) (Figure 1.5 A), whereas a more recent and comprehensive study characterized 5 stages (40) (Figure 1.5 B).

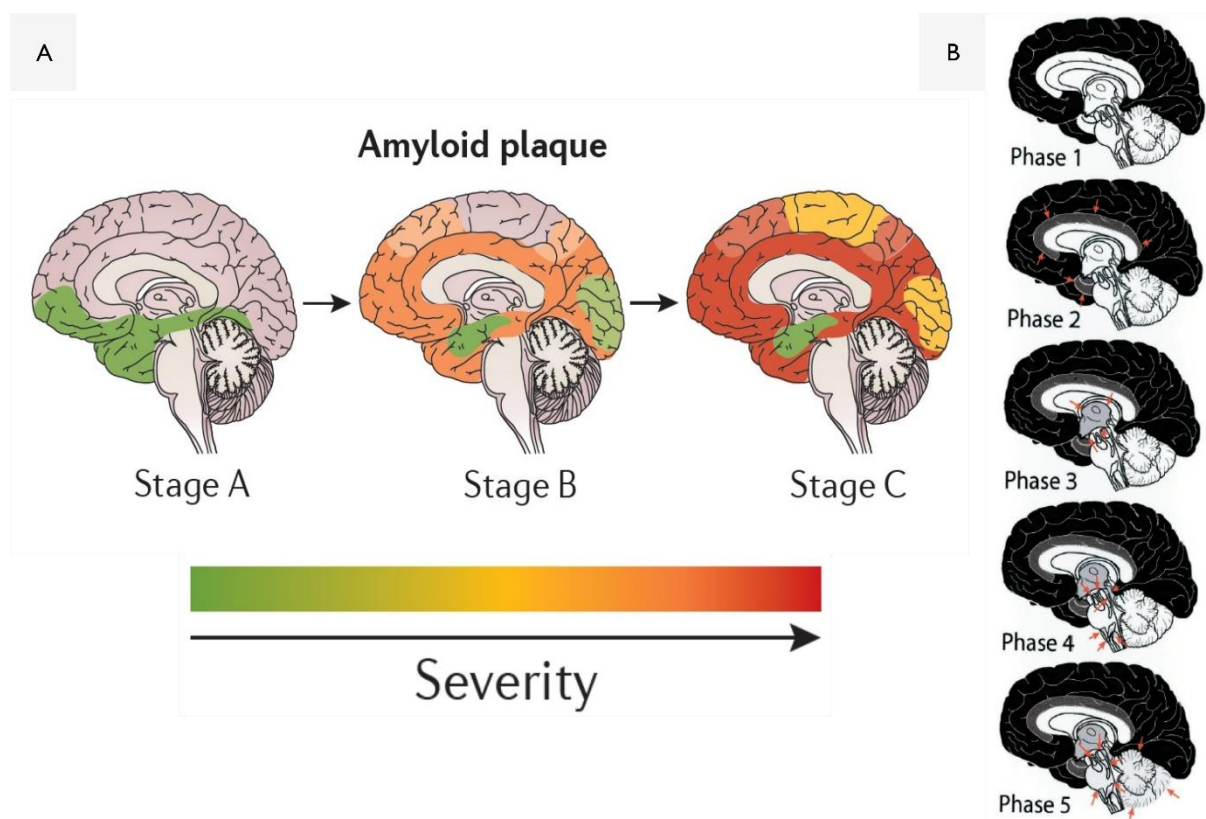


Figure 1.5 A β pathology staging systems. The staging system for A β pathology in the brain, as described by Braak and Braak (A) and as described by Thal *et al* (B). In B, orange

arrows indicate the progression of emergence of A β deposits characteristic to each phase. A is adapted from (5) and B is adapted from (40).

More vehemently exploring APP processing in the brain leads to two competing proteolytic pathways: amyloidogenic and non-amyloidogenic (Figure 1.6). As already stated, A β peptide is produced via the amyloidogenic cascade. It starts with cleavage of APP by β -secretase β -site APP cleaving enzyme-I (BACE1, that is very abundant in neurons), generating a soluble fragment (APPs β) and a still membrane-bound APP carboxy-terminal fragment (β CTF). The latter is further cleaved by the γ -secretase protein complex, generating AICD, as well as extracellular A β peptide (32, 33, 38). As for the non-amyloidogenic pathway, it starts with an α -secretase cleaving inside the A β region (thereby preventing the formation of the pathogenic peptide) and generating both an extracellular fragment (APPs α) and a membrane-bound APP carboxy-terminal fragment (α CTF). The latter is further cleaved by the γ -secretase protein complex, forming AICD and a shortened version of the extracellular A β peptide (p3) (38). In physiologically normal individuals α -secretase cleaves upwards of 90% of available APP, leaving the remainder to be cleaved by β -secretase (33).

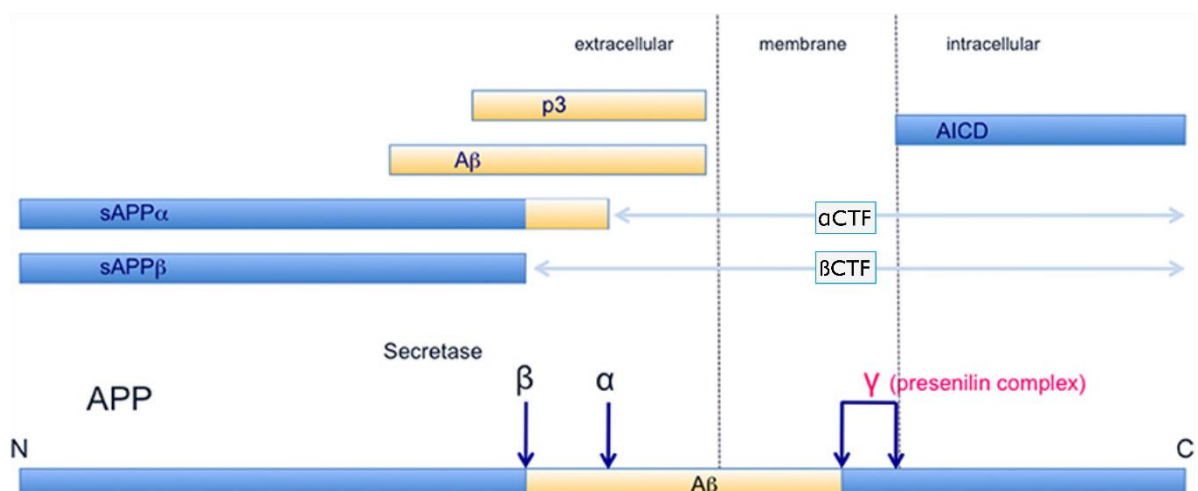


Figure 1.6 APP processing pathway. Adapted from (33). APP is a transmembrane protein that can be cleaved by different secretases. Depending on the cleavage site, downstream events may culminate either in the release of soluble fragments or in the generation of aggregate prone A β , among other intermediate molecules, which links APP processing to AD.

Note that multiple proteins of the “a disintegrin and metalloprotease” (ADAM) family function as α -secretases, but research advocates that the main one (responsible for most α -secretase activity and constitutively expressed in neurons) is ADAM10 (38, 41), suggesting its relevance in APP proteolytic processing. Furthermore (and to clarify), the

γ -secretase protein complex is comprised of four essential subunits: PS1 and PS2 (which are catalytic subunits (32)), nicastrin (NCT, that allows for initial substrate recognition), anterior pharynx defective 1a or 1b (APH-1a and APH-1b, respectively), and presenilin enhancer-2 (PEN-2, which is responsible for the stabilization of the presenilin fragments integrated in the protein complex) (38, 42).

Another deleterious aspect of A β deposition is the formation of fibrillar aggregates in the walls of blood vessels irrigating the brain (potentially obstructing them) (Figure 1.7), mainly cortical capillaries, small arterioles, and mid-sized and leptomeningeal arteries, a lesion referred to as CAA. It mainly consists of A β 40 that initially collects within the outer basement membrane of the vessels (supposedly during its clearance from the brain, after being released from neurons) and can lead to smooth muscle cell degeneration in the tunica media. In later stages, aggregates can infiltrate the surrounding parenchymal tissue all the while establishing plaque-like structures. Nonetheless, 6 other proteins have been identified that can produce this pathology in diseases other than AD, including other types of dementia and some mutation associated disorders. Most AD patients also present mild CAA pathology (80% - 90%), aside from SPs, although in many cases it is only confirmed at autopsy. This happens because CAA is usually asymptomatic, albeit it can contribute to cognitive decline in AD (12, 43).

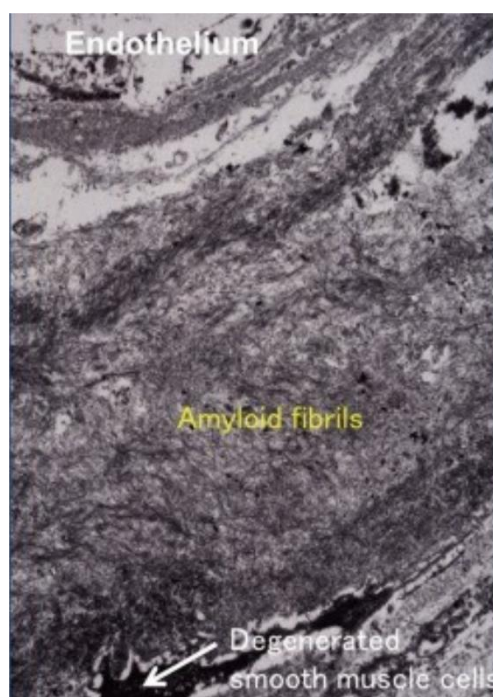


Figure 1.7 Cerebral amyloid angiopathy. An electron micrograph of the media, with clearly observable amyloid fibrils and smooth muscle cell degeneration. Amyloid fibrils can additionally cause vasculature double barreling. Adapted from (43).

NFTs initially develop in the nerve cell body (eventually spreading into dendrites and axons, which in turn may deteriorate and form neuropil threads, that are known to develop side by side with NFTs) and are composed of aggregated proteins, of which the main contributor is hyperphosphorylated (and consequently misfolded) tau, a microtubule-associated protein, mostly arranged in the form of paired helical filaments (a helical three-dimensional [3D] conformation containing pairs of fibrils with a diameter of 10 nm, with constant periodicity of about 80 nm), but also straight filaments (Figure 1.8) (12, 33, 37, 44-46). There are additional diseases characterized by aggregation of tau (known as tauopathies), but in AD, NFT deposition is exclusive to neurons (46). NFT bearing neurons eventually succumb to this burden, degenerating (which, along with other AD-related lesions, may ultimately cause the cognitive decline characteristic to this disorder) and leaving behind an extracellular assembly nicknamed “ghost tangle” (37). Nevertheless, whether the generation of these aberrant protein assemblies is an indispensable predecessor of neurodegeneration in AD or embodies a defensive reaction by injured neurons is, thus far, matter of discussion among researchers (12).

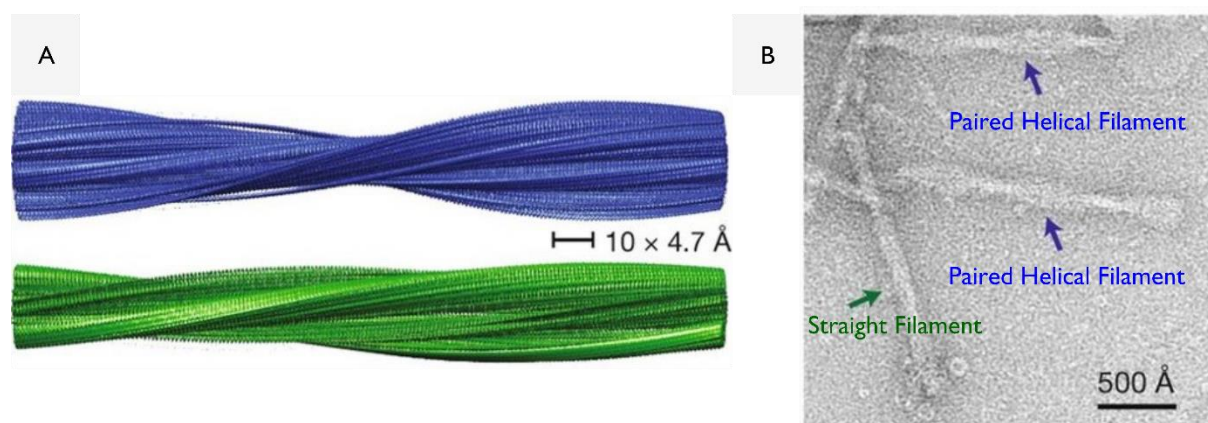


Figure 1.8 Tau filament structures from AD afflicted brain. Cryo-electron microscopy reconstructions of paired helical filaments (blue) and straight filaments (green) (A). Electron micrograph of negatively stained, purified tau filaments (B). Adapted from (45).

The development of these aggregates throughout discernible brain regions and alongside the progression of disease follows a distinct (and relatively conserved) pattern, corresponding with the sequential neuropsychological and cognitive changes (among other perturbations like the pattern of neurodegeneration) representative of AD, enabling the creation of a staging scheme of tau pathology (Figure 1.9) (with 6 levels of pathology development), that correlates with both dementia duration and severity and that can be used for the pathological diagnosis of AD (12, 33, 37, 40). Staging is elaborated by classification according to 3 broad range stages of increasing brain lesion dispersion, which

in turn are further classified as a mild or severe form of the previously chosen stage (Example: Stage 1 and 2 both comprise the transentorhinal stage, but are respectively classified as mild and severe). The three broad range stages are: 1) transentorhinal (relating to an asymptomatic disease state), 2) limbic (relating to incipient AD), and 3) isocortical (relating to completely established AD) (12, 33, 37).

Neuron and synapse loss displayed in AD mainly occur in the cerebral cortex and certain subcortical regions (47), therefore being the main contributors to cortical atrophy in the brain of afflicted patients (12).

The neuronal loss present in AD, exhibiting explicit brain distribution (similar to that of NFTs) (12) and ultimately leading to cognitive decline, is a fairly late occurrence in the progression of the disease, following events such as synaptic dysfunction, synaptic loss, and neurite retraction, among other irregularities (39). However, neuron death initiation in AD does, in fact, precede SP and NFT formation (48). Hence, though neuronal loss may very well be one of the best indicators of cognitive deficit (actually being a better correlate than the number of NFTs) (12), it may also be that, at the point when it is observable/measurable, the damage is already irreversible. In fact, it is believed that before clinically observable symptoms manifest in a given patient, a majority of the neurons selectively vulnerable for AD pathology, have already perished.

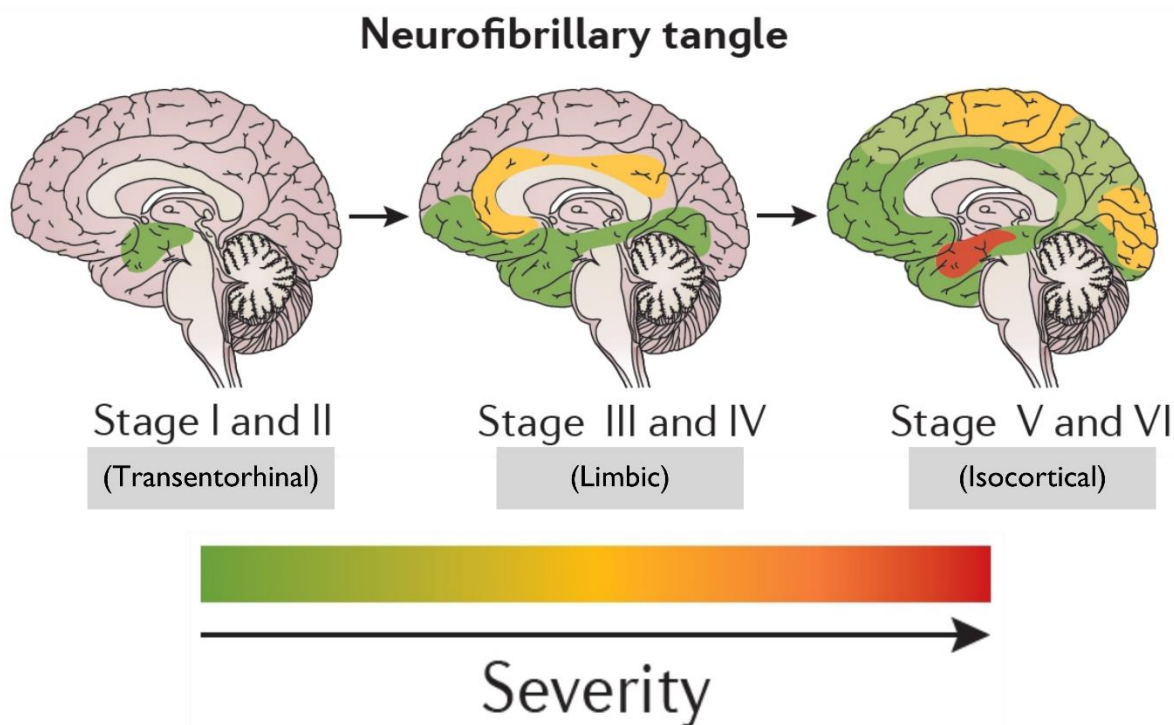


Figure 1.9 Staging system for NFT pathology in the brain, as described by Braak and Braak. The staging system is used to stratify patients according to disease severity, which appears correlated with the appearance and spreading of lesions such as NFTs. Adapted from (5).

As stated before, both astrogliosis and microgliosis (activated/reactive state of astrocytes and microglia, respectively) are suspected to be associated with A β deposition into dense-core SPs. Nonetheless (and contrasting with the increase in glial responses during the course of AD progression), the formation of the latter does not linearly correlate with the development of the disease, suggesting activated astrocytes and microglia might be more closely related to tau pathology, namely to NFT burden (12). In fact, research evaluating NFT burden, A β burden, and glial activation (among other AD hallmarks) in the temporal neocortex of AD stricken individuals concluded that, although astrogliosis and microgliosis transpire in the surroundings of both dense-core SPs and NFTs, their marked increase along the progression of disease correlates with NFT formation (as well as neuronal and synaptic loss), but not plaque formation (since it reaches a “ceiling” early in the clinical course of disease) (49, 50).

Notwithstanding this apparent connection between glial responses and NFTs, there are numerous molecular and morphological traits in astrocytes, like the marked increase in expression of the glial fibrillary acidic protein (GFAP) (51-53), that are implicated in NDs such as AD, and that may very well be associated to restraining SP formation. For instance, in a study investigating the effect of deletions in genes such as GFAP's, mandatory for

astrocyte activation, in mice manipulated to model AD (bearing mutated human APP and PSI genes), results indicated astrogliosis plays a pivotal role in restraining plaque growth and impairing plaque-related dystrophic neurites, while not influencing A β peptide formation (54). Hence, glial responses hallmarked in AD might be a protective mechanism that reacts to aberrant protein aggregation in the brain.

Aside from the previously stated and more widely studied hallmarks of AD, others exist that are still misunderstood like Granulovacuolar degeneration (GVD) and Hirano bodies. Both these lesions are observable in non-diseased individuals, but their severity and frequency are noticeably increased in the cytoplasm of hippocampal pyramidal neurons of age-matched AD patients and in the case of GVD, among other brain regions and NDs (12, 55-57). In fact, GVD (much like neurofibrillary lesions such as NFTs) in the hippocampus is a strong correlate to the characteristic decline of episodic memory performance observed in AD (55). Additionally, GVD burden per neuron correlates with the severity of dementia (56). While GVD is remarked as the accumulation of large (3 to 5 μ m in diameter) double-membrane bodies containing a central argyrophilic granule (12, 55, 56), Hirano bodies are eosinophilic rod-like inclusions (12, 57) and, even though their involvement in AD pathology is unknown, they have distinct profiles of immunoreactivity to proteins known to be associated with AD pathology: 1) in the case of GVD, the respective bodies show immunoreactivity for cytoskeletal proteins (including tau), tau kinases (suggesting association to NFT generation, although not directly involved) and many stress kinases, activated caspase-3 (linked to programmed cell death), and ubiquitin and autophagic markers (indicating they might actually be late-stage autophagic vacuoles) (12, 55, 56); and 2) in the case of Hirano bodies, the respective inclusions show immunoreactivity for cytoskeletal proteins (also including tau) and for carboxy-terminal fragments of APP (12) (namely AICD (57)). Since AICD is known to be involved in protein complexes that regulate the induction of apoptosis, it is not surprising that research shows Hirano bodies might safeguard neurons against AICD-mediated cell death (57).

1.1.1.2 Hypotheses for AD Pathology

The amyloid cascade hypothesis (Figure 1.10) first postulated by Hardy and Higgins (35) puts A β generation and deposition at the center of AD etiology. It states A β or APP cleavage products containing the complete A β sequence are neurotoxic, and that their deposition is the direct initiator of other pathological processes at the core of AD, such as NFT formation, neurodegeneration, and vascular damage (culminating in dementia),

although encompassing additional causes of AD that may trigger A β deposition or alter A β homeostasis (31, 32) (maintaining it as initiator of disease). It has since been altered to change the focus to soluble A β oligomers, although with no objective conclusions concerning their potential toxicity (32, 33). The main contributors for supporting this hypothesis are the identification of A β in SPs (34) and of mutations in APP, PSEN1, and PSEN2 that directly determine the early onset of AD featured in FAD (through enhanced accumulation of A β) (31, 34), as well as the observation of early-onset AD in individuals afflicted by Down syndrome (35). Albeit not definitive, the originally proposed mechanism for the A β cascade hypothesis enveloped disruption of calcium homeostasis and subsequent augmented tau phosphorylation as sequentially caused by A β peptide aggregation, ending with the formation of NFTs (35) and general increase in aggregate stress that leads to neurodegeneration in AD. Hence, the overall premise is that rare autosomal dominant forms of AD are essentially a fast-tracked model of (sporadic) AD.

Despite that (and even though the majority of up to date research substantially corroborates the premise of A β as the main disease initiator in AD (20, 32-34)), there is ever-increasing controversy in this subject and even some caveats to the hypothesis. These include the independent development of SPs and NFTs (with most mouse models bearing human A β not being associated with NFT pathology) and the unclear causal relation between both these lesions and neurodegeneration (as they could be causative or reactive), along with the generally limited success of clinical trials testing drugs (specifically antibodies) directed at molecular entities involved in the A β pathway (20, 32, 34).

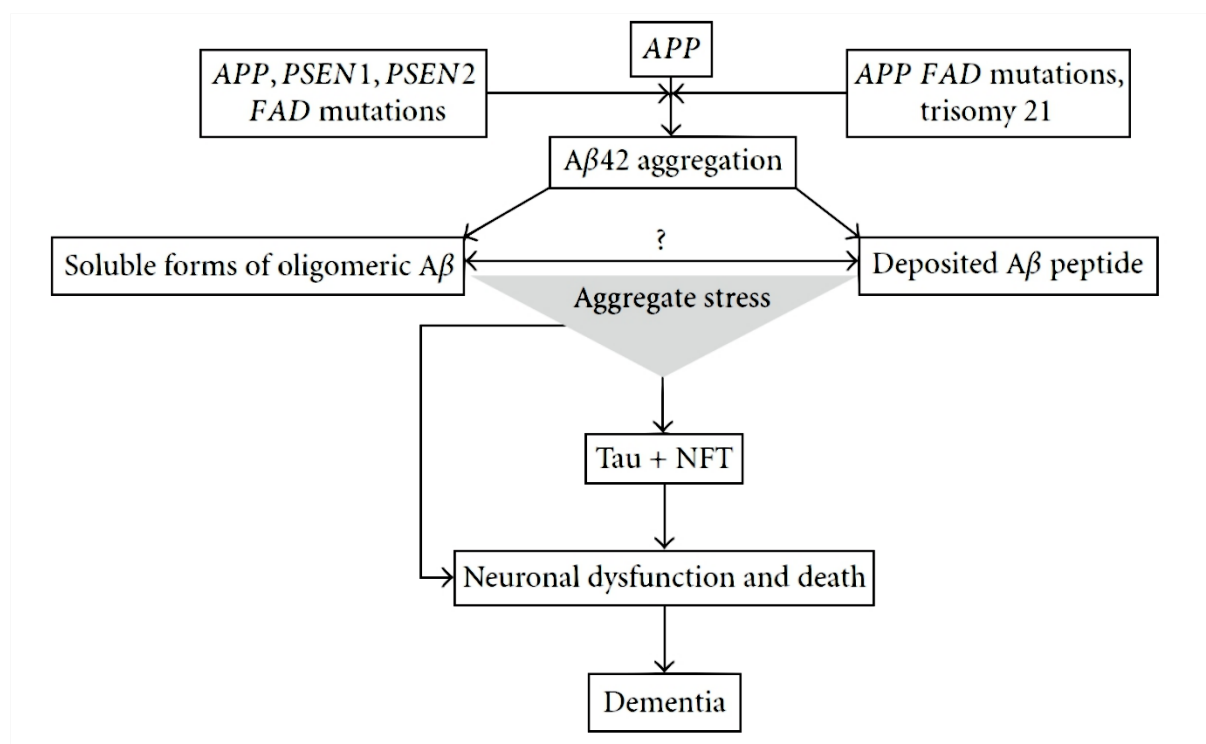


Figure 1.10 Schematic representation of the amyloid cascade hypothesis. Adapted from (34). Genetic factors influencing APP processing have a direct impact on A β aggregation. Aggregation may lead to deposit formation or into the generation of soluble oligomers. These events, coupled to other common AD pathologies and lesions culminate in neuron death and the onset of dementia.

In addition, a seemingly unsurpassable obstacle of this hypothesis is the weak temporal and anatomical correlation between plaque deposition, neuron death, and the clinical manifestations of AD, a commonality among sporadic AD and FAD alike (31). Therefore, while acknowledging A β as the initial trigger of other downstream processes (such as exacerbation of tauopathy, not to mention the consequent neuron debilitation and degeneration) and even essential to some of them like CAA, many in the scientific community consider it to be necessary, but not sufficient, to cause sporadic AD (31, 32).

As previously uttered, tau is a microtubule-associated protein that, under physiological conditions, is responsible for the stabilization of tubulin assemblies (additionally serving other purposes such as nucleic acid protection and synaptic function regulation). Alike many other proteins, tau exists in the human brain as multiple protein isoforms, specifically six, generated from alternative splicing of three exons (2, 3 and 10) in the respective mRNA molecule (the latter molecule also containing four repeat regions, determinant in microtubule binding, the second of which is contained in exon 10). According to the number of repeats expressed, tau in the human brain can predominantly exist as a three-

repeat (3R, without exon 10) or four-repeat (4R, with exon 10) isoform, primarily in neuron axons (32, 33) (Figure 1.11).



Figure 1.11 Tau mRNA alternative splicing gives rise to different protein isoforms. Adapted from (33). Alternative splicing of tau mRNA leads to the formation of different isoforms. Some of these have more propensity for particular modifications, such as phosphorylation which favors aggregation of tau.

This protein is subject to a variety of modifications (20, 32), being that phosphorylation is the most investigated and known to play a role in the regulation of microtubule-binding activity. In AD, hyperphosphorylation of both isoforms renders the protein prone to aggregation, impacting neuronal plasticity by the means of microtubule-binding impairment (which in turn leads to a variety of downstream abnormal cellular regulation events), and also driving the formation of lesions formerly referred to as NFTs and neuropil threads (capable of both driving and being modulated by neuroinflammation) (20, 32, 33). Moreover, microtubules are consequently destabilized, thereby negatively affecting axonal transport of neurotransmitters essential for normal cognitive functions like memory and learning (58). The premise of the tau hypothesis is that pathological processes like these, involving aggregation and propagation of this protein in brain cells (leading to neurodegeneration), comprise the main driving force of AD, tau being considered as the essential trigger of all downstream pathological proceedings throughout AD onset and progression (32, 33). Indeed, the generalized failure of candidate therapeutic strategies directed at A β (33) and the fact that AD progression (as well as the inherently associated cognitive demise) is more closely linked to tau pathology (32, 33), are two strong arguments in favor of this hypothesis. Coherently with the parallel progression of AD and tau pathology, it is believed that the initial trigger might be connected to increase in APP and/or its C-terminal cleavage products, that leads to incorrect sub-cellular localization of tau and consequent transport dysfunction. The accumulation of the mislocalized tau generates its propagation and foments the formation of the associated cytoplasmic inclusions (like NFTs) that further impair sub-cellular transport, thereby explaining the progressiveness of AD (33).

Conversely, the genetically determined etiology of other tauopathies (which is not the case for AD) and the observation of tau pathology in cognitively normal populations,

suggest that tau is needed but is also insufficient to prompt AD (much like what is said for A β in the context of the amyloid cascade hypothesis), and that in such a way tau pathology must be in fact downstream of this still unknown initial trigger of disease (32). Of note, the relation between amyloid and tau pathology is complicated by the fact that APOE's ϵ 2 allele, protective of AD (31, 32), actually intensifies the risk of developing other tauopathies (32).

The inflammatory hypothesis, tentative at explaining the pathogenesis of AD, is based on a model of self-perpetuating inflammation, of continuously increasing intensity, that drives neurodegeneration (58) (Figure I.12). AD is hallmarked by persistent neuroinflammatory processes such as astrogliosis (which increases linearly with cognitive decline) and microgliosis (20), that might play an important role in the etiology of disease and significantly contribute to its pathogenesis (51). This importance is substantiated by the fact that immune system components such as TREM2 and the complement system (as well as microglia themselves) are accountable for synaptic pruning (in physiologically normal situations it is defined as “the reduction in the number of synapses that occurs between early childhood and puberty” (59)), early on in the course of disease (20). In fact, numerous genes that aggravate the risk of developing AD are involved in inflammation and regulation of misfolded protein clearance by glial cells (51).

Both reactive microglia and astrocytes can be found in the periphery of some SPs (52) (Figure I.13) and NFTs (58), early in AD development, secreting pro-inflammatory cytokines (20) and a myriad of other inflammatory mediators, although their activation may occur upstream of A β deposition (51). Additionally, these cell populations can be primed for the inflammatory response, as a consequence of binding of misfolded and aggregated proteins (both A β oligomers and fibrils) to pattern recognition receptors on their surface, such as receptors for danger-associated molecular patterns (DAMPs) or pathogen-associated molecular patterns (PAMPs) (51, 52). Therefore, A β is a main inducer of glial activation in AD, possibly leading to synaptic loss further downstream (52).

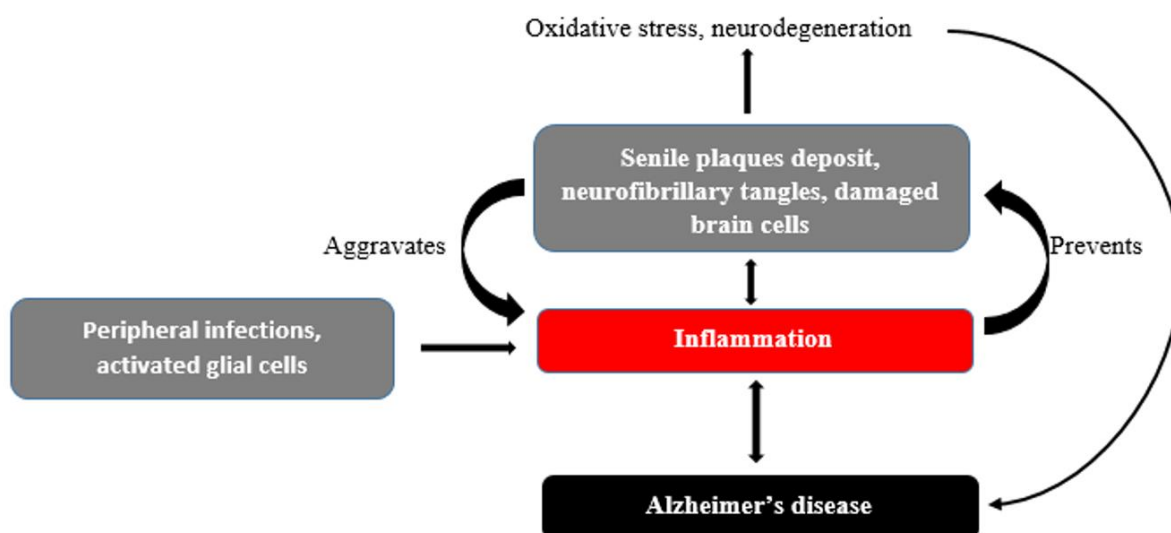


Figure 1.12 Self-perpetuating mechanism in the inflammatory hypothesis for AD pathogenesis. (58) Although inflammation is essential for immunity and oxidative stress is an unsurpassable (but usually manageable) byproduct of energy generation in cells, when both are affected in AD, a self-potentiated loop of exacerbation may be triggered. External insults might also trigger this cycle.

Other priming events may be associated with microglial senescence (which can be found in the surroundings of NFTs) and brain ageing. Microglia can also be activated upon binding of A β to immune receptors like cluster of differentiation 36 (CD36) and toll-like receptors 4 and 6 (TLR4 and TLR6, respectively). Consequently, A β fibrils are phagocytosed and directed to endolysosomal degradation (51). Compromised microglial A β clearance processes such as the latter, due to downregulation of phagocytic receptors, are inherently linked to sporadic AD, as evidenced by the identification of disease risk altering mutations in some genes encoding aforementioned receptors (TREM2) and allelic variants and single-nucleotide polymorphisms (SNPs) of cluster of differentiation 33 (CD33) (51). Besides impaired clearance, further microglial malfunction observed near SPs may occur due to continued exposure to A β and positive feedback loops between inflammation and APP processing, which lead to chronic inflammation in the afflicted brain regions (51). Astrocytes are also possibly responsible for A β elimination (albeit to a lesser extent than microglia and preferentially engulfing its oligomeric form (52)) by ApoE dependent mechanisms and secretion of extracellular A β -degrading proteases, such that their dysfunction/atrophy may affect A β clearance (51). Tau has also been implicated in the induction of pro-inflammatory signals, despite the fact that inflammation can induce microglial phagocytosis of tau oligomers (58), a feasibly neuroprotective mechanism.

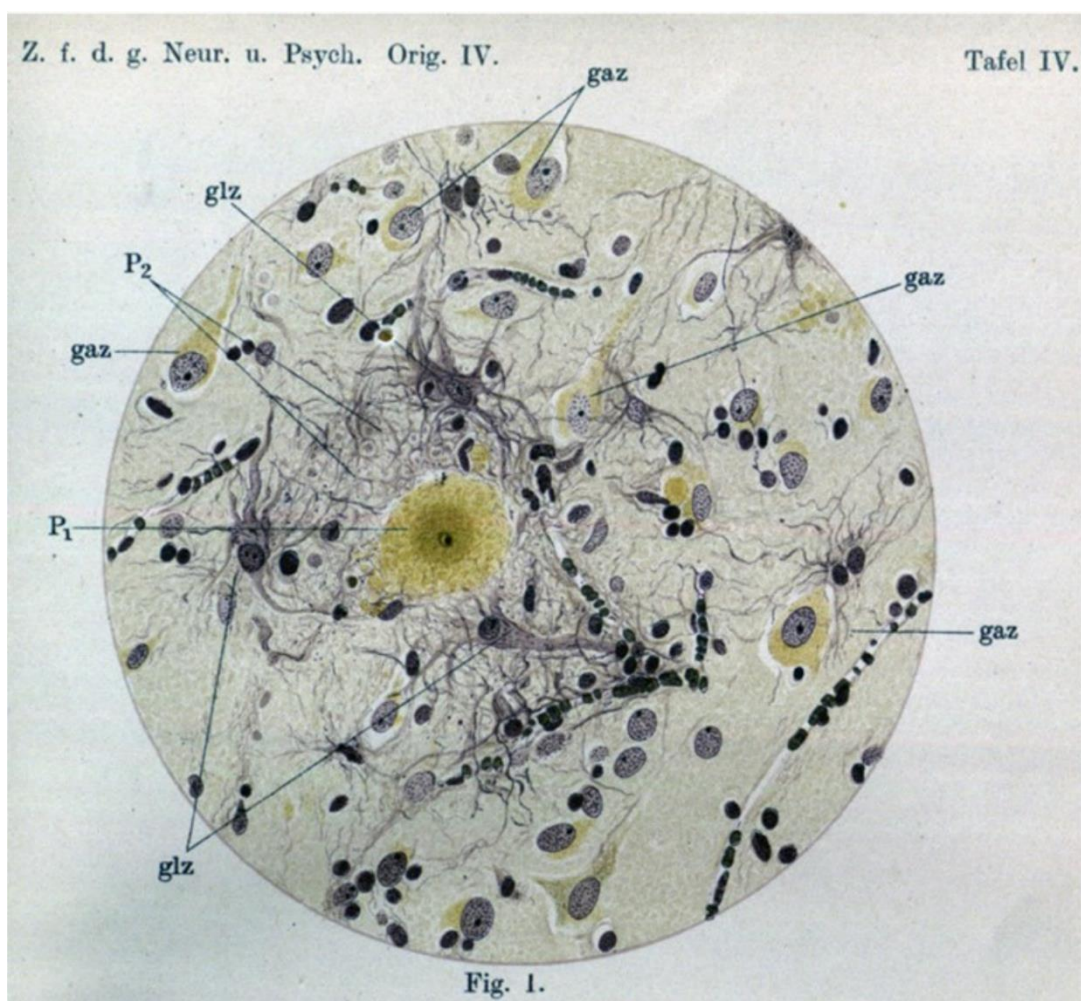


Figure 1.13 Plate drawing made by Alois Alzheimer himself, illustrating the relation between glial cells and plaques. It was originally drawn by Alois Alzheimer himself in 1911 and depicts microglia (glz) surrounding a SP (P1) close to neurons (gaz). Taken from (52), but the translated version of the original article can be found in (60).

Hence, regarding immune responses/glial cell activation in the context of AD, they can be considered either protective (namely aberrant protein removal) or harmful (such as unceasing glial cell activation) (20, 51, 52, 58). Note that the causal relationship between inflammation in AD and its other hallmarks is still a matter of discussion (58) and, although neuroinflammation is definitely a determinant factor in AD, it does not explain all mechanisms at play in the pathogenesis of the disorder, as evidenced by the limited success in creating clinical benefit of the administration of non-steroidal anti-inflammatory drugs (NSAIDs) to afflicted patients (20, 58). It is also hypothesized that comorbidities related to systemic inflammation could possibly accelerate AD progression (51) since peripheral pro-inflammatory molecules can potentially enhance inflammatory signaling in the brain by stimulation of peripheral nerves or by passing through the blood-brain barrier (BBB) (58). NSAID administration can also cause tau dephosphorylation, indicating peripheral inflammation might influence tau pathology and, consequently, AD progression (58). In

conclusion, many research results are conflicting, but all indicate neuroinflammation has a crucial role in AD pathology.

The oxidative stress hypotheses explains the features found in AD by linking neurodegeneration to free radical exposure that leads to alterations in the normal functioning of nerve cell membranes, resulting in dysregulated signal transduction cascades (mainly due to calcium imbalance in the cell) (61). Oxidative stress and its resulting cell damage are intrinsically implicated in the pathogenesis of AD (20), among other NDs and neuropsychiatric disorders (61, 62). It is conceivable that the brain be very susceptible to oxidative injury since it is a highly oxygen-demanding tissue (due to high energy demand), has copious amounts of lipids, and has a relatively dearth antioxidant enzyme pool, increasing the risk of reactive oxygen species (ROS) (over)exposure while undertaking mitochondrial respiration (19, 20, 61-63). Injuries related to reactive nitrogen species (RNS) can also be found in the brain of AD patients (64). AD is indeed related to such insults as indicated by the enhancement of glycol oxidation, lipid peroxidation, and protein nitration and oxidation (20), as well as other disease features discussed further down.

Additionally, A β is also known to induce oxidative stress (20), critical to both AD pathogenesis and progressiveness (19), (for instance, protein aggregates can injure cell membranes through increased levels of free radicals (5)) and oxidative stress itself has been shown to foment A β production (51), either through increase in APP levels or modulation of APP-processing related enzymes (BACE1, for example) (64). One mechanism through which A β fragments induce oxidative stress is iron and copper reduction in the brain, endorsing DNA damage (19). Actually, copper reduction by APP could instigate neuronal damage by the means of increased hydroxyl radical (\bullet OH) production (62) and A β , depending on its length after APP processing, and some of its precursors have high-affinity binding sites for copper and zinc, which may be associated with increased oxidative stress telltale of AD (63). What's more, A β could theoretically enter mitochondria (in the incipient stages that trigger AD) leading to elevated ROS-mediated oxidative stress (64). Further discussing AD lesions, both SPs and NFTs can set off oxidative stress reactions, possibly culminating in neurodegeneration (64). There is also evidence that links oxidative stress to pathogenic macroautophagic processes in AD (61).

Oxidative stress is linked to inflammation as well (albeit with an uncertain causal relation (19)), with cytokines being able to prompt inducible nitric oxide synthase (iNOS, which is

upregulated in the AD brain) in microglia and astroglia, favoring the generation of neurotoxic nitric oxide (NO) species, which in turn may modify proteins through nitration and S-nitrosylation, among other post-translation modifications (PTMs) (51). As an example, A β nitrated at tyrosine 10 (found at the core of SPs) is more aggregation-prone, linking iNOS increased expression to AD. Another enzyme upregulated in AD is the NADPH oxidase complex (PHOX) which is exceedingly expressed in microglia and susceptible to activation by inflammatory inducers like A β . Either isolated or in coordination with iNOS products, PHOX can lead to the production of hydrogen peroxide (known to activate microglia), superoxide and peroxynitrite (51).

Thus, it is possible that elevated production of free radicals (such as ROS) in the AD brain overwhelm or deplete the brain's antioxidant pool, thereby leaving it unprotected with regard to these insults and susceptible to degeneration. This marked increase in free radicals may be due to a panoply of events like mitochondrial dysfunction (mitochondrial function being both a source and target of toxic ROS (63)), A β extracellular deposits, and microglial activation (61).

All in all, numerous features of AD validate the oxidative stress hypothesis such as increased levels of trace metals (able to generate free radicals) in the brain, elevated levels of lipid peroxidation (suspected to be an early occurrence in the development of the disorder) in ventricular fluid, augmented protein and nucleic acid oxidation (protein oxidation potentially leading to the formation of advanced glycation end products, as a PTM (63)), energetic hypometabolism, and A β -mediated free radical generation (61, 62, 64). Still, some questions remain unanswered, for instance, the causal relation between ROS and brain lesions characteristic of AD is yet undefined, as each of them has been reported to stimulate the formation/induction of one another (61, 62). Moreover, clinical trials testing antioxidant therapy for the treatment of dementia have failed to demonstrate an obvious beneficial effect (61, 64), which might mean there are other unknown aspects at play in AD or that these trials did not evaluate all essential information (64).

Malfunctioning mitochondria and imbalanced energy metabolism are stereotypical of AD. Mitochondrial function worsens with advancing age (as do other hallmarks of AD) (Figure 1.14) and thus, the mitochondrial cascade hypothesis tries to explain why aging is the major risk factor for AD. This hypothesis for the explanation of AD pathogenesis, which explores the previously stated traits of the disorder, can be divided into two general hypotheses, one that proposes a primary involvement of mitochondrial dysfunction in the

development of disease and another in which the role of this deleterious event is secondary. If and when considering a primary role of these specialized cellular structures in the etiology of AD, the A β cascade hypothesis must be disregarded, since it puts A β aggregation upstream of all pathological occurrences. Conversely, regarding mitochondrial dysfunction as important but not pivotal to the onset of AD and accepting A β deposition as the major initiator of disease are not mutually exclusive realities, being that this peptide may very well prompt mitochondrial dysfunction (65).

One of the first studies linking dysfunctional mitochondria to A β demonstrated (in vitro) a differential toxic effect of this peptide in neuronal NT2 cells, both bearing (NT2 ρ^+) and not bearing (NT2 ρ^0) their respective mitochondrial DNA (66). Supplementing the media with A β induced cell death in NT2 ρ^+ cells but did not significantly affect the viability of NT2 ρ^0 cells, indicating a central role of mitochondria (more precisely, of some core respiratory chain subunits) in mediating A β toxicity (65, 66). Another possible effect of A β exposure is an imbalance in calcium homeostasis, which can affect mitochondria, ultimately leading to less production of ATP (65). Built-up A β can also hinder select mitochondrial import channels, inducing their dysfunction and consequently resulting in cell death, through augmented ROS generation (21). Likewise, tau deposits are also a source of neuronal mitochondria toxicity, impairing their normal functioning by hampering the oxidative metabolism typical of these organelles (19). In addition, APP may also hinder normal mitochondrial function. It has a mitochondrial targeting motif, but upon entering the organelle, it ends up being arrested amidst internalization, clogging the mitochondrial import infrastructure with its C-terminal end projected into the cytosol (an occurrence which is associated with diminished cytochrome oxidase activity) (65). All of this evidence seems to point to a secondary role of mitochondrial dysfunction in the etiology of AD, suggesting it as being caused by altered A β metabolism, in accordance with the A β cascade hypothesis.

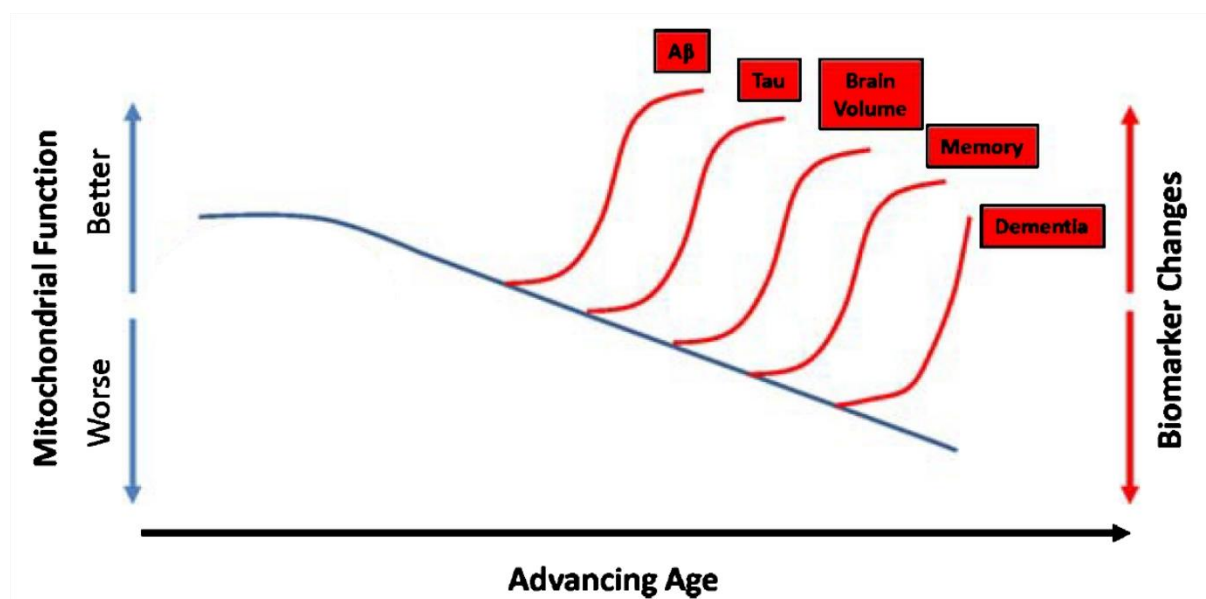


Figure I.14 Relation between mitochondrial dysfunction and other hallmarks of AD. With increasing age, features and hallmarks of AD tend to develop alongside a depreciation of mitochondrial function. Adapted from (65)

Yet, it may very well be the other way around, with mounting evidence pointing to the influence of altered energy metabolism on APP processing and A β homeostasis (incrementally, it may also affect a panoply of aspects associated with tau, like its production and clearance, among others). This theory (as reviewed in (65)) comprises multiple indications, regarding inhibition of cytochrome oxidase *in vitro* and mitochondria-derived ROS as favoring the amyloidogenic pathway of APP processing. In turn, the consequential accumulation of A β may be conducive to other functional changes and pathologies observed in AD patients. Other supporting evidence comes from experiments using cybrid human cell lines containing mitochondrial DNA originating from AD patients (67). Cybrid cell lines: eukaryotic cell lines produced by the fusion of a whole-cell with a cytoplasm. Cytoplasm is a cell which had its nucleus removed. In conjunction with other information regarding haploid mitochondrial genome variants that condone increased risk of developing of AD (68), this evidence suggests a genetic cause for mitochondrial dysfunction observable in patients with the disorder. Thus, in coherence with other AD hypotheses, there is a lack of consensus concerning the causal relationship between energy metabolism (that involves mitochondria) and aberrant protein aggregation (65).

A non-obvious demarcation of AD is the fact that the disease might be instigated by external pathogens (including those in the gastrointestinal tract microbiome). Several, lesser-known hypotheses link chronic and/or cumulative infections and pathogenic species

to AD onset, relating it to several viral, bacterial, protozoan and even fungal pathogens (32, 58). These may very well be capable of entering the CNS through multiple pathways, such as the blood-brain-barrier (BBB), as well as nerves connecting to the oral-nasal pathway (like the trigeminal nervous system) and to the enteric nervous system (ENS, like the vagus nerve) (32). On the other hand, they may secrete toxins into the systemic circulation, eventually affecting neurons in the brain, as is the case of virus and microbiota dysbiosis (defined as microbial imbalance or maladaptation) that can also influence systemic inflammation and dysregulate neurotransmitter production (32, 69).

According to the literature, some indications of the involvement of these pathogens in the etiology of AD are, for instance: 1) the increased abundance of nucleic acids originating from more than one human herpes virus serotype in AD patients (some of which correlate with severity of disease), 2) the indication that reinsertion of APP mRNA into the genome by reverse transcription may occur in the human brain (more so in the AD brain), leading to a high number of APP variants (which could be related to viral infection), 3) the possible relation between AD and periodontitis (32, 58), 4) the observation of discriminating increases (phylum Bacteroidetes) and decreases (phylum Firmicutes and genus *Bifidobacterium*) in specific bacterial populations existing in fecal samples of AD patients, 5) *in vivo* studies with microbiota manipulation of AD mouse models demonstrating a beneficial effect on plaque pathology, and 6) the potentially antimicrobial and antiviral nature of the A β peptide. All of these evidences are reviewed in (32).

Yet, some considerations still suggest that although these pathogens have a role in the course of the disease, they may not be the primary initiators of AD. Regarding viral infection (specifically herpes simplex virus type I, HSVI), unlike AD (that is more prone to develop in women), it seems to be gender independent (32). Additionally, the association between this viral infection and AD may be confounded by the fact that APOE genotype could possibly influence viral entry into the brain, one of many examples indicating that viral infection might be consequential of AD rather than causal (32).

Autophagy is an essential process in the maintenance of cell homeostasis that consists in the regulated degradation and subsequent recycling of cellular machinery such as organelles and proteins, as well as disposal of cellular waste (70-74). Microautophagy, chaperone-mediated autophagy, and macroautophagy are the three known autophagic mechanisms (70-74), the latter (in which cytoplasmic contents are engulfed into what are called autophagosomes) being both the major one (70, 74) and the most implicated in AD.

All three mechanisms direct cellular components for lysosomal degradation (74). Impaired autophagy is believed to be connected to neurodegeneration in several NDs, including AD and its abnormal protein aggregate hallmarks like accreted A β and tau (70, 73, 74). Furthermore, anomalies in the lysosomal degradation pathway pre-date the appearance of these hallmarks (in their macroscopic form, at least) in the AD brain (70). During maturation, autophagosomes translocate retrogradely toward the neuronal soma by the means kinesin-mediated transport along the microtubules (73), a process which is hindered in AD (74). This implicates a great neuronal dependence on intense transport and efficient proteostasis (73) and a possible involvement of aberrant tau protein (70), mainly due to the great distance between neuronal processes (where autophagosomes are formed) and the neuronal cell body (where lysosomes are situated) (18). This dependence is further exacerbated due to the fact that, like any post-mitotic cell, neurons are unable to dilute aberrant components through cell division (70). Thus, shortcomings in autophagosome maturation and trafficking ultimately lead to swelling in dystrophic and degenerating neurites in AD (18). Neurodegeneration-like symptoms of dysfunctional autophagy encompass constraints to autophagosome-lysosome fusion, amassment of the aforementioned proteins inside cells, and lysosomal lumen pH increase (lysosome enzymes require an acidic milieu to properly function) (74). Additionally, proteasomal degradation (in cooperation with autophagy (73)) also plays a part in protein recycling inside the cell, requiring the polyubiquitination of target proteins (a process that has been associated with multiple NDs, including AD, specifically when it is irregular) (74).

There are two pathways of A β elimination, but the one most predominant in the AD brain refers to the accretion of the peptide in autophagosomes and other autophagic vacuoles (which also contain the essential machinery and substrates for A β generation (70)) of dystrophic neurites, mostly in SPs, indicative of impaired autophagy and involvement of this process in A β metabolism (73, 74). In fact, there is evidence that suggests that not only is A β secreted from neurons through autophagy, but that the impairment of this process in AD mouse models leads to increased intracellular A β and consequent neurodegeneration and memory loss (75), indicating a role of malfunctioning autophagy in A β pathology and SP formation (70, 73, 74). In this line of thought, mammalian target of rapamycin (mTOR, an inhibitor of autophagy) signalling (particularly the mTORI complex, that controls autophagy (73)) and endocannabinoids (lipophilic activators of cannabinoid receptors) seem to be somehow linked to imbalanced autophagy and, therefore, to the pathogenesis of AD (74). Particularly, mTOR inhibition has been shown to reduce

extracellular plaque burden and ameliorate cognitive function in animal models, through increased autophagy and induced A β secretion (73). Conversely, reduced plaque burden has also been observed in autophagy-deficient AD mice models. Opposing results such as these may not be as controversial as it seems because different animal models are illustrative of different disease stages in which the autophagic process might be either pathological or protective (70). Therefore, changes in the mTOR pathway sustain the idea of autophagic impairment in AD (18). Forfeiture of basal levels of autophagy is also associated with accrual of ubiquitinated protein inclusions (70). Moreover, neuroinflammation (74) and oxidative stress (70) in AD may be related to impaired autophagy, being that the latter might be a defensive mechanism in the AD afflicted brain (74). NFT generation may also be related to hindered autophagy (70). Additionally, peripheral infection may also be relevant to altered autophagy since HSV1 has been shown to disturb the autophagic process, possibly by means of A β and NFT degradation impediment (70). Overall, the existing evidence validates the determinant involvement of dysregulated autophagy in AD and especially in A β pathology (73), either through impaired A β clearance, generalized insufficient autophagy, or favouring of the amyloidogenic pathway of APP processing in autophagic vacuoles (70).

The CNS and ENS are intrinsically linked in constant communication through several mechanisms like neuronal signaling (among others) mediated by, for example, the vagus nerve. This crosstalk between nervous systems denotes what is known as the brain-gut axis, to which can be added the interactions between gut microbiota and the barriers containing them in the gastrointestinal tract, therefore ultimately connecting microbiota to the CNS. This connection has been drawn in as a potential interferent in the pathogenesis of multiple NDs, including AD, as alterations in gut microbiota that enhance the permeability of the gut barrier and/or that lead to systemic inflammation (for instance, alterations that elicit peripheral immune cell activation and impact cytokine profile) may negatively affect the BBB with consequential features in the brain, stereotypical of NDs, like neuroinflammation and neurodegeneration (69). In fact, BBB damage has been observed in AD patients after death, as well as increased abundance of blood-derived components in the brain (69). As previously stated, another mechanism by which these microbes affect neurons in the brain is by producing numerous neuromodulators and neurotransmitters (32, 69).

Although through poorly understood mechanisms, gut microbiota definitively influences the formation of SPs (69). The potential antimicrobial function of A β (32), mostly in its aggregated form and by means of pore-forming structures (69), associates the peptide with the innate immune system. An eventual dysregulation of this activity or the presence of bacterial amyloids may lead to harmful effects in the CNS (which is congruent with malicious effects of dysregulation of other antimicrobial peptides), for instance through cross-seeding (and misfolding) of human A β and induction of microglial priming (69). Priming of the immune system by these exogenous bacterial amyloid proteins (by molecular mimicry) may augment the immune response to endogenous neuronal A β (69). The fact that APP expression in the ENS is a common event substantiates this hypothesis (69).

1.1.2 Parkinson's Disease

As mentioned earlier, the increasing aging of the global population is amounting to a greater burden of NDs in society, of which PD is not only an integral constituent but also considered the fastest growing neurological disorder (76). Albeit only first comprehensively described from a medical point of view in 1817 by James Parkinson (77), remnants of earlier descriptions that fit Parkinsonism have been found, that still today represent potential sources of neurological understanding of the disease (78). The main brain features of PD that allow for discriminative and unequivocal *post-mortem* diagnosis are marked progressive degeneration of dopaminergic neurons in the SNpc (among other brain areas) and the observation of intracellular protein aggregates (LBs and LNs), mostly composed of filamentous α -synuclein (6, 71).

Clinically, it is characterized not only by motor disturbances like postural instability (mainly in more advanced states), tremor while at rest, muscular rigidity, and (foremost) bradykinesia (which consists of slowness and difficulty in moving on demand), but also by non-motor traits covering sleep disorders (such as rapid eye movement sleep behaviour disorder and sleepiness during daytime), depression (and other mood disorders), hindered smell (also known as hyposmia), autonomic dysfunction (that increases with age, disease severity and surprisingly, enhanced doses of dopaminergic medication, comprehending for instance, constipation and urinary incontinence), anxiety, pain (possibly consequential of irregular nociceptive signal processing), and cognitive decline (6, 79-82). Non-motor traits, which may be the product of susceptibility in select CNS and autonomous nervous system neuron populations (6), can frequently prelude motor disturbances by more than 10 years

and due to this largely varied multitude of symptoms, clinical diagnosis of PD is often problematic (82).

PD is one of the most frequent types of ND (the most if specifying for movement disorder NDs (6, 71)), second only to AD (79, 80), with a diluted overall prevalence of about 0.3% that abruptly increases (as does its incidence (80)) with advancing age (82) (as an example, the prevalence in individuals over 80 years of age is over 3% of the respective population (79)) (81). Unlike some other neurological pathologies, the risk of PD has enlarged in high-income countries (mainly in Western society) (83) and one study investigating the possible inverse relation between prevalence and incidence of PD and socioeconomic status found an increase in its prevalence over a period of 20 years (84), which might be linked to improved healthcare and consequentially lengthier survival time of afflicted individuals (81). In fact, on a worldwide perspective, the number of people affected by PD has risen from about 2.5 million in 1990 to about 6.1 million in 2016, being that this approximate doubling of the afflicted population is expected to repeat itself in coming years (76). This may lead to over 12 million worldwide PD cases by 2050 (83). Additionally, in 2016 alone PD was responsible for a cumulative 3.2 million DALYs (76), evidence of the global scope of not only disease mortality, but also to the deterioration of quality of life inherent to PD.

Although still unknown, the etiology of PD is regarded as heterogeneous and multifactorial (83), with age being the most relevant risk factor (76, 79). The disorder affects people of all races (6), yet, incidence appears to fluctuate according not only to race but also ethnicity, environment, and genotype (81). Because race and geography are regularly associated it is difficult to ascertain how each affects the risk of developing PD (81). Overall, women seem to be somewhat spared as PD is a dimorphic disorder (83), considered to be two times more frequent in men than women (81, 82) (more precisely, 1.4 times more common in men, according to one study (76)). This may be explainable by the protective effect of female sex hormones or by gender-associated variances (occupational differences, for instance) in contact with environmental risk factors (76, 82).

Regarding environmental risk factors, some of the first evidence of external toxins influencing the development of PD came from the observation of irreparable parkinsonism in a chemist, caused by chronic exposure to 1-methyl-4-phenyl-1,2,3,6-tetrahydropyridine (MPTP) (85). It mainly acts by inhibiting complex I of the mitochondrial electron transport chain, which elucidated the involvement of mitochondrial dysfunction in the development of PD and since then, multiple compounds that lead to mitochondrial dysfunction have

been identified, namely solvents and insecticides (79). In fact, multiple pesticides have been linked to the onset of PD (and other NDs) regarding, for example, organophosphorus compounds (86), as well as organochlorine compounds (like β -Hexachlorocyclohexane [β -HCH], a by-product of insecticide production) (87). This might help explain the association between PD and occupational exposure to agricultural chemicals, not unlike those used in farming in rural communities (88).

PD can be classified as late or early-onset, depending on the age of incipience of parkinsonian symptoms. Early-onset PD comprises between 3% and 5% of all cases and can be further divided into juvenile-onset (before 21 years of age) and young-onset (amid 21 and 40 years of age) (82). There is a tendency to correlate (heritable) genetic causes of PD (5% to 10% of all PD cases (79, 81, 82)) with a younger age of onset. As reviewed in (82), multiple genes are implicated in this genetic predisposition to PD, such as those encoding: 1) parkin, 2) leucine-rich repeat kinase 2 (LRRK2), 3) α -synuclein, 4) PTEN (phosphatase and tensin homolog) induced putative kinase 1, 5) protein deglycase DJ1, 6) ubiquitin C-terminal hydrolase like 1, and 7) ATPase type 13A2 (ATP13A2). The respective gene nomenclature is: 1) *PARK2*, 2) *PARK8*, 3) *SNCA*, 4) *PINK1*, 5) *PARK7*, 6) *UCH-L1*, and 7) *ATP3A2* (82). Some of the pathogenic protein products of these PD-associated genes can lead to the development of neuronal pathologies much like the ones observed in the sporadic form of PD and there are plenty overlapping pathways between the latter and the genetically determined forms of PD (81). Heritable forms of PD may have different clinical features and hallmarks depending on mutation (79). Thus, it is clear that genotype, environment, and the cross-talk between them can modulate the risk of sporadic PD (81). Another type of disease classification takes into account the abovementioned clinical observations and separates those afflicted into two groups: tremor-dominant PD (characterized by relative paucity of other motor symptoms) and non-tremor-dominant PD (82).

Being a progressive disorder, PD benefits from multiple rating scales created along the years, none of which is completely satisfactory (89), but that cumulatively offer a wide range of instrumental features for the classification of PD severity and associated pathologies. Examples of such staging tools are the Braak staging system (90) (which takes into account the hallmarked brain lesions of PD, as well as their progression through the brain during the course of disease, but that may also require patient evaluation according to the respective and previously mentioned AD staging system, due to possible

confounding factors), the Hoehn and Yahr scale (91) (which regards clinical observations and is allegedly the most popular and easy system to evaluate disability of PD patients (89)), and the Unified Parkinson's Disease Rating Scale (UPDRS) (89).

All things considered, PD is an ever increasingly common ND associated with augmented morbidity and mortality, as well as pronounced effects in both quality of life and working capacity that, if left unchecked by the medical and research community, will certainly increase the already profound burden of PD on society (6, 82).

1.1.2.1 Hallmarks of PD

It is well understood that the major hallmarks of PD, α -synuclein deposition into LBs and LNs and early dopaminergic neurodegeneration in the SNpc (which is the main driving force of the development of motor symptoms in this disorder, also consequentially linked to dopaminergic neuron loss, as well as dopamine deficiency, in the striatum (6, 81, 82)) are clearly involved in the pathogenicity of PD (71, 79, 80, 82, 92). The abovementioned motor symptoms are clearly visible upon loss of about 80% of striatal terminals and 50% to 60% of nigral soma of dopaminergic neurons (6). Nonetheless, other hallmarks exist (each influencing their respective pathogenic pathways (81)) such as effects on other neurotransmitter systems, imbalanced protein degradation systems (proteasome dysfunction and autophagic alterations), mitochondrial dysfunction (along with consequential increase in ROS production and disruption of calcium homeostasis), other oxidative stress radices (altered iron metabolism and dopamine oxidation), synaptic dysfunction, and neuroinflammation (microgliosis and reactive astrogliosis, as well as elevated levels of pro-inflammatory cytokines) (79, 80), some of which are both interconnected and known to sensitize neurons to death (6).

As stated before, α -synuclein is the most abundant protein contained in LBs (81) and LNs, an observation transversal to both sporadic and genetically determined forms of PD (79, 92). The previously mentioned macromolecular forms of aggregated proteins (LBs and LNs) affect subcellular transport in neurons and are thus connected to synaptic dysfunction (79). The aggregation of α -synuclein's fibril and oligomeric assemblies (that can result in neurodegeneration) may be caused by mutations (like amino acid substitutions), but also by generalized overexpression of the protein (79, 92). Overexpression is known to inhibit neurotransmitter release (79), which might lead to synaptic dysfunction. The aggregated forms of this protein may also be post-translationally

modified by truncation, nitration, ubiquitination, and phosphorylation, which may modulate their toxicity (72, 92). Additionally, oxidative stress involving dopamine has been linked to increased α -synuclein aggregation, which might explain the extended vulnerability of dopaminergic neurons, although the same cannot be said for non-dopaminergic neurons perishing early in the course of disease (92). This (aggregative) proteinopathy can be further potentiated by heterozygous mutations in the lysosomal enzyme β -glucocerebrosidase, that thereby loses function, accumulates, and eventually stabilizes oligomeric intermediates of α -synuclein and meddles with lysosomal clearance, ultimately resulting in a 5-fold increased risk of developing PD for mutation bearing individuals (79). α -synuclein is caught up in a myriad of molecular mechanisms involved in PD, discussed further down, with some examples being ENS dysfunction and cell-to-cell transmission (80).

Although necessary for the unequivocal diagnosis of PD, LBs (and neuron loss in the SNpc) are not exclusive of this disorder, being observable in a plethora of other synucleopathies (6, 81, 92). Additionally, the role of these lesions in the course of disease is still very debatable, being hypothesized not only as pathological entities but also either as a neuronal protective measure or as a failed attempt of eliminating toxic proteins (6). Thus, α -synuclein (and its deposition) is considered a marker of PD, but with no unambiguously proven causal relation to the disease (92).

Degradation pathways in brain cells of PD afflicted patients appear hindered (including lysosomal defects (71) and being mostly observed in the SNpc), promoting the toxic accumulation of harmful proteins in neurons and representing yet another hallmark of the disease, which involves both autophagy and the ubiquitin-proteasome system (79, 80).

As stated before, neurons are especially dependent on autophagy for the maintenance of proteostasis due to their post-mitotic nature (70, 71). Abnormally conformed (and thus, aggregation-prone) α -synuclein clearance, such as in the case of its mutated forms, along with autophagy of defective mitochondria (known as mitophagy), in particular, are significantly dysfunctional in PD (72, 79). This may lead to their accumulation, which is especially preponderant in the case of mutated forms of α -synuclein that may inhibit their own elimination in the chaperone-mediated autophagic pathway (supposedly critical in limiting the protein's oligomerization (18)), potentiating their accrual in a vicious cycle-like fashion (72, 79). Diminished rates of chaperone-mediated autophagy may also prompt neuron death, mainly due to inadequate degradation of other proteins (18). Different PD-

associated mutations may affect different stages in the maturation process occurring in autophagy (71) and different α -synuclein mutations impart different levels of toxicity, but generally the latter may lead not only to cell death (due to increased aberrant protein accumulation and inhibition of cell survival proteins) but also to autophagosome accumulation and impaired dopamine release (72). Incrementally, the fact that PD-associated proteins (including, for instance, PINK1 and Parkin) are implicated in the control of mitophagy, corroborates the involvement of impaired degradative mechanisms in the development of disease (71, 72, 79). Likewise (and as reviewed in (80)), mutations in the genes encoding for α -synuclein and ubiquitin-proteasome system enzymes (including parkin and C-terminal hydrolase L1) have been linked to genetically determined forms of PD. Several other observations have been made in patients and animal models that connect abnormally expressed α -synuclein to both of the cellular component degradation (and quality control) mechanisms (71, 72, 80). α -synuclein may also inhibit other forms of autophagy by blocking autophagosome formation, increasing Golgi fragmentation, and hindering secretion (72). Thusly, malfunctioning clearance mechanisms are inherently connected to α -synuclein deposition and accumulation in PD (71).

Aside from the previously mentioned pathogenic role of β -glucocerebrosidase (the mutation of which being the most common genetic risk factor for PD (71)), lysosomal dysfunction in PD may also come from non-functioning ATP13A2 that is linked to several impairments in lysosomal acidification and proteolytic activity, to name a few (79). Moreover, diminished levels of this ATPase in neurons of sporadic PD patients have been reported, as reviewed in (79). Pathogenic processes associated with autophagy in PD include oxidative stress and mitochondrial dysfunction (72), which are discussed further down. Cumulatively, most findings suggest that autophagy in PD (as in many other diseases) can be disadvantageous when either insufficient or excessive (72).

As previously stated, mitochondrial dysfunction is hallmarked in the pathogenesis of PD, which is evidenced by the effect of some external toxins in inducing PD-like symptoms as a result of nigral dopaminergic cell loss (79). These toxins act by inhibiting complex I of the mitochondrial electron transport chain and include not only the abovementioned compound, MPTP (85), but also other molecular entities used in pesticidal control like rotenone and paraquat (79). Moreover, the impact of mitochondrial dysfunction in PD pathogenesis is shown by the fact that, in genetically determined forms of PD, most of the affected genes encode for effectors in mitochondrial function like the aforesaid PINK1 and

Parkin proteins (71, 72, 79), together with DJ-1 (which is engaged in oxidative stress responses) (79).

Nigral dopaminergic neurons and other central and peripheral neuron populations, that exhibit increased susceptibility to degeneration in PD, share several characteristics that may help to explain the observed mitochondrial dysfunction and enhanced vulnerability in the course of disease like highly branched axons, pacemaker activity, elevated oxidative stress, and calcium buffering stress (79). These cellular features (distinctively, the high energy-consuming pacemaker activity), together with the already high energy demand of the brain (about 20% of total body energy, while at rest), may difficult the energetic balance of these neuronal populations (79), which could be especially relevant in stressful conditions like the ones evidenced in the course of PD. The highly branched morphology of these neuron populations means their synapses are numerous and widespread, which together with high energy and calcium buffering resource demands may elicit their exhibited susceptibility to mitochondrial dysfunction and axonal transport deficiencies (79).

A by-product of normal mitochondrial function (namely due to mechanisms of the electron transfer chain) are ROS, whose production may reach levels of up to 1% of all oxygen used (79) and which, under these circumstances, is quite manageable for the respective cells. However, upon mitochondrial dysfunction (potentially coupled to inefficient antioxidant networks (10)), there is an enhanced surplus of these molecules, which has harmful effects in multiple cellular features (as reviewed in (79)). These comprehend dysregulation of signaling cascades (93) and oxidation events affecting lipids, proteins, and DNA (10, 94), as seen in nigral tissue of PD patients (95, 96). Thus, oxidative stress and mitochondrial dysfunction go hand in hand in PD, as shown by the observation of lower levels of complex I of the mitochondrial electron transport chain along with higher levels of oxidative markers, in the brains of sporadic PD patients (as reviewed in (79)). Note that increased production of ROS is also found in genetic PD cases (80). Other processes in which mitochondria are involved, like programmed cell death and inflammatory responses, may also affect the pathogenesis of PD (79). Aside from mitochondrial dysfunction, other procedures occurring in dopaminergic neurons that act as a root of oxidative stress are dopamine metabolism and neuroinflammation (80).

Another aspect transversal to all types of PD that is also related to oxidative stress is iron deposition in the SNpc (79, 80). Iron can mediate hydroxyl radical generation (the most

detrimental ROS) through what are called Fenton reactions, thereby significantly contributing to oxidative stress (79, 80). This is especially relevant when regarding nigral dopaminergic neurons as this tissue has the highest iron content in the brain, probably due to its binding to neuromelanin (also very abundant in this brain tissue) (79).

Concerning inflammation in the PD brain (that involves both arms of the immune system), the main players at hand are microglia and astrocytes (80), with the former being determinant in environmental danger interpretation, pivotal in prompting either beneficial or detrimental outcomes of a given immune response (79). The latter outcome is generally observed since, upon microglial detection of misfolded α -synuclein, an augmentation of ROS and proinflammatory cytokine-mediated neurotoxicity is elicited (79). On the other hand, inflammation itself may be able to potentiate α -synuclein aggregation and oxidation in afflicted neurons (80). Nigral susceptibility to inflammation may also be caused by a decreased astrocyte population in this tissue (which would regulate microglial-mediated inflammation) (79). Furthermore, reactivity of microglia to neuromelanin in the SNpc could be contributing to additional susceptibility to this pathogenic process (79). Thus, it is safe to assume neuroinflammation should be modulating PD progression, albeit as of yet with no determined causal relation to the disorder (79, 80).

1.1.2.2 Hypotheses for PD Pathology

The etiology of PD, be it familial or sporadic, is not yet definitively ascertained, as evidenced by the lack of efficient and all-encompassing therapeutic strategies for this highly multifaceted disease. Still, plenty postulated hypotheses exist that try to explain the causation of PD, most of which address the combined or discrete role of aging, oxidative stress, mitochondrial dysfunction, impaired calcium handling, inflammation, environmental toxins, hereditary factors, axonal transport, protein misfolding, and impaired clearance in this disorder (mainly regarding α -synuclein metabolism) (81, 97, 98). Two of the most relevant and vehemently discussed hypotheses are subsequently addressed in this section.

According to the aforementioned PD staging system suggested by Braak and colleagues (90), the disease progresses through susceptible brain regions in a stereotypical (and predictable) fashion of caudal-rostral spreading (99) (Figure 1.15), beginning in the lower brainstem, specifically in the dorsal motor nucleus of the vagus nerve (DMV), but also in the anterior olfactory structures. Based on this staging scheme and on evidence of the existence of a prolonged prodromal phase preceding sporadic PD onset, characterized by

hyposmia and vagal dysfunction (among other non-motor disease features), the Dual-Hit hypothesis was proposed (99), also known as the “ascending spread hypothesis” (79). Therein, a supposed neurotropic pathogen (suggestively viral) may enter the brain either through an anterograde nasal route or a retrograde gastric route (the latter being secondary to swallowing of nasal secretions in saliva), hence the name “dual hit” (99, 100). Other potential disease triggering insults include unconventional pathogens with prion-like properties and slow-acting neurotoxins, known to be taken up at synapses (99). These insults might trigger α -synuclein deposition in the ENS, which could spread “transsynaptically” to reach the CNS (101).

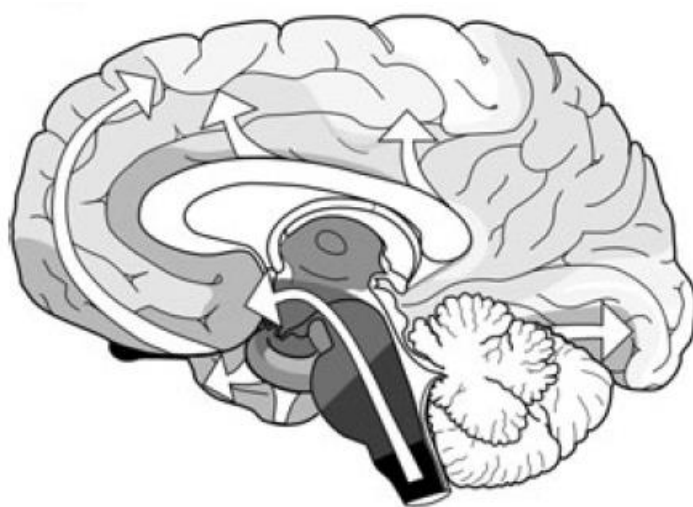


Figure 1.15 Caudal-rostral spreading of LB pathology, in accordance with Braak's hypothesis. Taken from (99). Arrows indicate the trajectory these lesions take upon entrance into the brain. Darker regions are affected earlier.

Enteric and olfactory dysfunction are hallmarked both early and late in the course of PD (102). In fact, the olfactory bulb and the ENS (particularly the plexus of the stomach), are affected by α -synuclein pathology early in the course of disease (82, 99) and olfactory testing has even been demonstrated to have some predictive power (regarding the presence of LBs at autopsy) (103), however modest and mostly unreliable (especially due to the fact that about 10% to 20% of PD patients do not show signs of impaired smell (99)). This early enrolment of the gastrointestinal tract in the development of PD may substantiate the idea that environmental factors are involved in the etiology and progression of the disease, especially regarding the local effect of pesticides on the ENS (101). Additionally, early ENS lesions are usually escorted by mild CNS lesions which, along with the involvement of the olfactory system, suggest that a shared pathogenic insult may likely induce the disease, starting at these more susceptible regions of the nervous

system (99). Moreover, dysphagia hallmarked in PD may be mostly due to vagal dysfunction (99) and constipation has been suggested as an omen to the development of the disease (100), further confirming the contribution of ENS alterations to the onset of disease. Furthermore, multiple changes in the gut microbiome may be connected to some clinical features of PD (82, 101, 102). Hypothetically, these microbiome alterations may prompt intestinal inflammation and eventual increased barrier permeabilization therein, consequently leading to oxidative stress in the ENS and triggering α -synuclein pathology that could propagate from there to the CNS (102).

In summary, the main argument for the role of these neuronal structures as access ports for possible insults into the nervous system is the fact that both are, through inhalation or ingestion, continuously exposed to the external environment where these potentially hostile entities may lie (99-101). However, this hypothesis (and the inherent staging system) does not explain the full spectrum of PD cases, therefore giving an enormous contribution to the understanding of the disease, but mostly being applicable only for a subset of afflicted individuals characterized by young-onset and long disease duration (102).

The prion hypothesis for the etiology of PD states that neuron-to-neuron-mediated α -synuclein pathology spreading may be involved in prompting the development of the disease process. It is proposed that this spreading is enacted due to a diversity of molecular structures of aggregated forms of this protein. Depending on their interaction with different protein assemblies, these may propagate through different brain regions which might explain why many PD patients do not follow the same disease course, as well as shedding some light upon the autonomic dysfunctions hallmarked therein. (97)

Thus, the main assumption of this hypothesis is that some α -synuclein assemblies act as prion-like proteins, seeding aggregation (Figure 1.16) and propagating through neuronal uptake and axonal transport, eventually being released to the extracellular space and being taken up by other neurons (97, 104). Astroglia and microglia might also be partially responsible for the spreading of these pathological aggregates (97).

Unfolded α -synuclein may take up many isoforms, some of which may demonstrate this prion like behavior of seeding and aggregation cycles.

As reviewed in the literature, there are various routes of neuron-to-neuron α -synuclein spreading, not all requiring direct cellular contact (although following known anatomical

pathways) and potentially requiring extended periods of time (97, 104). One hypothesized long-range spreading route may be the cerebral vasculature. Inside neurons, the pathogenic assemblies may also undergo long-distance axonal transport. The seeding process is engaged when the internalized pathogenic protein assemblies induce the aggregation of endogenous cytosolic α -synuclein in the receiving neuron by a process not yet determined (97). This would mean that α -synuclein can self-aggregate and translocate to unaffected cells, thereby continuing the process in a vicious cycle and thus extending the disease process (98).

Natively unfolded α -synuclein may attain many different conformational states, whose lateral and longitudinal interactions (of the exposed amino acid stretches) with other α -synuclein proteins dictate the ability to incorporate additional monomers into a proteinaceous assembly. These exposed residue stretches also influence the interaction with other molecular entities, which is determinant in the spreading pathways taken by pathological assemblies. Additionally, these may also impact other pathological aspects, such as seeding propensity and are at the basis of the notions of α -synuclein fibril “strains” (97).

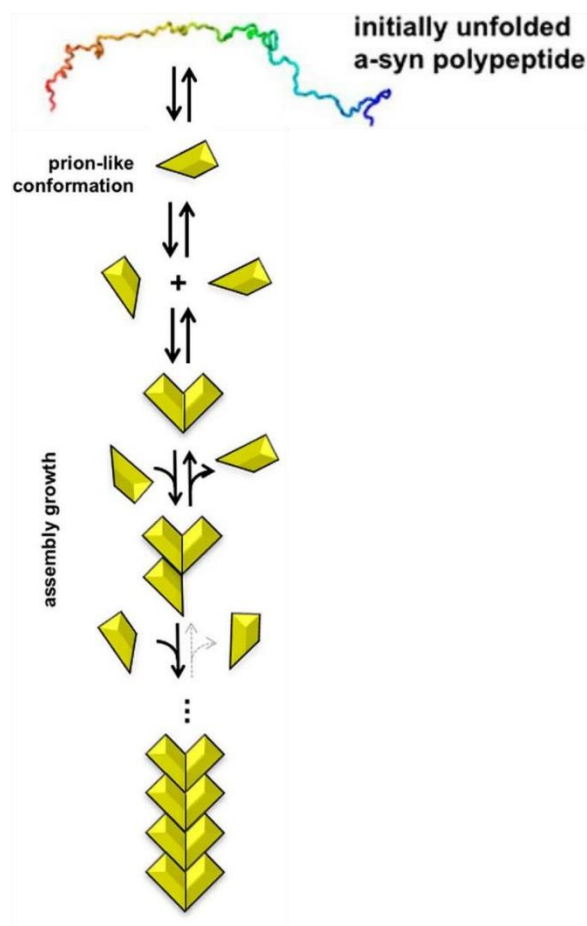


Figure I.16 Theoretical prion-like spreading of aggregation-prone α -synuclein. (97)

All in all, multiple factors may predispose cells to exhibit this prion-like behavior of α -synuclein like genetically determined (or age-related) hindered protein assembly clearance and its increased excretion/production (97, 98). In turn, the resulting formation of pathogenic oligomers and aggregates may induce neurodegeneration of the afflicted neurons (98), namely nigral dopaminergic neurons (104), which eventually leads to the onset of disease and its hallmark clinical symptoms. This hypothesis fits well with Braak's dual-hit hypothesis as it is conceivable that the prion-like model of α -synuclein spreading may occur through both enteric and olfactory routes (97, 104).

I.2 Biomarker Discovery in Neurodegenerative Diseases

According to the Food and Drug Administration (FDA) and the National Institutes of Health (NIH), a biomarker is regarded "as a defined characteristic that is measured as an indicator of normal biological processes, pathogenic processes, or responses to an exposure or intervention, including therapeutic interventions" in the Biomarkers, EndpointS and other Tools glossary (<https://www.ncbi.nlm.nih.gov/books/NBK326791/>)

and, according to the European Medicines Agency (EMA) (<https://www.ema.europa.eu/en/glossary/biomarker>), as “a biological molecule found in blood, other body fluids, or tissues that can be used to follow body processes and diseases in humans and animals”, two fairly congruent and comprehensive notions. Many sub-definitions exist (105) (and <https://www.ncbi.nlm.nih.gov/books/NBK326791/>), but in the context of NDs discussed in the present document, the most relevant appear to be those empowered by diagnostic, prognostic, predictive, and monitoring capabilities. Nonetheless, in the scope of proteomics research applied to neuroscience, much restraint is taken up by researchers regarding the use of this term, mostly because it diverges significantly from the observation of differentially expressed proteins somehow connected to a given disease, in a limited sample set (106). Thus, a more conservative definition for these still unvalidated observations is the notion of “biomarker candidate” (106).

As of today, few FDA-approved therapeutic opportunities exist for dealing with AD and PD and those that do exist are the result of discoveries made in the past century (107). This is the outcome of what is figuratively known as the “Valley of Death”, a vacuum existing between basic science discoveries and their eventual clinical application, which leads to mass failure of clinical trials (107). Although there may be many causative agents here at play, one possible solution might be the use of biomarkers as surrogate endpoints in these clinical trials, something that has had noticeable success in cancer trials (107). These would, in fact, be an improvement to the classically used endpoints, being a more cost-effective and uncomplicated measurement alternative, with the advent of also having higher precision (108). Biomarker-based diagnostics may also prove helpful in clinical trials as patient selection criteria (109).

To what concerns ND proteomic research, it would definitively be advantageous to have a broad spectrum of biomarkers in blood and other biofluids (110), as this would comply with criteria defined at a series of National Institute on Aging and Alzheimer Association consensus conferences (111). In summary, and as reviewed in (24), such biomarkers would be non- or minimally invasive, easy to collect and process, low-cost, neuropathologically validated (and therefore essential to the neuropathology of disease), and discernible from what is observed in other NDs, all the while preferably being detected ahead of the onset of symptoms and not being affected by treatments to said symptoms.

1.2.1 Established and Potential AD Biomarkers

Currently, clinically used biomarkers for the assessment of AD progression comprise measuring cerebrospinal fluid (CSF) A β and (total and hyperphosphorylated) tau levels, visualization of their fibrillar forms through positron emission tomography (PET), and deducing hippocampal atrophy by magnetic resonance imaging (MRI) (65, 112). Phosphorylated tau levels in CSF are, as of today, the most specific biomarker of AD (113). PET imaging for the ascertainment of tau pathology may allow for pathologically-based clinical staging of AD, but aside from the obvious invasiveness of CSF collection (114), some of these methods may be inadequately used as they are not validated by assessment of neuropathology at autopsy (107). Some of those, which are autopsy-validated, are used to validate biomarker candidates, but this may prove cumbersome due to the already limited sensitivity and specificity of the former (107). Furthermore, AD may not be limited to the brain, as different APP isoforms populate other tissues and A β can be found in multiple peripheral tissues (including, but not limited to, blood vessels (115)), with some indications existing that suggest other parameters, like energy metabolism, could predate these canonical biomarkers regarding not only the disease, but also brain ageing (65). Several other established CSF, blood and imaging AD biomarkers exist, as depicted in an illustrative poster in (113).

Several candidate AD biomarkers have been discovered through extensive research, with varying degrees of potential clinical value. These include, for instance: 1) plasma complement factor H (CFH) and α -2-macroglobulin, using mass spectrometry (MS) and semi-quantitative immunoblotting (116), 2) plasma gelsolin, using MS and western blot analysis (117), 3) a combination of plasma clusterin, factor I, and terminal complement complex, using a novel multiplex assay (118), as well as plasma clusterin alone (along with a multitude of other proteins), using MS and immunodetection (119), and 4) truncated tau (Tau-A and Tau-C) from serum, using enzyme-linked immunosorbent assay (ELISA) (120). Other potential plasma biomarkers involve different length A β peptides (and their ratio), tau (and its phosphorylated form), BACE1, and neurofilament light (NFL) (109). NFL has also been found relevant in serum and CSF samples, being very promising as a potential AD biomarker (113). Additionally, serum proteinaceous hormones may prove helpful in differential diagnosis of AD (121).

These examples are only the tip of the iceberg, with several others being reviewed, specifically regarding hypothesis-free discovery methods (112), potential biomarkers in serum (122), and potential biomarkers in plasma (113).

1.2.2 Established and Potential PD Biomarkers

Concerning PD, neuroimaging techniques combining the use of specific ligands associated with dopamine (including, for instance, dopamine transporter [DAT] protein) and single-photon emission computed tomography (SPECT), the combination of which is referred to from here on out as DAT-SPECT, have allowed for the measurement of function at presynaptic terminals and post-synaptic binding sites, which may have some prognostic value (123). This is used in the clinical, as well as research settings, in order to improve the accuracy of PD diagnosis, with several radioligands (114). Still, this imaging tool has some limitations like the possible underestimation of terminal density, attributable to compensatory responses (124, 125), and unknown accuracy (with varying reports of sensitivity and specificity), making clinical diagnosis persist as the gold standard (123). Furthermore, although both PET and SPECT are widely available (with DAT-SPECT having some utility in early PD diagnosis, as well as in its differentiation from other non-degenerative parkinsonian diseases), DAT imaging remains unobtainable in many countries, with DAT-SPECT still being very costly but also inferior to movement disorder specialists regarding the establishment of diagnosis (123). Another alternative is the use of ultra-high field MRI which is able to detect distinctive PD-related changes in SNpc morphology (126).

Internationally standardized criteria for PD diagnosis are still lacking, thus, efforts are being made to discover biomarkers early in the course of pathology, preferably in its prodromal or pre-clinical phase (114). Such efforts to yield clinically significant molecular biomarkers of PD are well represented in the “S4” multicenter observational study, short for “The Systemic Synuclein Sampling Study”, in which the main aim is to ascertain the sensitivity and specificity of a particular immunohistochemical staining, for pathological α -synuclein, in a myriad of samples (including CSF, blood, and saliva, but also biopsies from skin, colonic submucosa, and submandibular gland tissue) originating from both a broad spectrum of PD afflicted subjects (determined by DAT-SPECT), as well as healthy individuals (127). Collection of some of these sample types frequently resulted in mild adverse effects, but none were reported either for saliva or blood collection (125). Other relevant peripheral tissues, deserving of investigation for α -synuclein deposition, comprehend the esophagus,

the stomach, and the olfactory bulb (128). Exploring these tissues makes sense, taking into consideration knowledge that altered α -synuclein metabolism (central to PD pathogenesis) may manifest not only in the CNS, but also in the periphery, being that this protein may pass through the BBB (114). Additionally, examining the fecal microbiome of PD stricken individuals might also be interesting and of potential diagnostic value (114).

As previously stated for biomarkers of NDs, idyllic biomarkers for PD should constitute irregular observations (early in the course of the disease and preferably before the onset of symptoms), correspond to disease severity, and be unaffected by treatments (129). Furthermore, regarding the inherent criteria for an ideal biomarker, blood-based biomarkers would also ensure cost-effectiveness and non-invasiveness in clinical application (130). Concerning these considerations, some potential biomarkers have been discovered, with some examples following (mostly blood-based).

Immunoglobulin G3 (IgG3) in serum from PD patients has been found to be significantly elevated, compared to control subjects, as determined by peptoid ELISA, having modest accuracy in identifying the disease (129). Reduced levels of Mannan-binding lectin and increased levels of tumor necrosis factor- α (TNF- α) have been found in serum from PD patients, as determined by ELISA and a chemiluminescence immunoassay, respectively (131). Yet, there was no statistically significant correlation between these potential serum inflammatory biomarkers and clinical neurological and psychological status of the assessed patients. Blood-borne autoantibodies may also serve as potential biomarkers for NDs, PD in particular, because it is plausible that the stereotypical dopaminergic cell loss found in this disorder produces cell-type-specific debris that may enter the peripheral circulation, eliciting activation of the immune system through the generation of these disease-specific autoantibodies (130). Several other proteins have been marked as relevant in the search for PD biomarkers such as haptoglobin, transthyretin, apolipoprotein A1, ApoE, CFH, and a complement c3 fragment (132), but also DJ1 (114). A combination of phosphorylated and total α -synuclein concentrations may assist in differentiating between PD and more atypical parkinsonian disorders (133). Plasma glycopeptides have also been investigated, through MS, in this line of research (134). Plenty other promising potential biomarkers have been investigated, as reviewed in the literature (114, 135).

1.2.3 Blood as a Potential Biomarker Source: Pros, Cons, and Fractionation

The following section mainly regards blood (and its fractions) as a source of potential biomarkers in the context of MS-based research. Also, most of the contents herein were written as an integral part of a published book chapter by Miguel Rosado et al (136).

The identification of biomarkers capable of being used for diagnosis, prognosis, risk stratification, and therapeutic monitoring is still one of the major aims of clinical research. Among the several clinical biospecimens already used for biomarker discovery, special attention has been given to blood-derived samples mainly due to the non-invasive and simple blood collection methods that allow translation into routine clinical practice (137-139). However, despite technical developments in the analytical technologies used for biomarker discovery, in particular, the progress in sensitivity and specificity of analyte quantification by MS (140), applying these methods to biomarker discovery in blood samples has been shown to be technically very challenging (141).

Whole blood is almost never directly used for biomarker discovery. Instead, it is first fractionated into its different components, namely, plasma (or serum), buffy coat containing white blood cells and platelets, and red blood cells. The analysis is then typically performed on one of these fractions (Figure 1.17) (139, 142, 143). Serum, plasma, and buffy-coat, in particular, peripheral blood mononuclear cells (PBMCs), are the blood fractions that are most commonly used in biomarker discovery studies (144). However, the number of publications in this field has recently reached a plateau likely reflecting the technical difficulties in biomarker characterization resulting in reduced translation of these analyses into clinical applications (145).

The direct search of biomarkers in blood-fractions is limited by some characteristics of the blood-based samples, such as: (i) the high diversity of biomolecules and extremely high range of concentrations (up to 12 orders of magnitude); (ii) the large inter- and intra-individual variability of biomarkers in the study population; and (iii) the weak characterization of the human subjects that have been recruited in the discovery phase (141, 143, 146-148). For example, the large concentration range of different proteins in blood samples precludes a deep proteome coverage, with blood-based screenings being typically limited to identifying the few hundred most abundant species. Among other things, this can fail in capturing some important blood biomarkers that happen to be present in low abundance. To overcome this, two strategies have been applied: first, the

depletion of the highly abundant components—in particular proteins—and second, extensive sample fractionation (145, 149, 150).

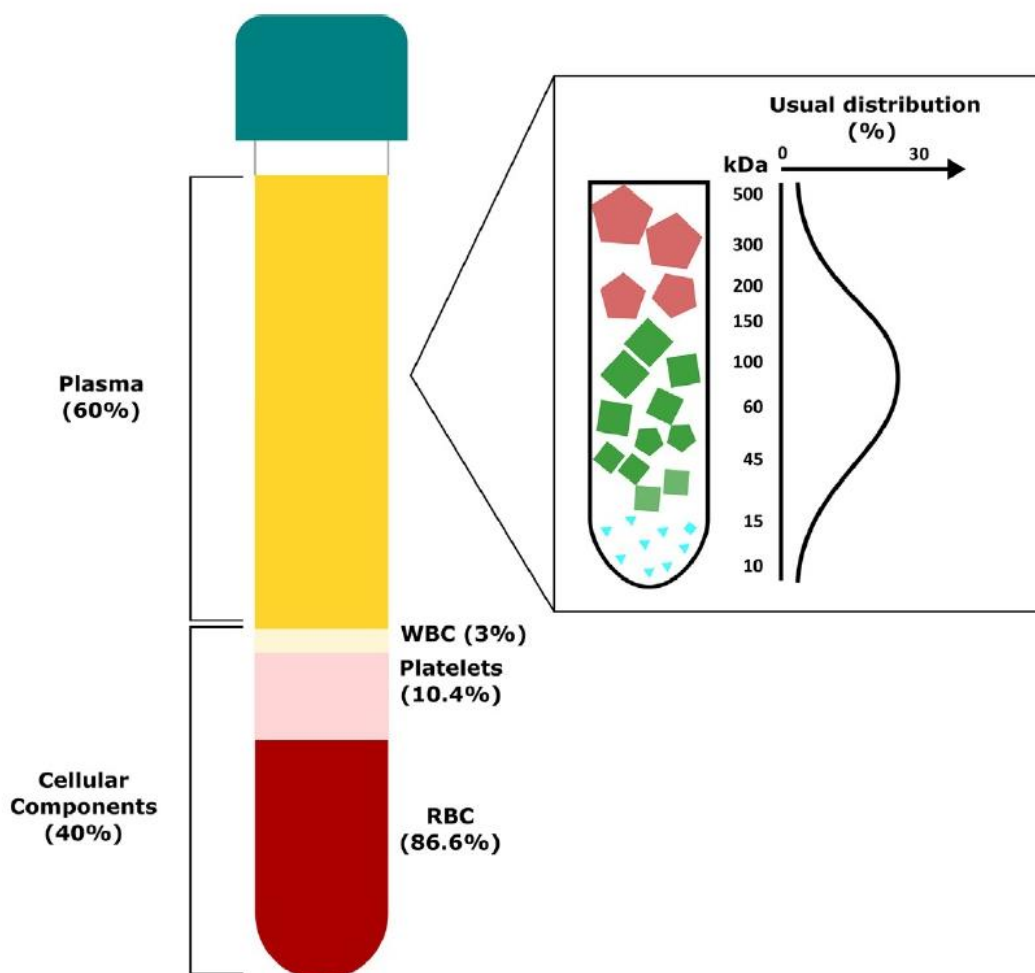


Figure 1.17 General overview of whole blood composition. The blood can be divided into two main fractions: an extracellular fluid called plasma that constitutes near 60% of the blood, and a cellular fraction (40% of the blood content) which can be divided into white and red blood cells (WBC and RBC, respectively) and platelets. Moreover, the plasma can be further fractionated according to the molecular size of the components (as indicated in the depicted rectangles). (136)

Because serum and plasma contain a very wide range of protein concentrations and molecular weights (151, 152), it is of pivotal importance to reduce the sample analyte complexity by selecting different fractions for subsequent MS analysis. If the protein of interest is present at low concentrations, this can be achieved by removing the highly abundant species whose presence may hinder quantification of the rarer target protein (153-155).

Several size-dependent separation methods of plasma/serum proteins exist, but in the context of the present work, the most relevant (and further discussed) is centrifugal ultrafiltration (CUF).

CUF is a high-throughput fractionation method (154) used to separate components in a liquid mixture (such as a biological fluid) based on the principle of size exclusion. It typically consists of two compartments separated by a semi-permeable membrane with a nominal molecular weight cut-off (NMWC) of a given mass expressed in the range of kDa (156, 157). When subjected to centrifugal force, the components with molecular weight under the NMWC limit pass through the membrane (the filtrate), while the remaining constituents are retained (the retentate) (157).

Although sometimes time-consuming (156), CUF is considered as a highly reproducible (156, 158), cost-effective (154, 156) and non-laborious (154, 156, 159) method compatible with automation (158).

The method's sensitivity and specificity depend on the selectivity of the semi-permeable membrane, but this parameter is still a matter of discussion in recent literature (153, 154, 159, 160). Consequently, there is a lack of consensus in the scientific community on the enrichment capabilities of CUF especially for the low molecular weight fraction (LMWF) of samples (153, 154, 156, 158, 159). This is likely due to two main characteristics of these devices: (i) the heterogeneity of pore sizes in the semi-permeable membranes (the NMWC is only an average of the pore size distribution) (156); and (ii) the fact that highly proteinaceous solutions (including blood-based samples) can clog the membranes, resulting in a phenomenon known as "membrane fouling" (156).

To overcome these limitations, some authors advise the implementation of the "1.5-2 rule" during the selection of the NMWC; i.e., the NMWC should be at least 1.5 times smaller than the molecular weight of the proteins to be retained (157). Also, adopting the use of devices with a vertical or angular membrane configuration and changing from direct flow filtration to tangential flow filtration decreases membrane fouling thereby enhancing method reproducibility (156, 157). Moreover, some authors suggest that the use of high sample volume (153), acetonitrile in sample buffer (153, 157), or even adding a previous solvent extraction step (158) can improve results. The two latter interventions are thought to act through the disruption of protein-protein interactions between small proteins/peptides and abundant high molecular weight protein carriers, such as albumin

(157). However, the use of organic solvents is not universally accepted, since under these conditions the proteins are no longer maintained in their native form (159).

Additionally, some authors also recommend pre-rinsing of the devices with buffer or deionized water in order to eliminate trace amounts of the preservatives used to protect the membrane, such as glycerine or sodium azide, that could interfere with sample analysis (157).

1.3 Bottom-Up Proteomics Approaches

Proteomic approaches have proven to be remarkably useful in the search for ND biomarkers (AD and PD potential biomarkers being at the center of most proteomics research efforts (161)), with the advent of technologies spanning sensitivities for a wide range of analyte abundances (originating from several technological breakthroughs and careful experimental design) and giving rise to never before seen accuracy and throughput (24). However, those referring to standard immunochemical methods still fall short of providing enough sensitivity to reliably quantify many CNS-derived, blood-borne molecules (109), mostly due to their dependence on the use of antibodies, which can be difficult to test in human biofluids (possibly cross-reacting with proteins structurally similar to their targets) and whose production is a process inherently plagued by large batch-to-batch variation (24). Thus, MS (particularly regarding bottom-up proteomics, the most widespread proteomics workflow (162)) plays a central role in these exploratory efforts, with MS-based proteomics being the leading technology for a high-throughput qualitative and quantitative analysis of protein mixtures (161).

The generic aim of MS is to produce ions from a given sample and to separate them according to their mass-to-charge ratio (m/z), subsequently retrieving quantitative and qualitative information about the respective sample analytes (163). The overall workflow of all bottom-up proteomics experiments is similar, beginning with protein extraction from the target sample, progressing to digestion with a sequence-specific enzyme (predominantly trypsin) and subsequent chromatographic separation, eventual ionization, for instance, by electrospray ionization (ESI), and finalizing by being inserted into the mass spectrometer (162). There, the resulting peptide ions can be fragmented, the most used method being collision-induced dissociation (CID) (161), thereby generating MS/MS spectra, which (through the use of MS-specific computational pipelines) allow for peptide identification and quantification (162).

Reducing sample complexity by peptide separation before MS analysis may prove beneficial to protein identification (164). Upon obtaining a peptide sequence, results can be checked for false positives with randomized or reversed sequence databases, both of which have proven to have comparable utility to this end (165). Sample fractionation and result validation (by alternative techniques) before and after MS analysis, respectively, are also generally considered a part of the aforementioned workflow and instrument parameters such as mass accuracy, resolving power, sensitivity, and throughput should be vehemently considered beforehand (161).

1.3.1 The Mass Spectrometer: Functioning and General Layout

The general workflow has already been described but the intricacies of the actual mass spectrometer have not, as will be done in this section. As previously stated, upon elution with a solvent gradient from the chromatographic column (in the case of RPLC), analytes are ionized (24). From the ionization source they follow directly into a mass analyzer, of which quadrupole and time of flight (TOF) mass analyzers (that can be coupled) will be described, and proceed to a detector, all under high vacuum conditions (163), as dictated by the general layout of a generic mass spectrometer (Figure 1.18).

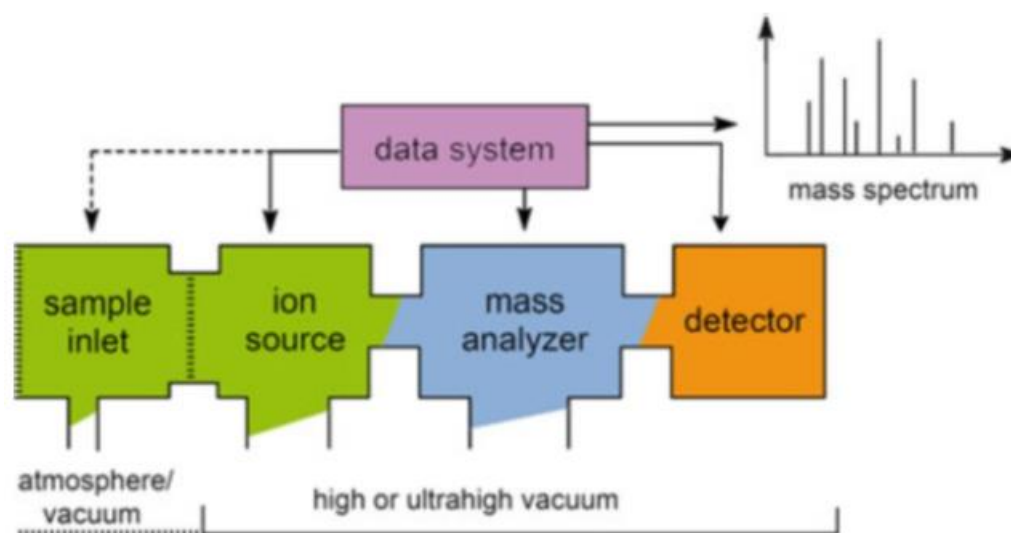


Figure 1.18 Generic layout of a mass spectrometer. Samples pass from one end of the mass spectrometer to the other, after insertion in the equipment, mostly being in a vacuum environment with the exception of when the mass analyzer is used as a collision cell. All steps are controlled and calibrated by the data system. Adapted from (163).

1.3.1.1 High-Performance Liquid Chromatography

High performance liquid chromatography (HPLC), referred to here as a high pressure version of RPLC, is used in the context of MS to retain peptides (in accordance to their

specific hydrophobic interactions with the material lining the inner-most part of the column, i.e. packing material – generally C18), which are eluted by a polar mobile phase (such as acetonitrile or a mix of water and methanol), thereby chromatographically separating these analytes (166). It is easily coupled to MS and its solvents are compatible with the subsequent proteomics workflow, making it a pivotal peptide separation tool (167). Additionally, this procedure achieves in-line desalting (essential for ESI), generates higher analyte fluxes into the ion source (resulting in increased sensitivity), and facilitates automation (168).

1.3.1.2 Electrospray Ionization

ESI is an ionization method used in MS in which analytes (in this case peptides) contained in an acidic, aqueous solution are sprayed (at atmospheric pressure) through a small diameter needle (in the micrometer range, for regular ESI), subject to a high positive voltage, thereby producing what is called a Taylor cone while sputtering electrically charged, peptide-ion containing droplets (163, 168). The peptides are ionized by protons in the acidic environment of the elution solution, giving the droplets a positive charge and directing them to the following compartment (the mass analyzer), by being repelled from the highly positively charged needle (163, 168). These droplets are repetitively disintegrated and evaporated during this trajectory (due to the proximity of positive charges in the solution and sometimes favored by a counter-flow of neutral gas, such as nitrogen) (163, 168). Upon reaching a “critical” size, the sheer number of closely enclosed positive charges desorbs the peptide ions from the droplets into the gas-phase (168), through what is known as a Coulomb explosion (Figure 1.19). From then on out, the trajectory of the peptide ions is manipulated by appropriate electric fields in the mass analyzer (168).

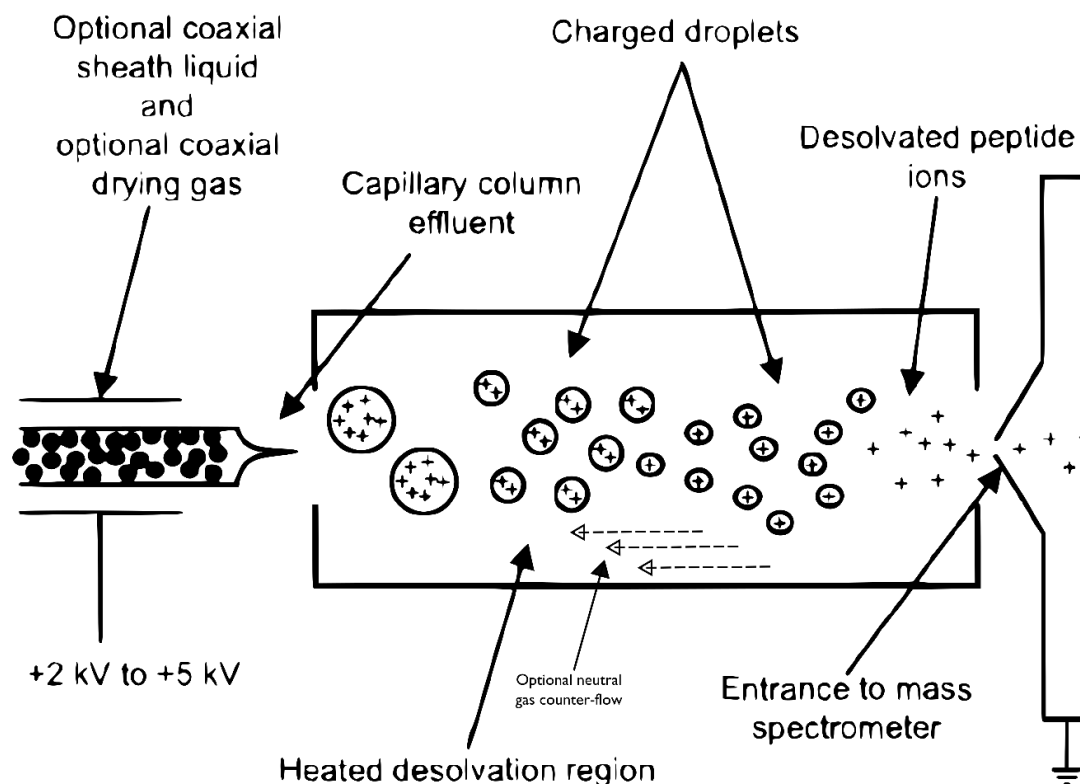


Figure I.19 Overview of ESI coupled to a mass spectrometer. Adapted from (168).

This is considered as a “soft” ionization method because it does not frequently promote stochastic analyte fragmentation (167, 168). However, it is regularly coupled not only to liquid chromatography but also to quadrupole mass analyzers, allowing for efficient peptide sequencing through the generation of MS/MS spectra, resulting from analyte fragmentation (167).

I.3.1.3 Quadrupole Time-of-Flight Mass Analyzer

Quadrupole mass analyzers (also known as quadrupole mass filters) are made up of four rods organized in sets of two (168). The rods in each set are electrically connected and through coordinated application of voltages from different types of current in each set, it is possible to manipulate (through oscillatory movement) the trajectory of ions contained in the mass analyzer, being that only those with a select m/z have a stable trajectory, hence passing through the apparatus and on to the next compartment of the mass spectrometer (168).

CID normally occurs by the opposite directional movement of a beam containing sample ions and a neutral gas stream (like helium, nitrogen, or argon, at a considerably higher pressure than the surrounding vacuum environment), in a collision cell (163, 168), that can be a quadrupole. The resultants from the implicated collisions are generally termed

analyte can be obtained (163). In tandem mass spectrometers, these collision cells are located between two mass analyzers the first of which selects “precursor ions” for fragmentation, and the second of which analyzes for resulting “fragment ions” (168).

In the TOF mass analyzers (Figure 1.20), ions are given a certain amount of kinetic energy and pass through a field-free region of known length until reaching a detector (163, 168). The velocity at which each ion transverses the field-free region is inversely proportional to its m/z , being that (in general) lighter ones will travel faster than heavier ones (163, 168). Therefore, by measuring this “flight time” it is possible to determine the m/z of a given ion (168). However, for this procedure to properly work, ions must be accelerated at roughly the same time (163) and with the same amount of kinetic energy (168). Thus, in order to circumvent this issue (and minimize its effects on mass resolution), TOF instruments can be coupled to an ion reflector (168).

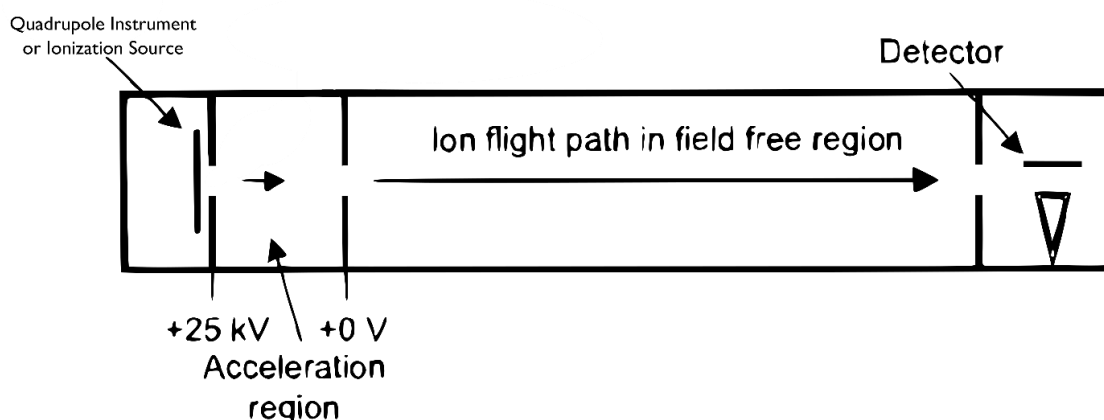


Figure 1.20 Illustrative representation of a linear TOF instrument. Adapted from (168). After receiving the designated kinetic energy, peptide ions fly through the field free zone, and time of flight until they the detector is used to calculate the m/z .

1.3.2 Sample Preparation for Mass Spectrometry

This part of the proteomics workflow is subject to a lot of variation across laboratories, but some procedures can be regarded as essential when dealing with protein digests prepared for subsequent MS analysis.

During the workflow, samples must be frequently dried. Thus, with the purpose of evading protein modification, aggregation, and precipitation, sample solubilization should be done using chaotropic agents (like urea), detergents (like Triton X-100 and sodium dodecyl sulphate [SDS]), reducing agents (like dithiothreitol [DTT] and triscarboxyethylphosphine [TCEP]), and protease inhibitors, mixed in sample buffer (167). Special attention should

also be given to some of these reagents as they could interfere with protein digestion and separation, or even with MS-analysis itself, and thus need to be removed at the proper time points (167). Microscale solid-phase extraction may also be performed using C18 filled tips, so as to desalt, concentrate, and fractionate peptide (and proteins) from samples (167). One- or two-dimensional electrophoretic separation as a pre-fractioning procedure is also common practice (167).

1.3.3 Tandem Mass Spectrometry

In tandem MS, two mass analyses are elaborated during the course of a single experiment (168). Briefly, tandem mass spectrometers make use of the ion separation occurring in mass analyzers to isolate those with particular m/z values and subsequently fragment them for further analysis, obtaining structural information about the original, non-fragmented, ion (and, thereby, about the assayed analyte) (168). In bottom-up proteomics this information refers to an amino acid sequence (168).

1.3.4 Data Acquisition Methods: DDA and DIA

Data acquisition in MS regards the way ions (and their fragments) are selected in mass analyzers during tandem MS. The selection process in the first mass analyzer is commonly referred to as the MS1 level and the selection process in the second mass analyzer (after fragmentation in the collision cell) is commonly referred to as the MS2 level. There are multiple variations and workflows, but most can be generalized either as data-dependent acquisition (DDA) methods or data-independent acquisition (DIA) methods, which are further discussed below.

Regarding DDA methods (also sometimes named information-dependent acquisition (164)), precursor ions are selected at the MS1 level spanning the full range of m/z (resulting in mass spectra of all ions co-eluting at a given time-point) and, at the MS2 level, fragmentation spectra are acquired for as many precursor ions as possible, during the predetermined cycle time (usually about 1 second) (162). Conversely, a limited number of precursor ions may be selected for fragmentation (typically the most intense) and subsequent analysis at the MS2 level (164). This acquisition process is alternated between MS1 and MS2, with peptide quantification information being achieved at the MS1 level (through precursor ion peak signal integration) and peptide identity being attained at the MS2 level (162). Additionally, peptide quantification can also be obtained at the MS2 level, by using fragment ion intensities in a similar fashion to quantification at the MS1 level (162).

Absolute protein quantification can be estimated from the peak volumes of all peptides identified as belonging to that same protein (162). A caveat of this technique is that it may be affected by samples with a very broad dynamic range of analyte concentrations, as it is biased to largely abundant ones (namely proteins) (169).

As opposed to DDA, in DIA methods, selection of precursor ions for fragmentation and fragment ion spectra acquisition is tiled in determined m/z ranges (within the most frequent peptide mass range), therefore eventually spanning the entire range and thus being untargeted (24, 162, 164). To this end, each tiled scan is repeated at all cycles, allowing for improved sensitivity, higher throughput, and shorter chromatographic elution gradients, resulting in highly complexed spectra that can be deconvoluted after acquisition (24, 162). Presently these approaches can span a dynamic range with 4 to 5 orders of magnitude but still prove superior to DDA regarding the elimination of issues with missing values, as it allows for the entire range of potential precursor ions to be impeccably analyzed at the MS2 level (162). As in DDA, quantitative information comes from the MS1 level, and peptide identification from the MS2 level, the latter making use of a DDA-obtained “library”, containing peptide query parameters (like retention time [RT], precursor ion m/z , and MS/MS spectra), to assist in the MS2 spectra deconvolution process (164).

1.3.4.1 Sequential Window Acquisition of All Theoretical Mass Spectra

In 2012, a revolutionary type of DIA method was developed, the Sequential Window Acquisition of All Theoretical Mass Spectra (SWATH) method (Figure 1.21) (170). Therein, upon a single sample injection, fragment ion spectra of all precursor ions inside a defined precursor RT and m/z range are produced and saved as complex fragment ion maps. Using the latter, a targeted data extraction strategy is performed to acquire quantitative information of particular peptides, in accordance with information previously established in spectral libraries (in the form of peptide query parameters). The recording of consecutive fragment ion spectra from all precursor ions is accomplished using precursor isolation windows (to select precursor ions for fragmentation in “swaths”) and makes use of both quadrupole and TOF mass analyzers. These swaths typically range 25 Daltons (Da), with 32 of these “windows” spanning across a total range between 400 m/z and 1200 m/z in just about 3.2 seconds (well enough to reconstruct a 30-second-long chromatographic peak for each analyte).

Ever since, variations to this method have been created that allow for the various precursor isolation windows, across a single cycle, to have variable lengths (171), effectively reducing the number of simultaneously selected precursor ions in densely populated mass ranges (164).

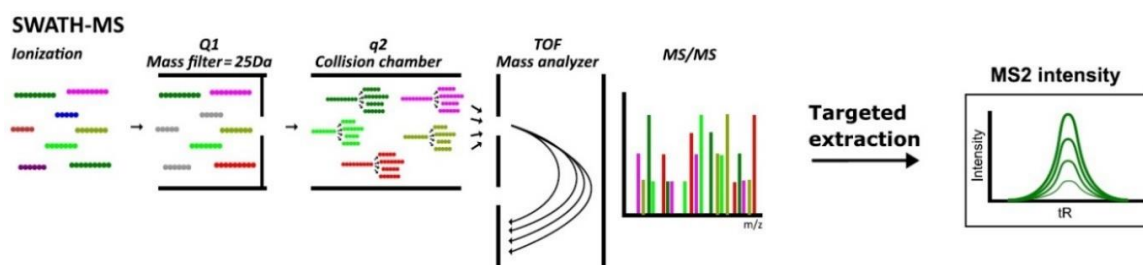


Figure 1.21 SWATH data acquisition method for MS/MS spectra. (164) In SWATH-MS, after ionization and MSI scanning, peptide ions are fragmented in the MS2 level for subsequent detection after passing through the TOF instrument. MSI and MS2 values are then used to determine identity and quantification, respectively.

2. Objectives

As NDs threaten to plague the worldwide ageing population, the search for biomarkers of these brain-related diseases will intensify, with an ever increasing need to meet the demands not only for new therapeutic opportunities, but also for new methods of earlier and more sensitive diagnosis, that encompass heterogenous diseases such as these.

Protein biomarkers would be ideal, as hinted by the nature of many of these disorders in which aggregation, abnormal processing, and even hindered clearance of proteins is evidently connected to the respective pathologies.

Although some attempts at these feats of biomarker discovery have been fruitful, most have failed to yield proper biomarkers of diseases like AD and PD while limiting research for them to the nervous system. In fact, no longer is there any doubt that these diseases plague affected individuals on a systemic level, with multiple accounts of associated pathologies, peripheral to the CNS.

Blood and its fractions could shed some light on these vastly unexplored features of NDs. Yet, the protein dynamic range of this biofluid challenges even the furthestmost sensitive modern technologies of detection and quantification. Mass spectrometry-based proteomics has the potential to be the leading tool for biomarker exploration regarding the at most complex samples, not unlike blood and its components.

Therefore, in the present work the aim is to optimize a non-denaturing serum fractionation protocol based on molecular size, in order to better observe its HMW fraction, whilst searching for proteins involved in altered degradation mechanisms or possibly abnormally complexed protein assemblies, using mass spectrometry to identify and quantify those that might help differentiate between healthy individuals, AD patients, and PD patients.

3. Experimental Procedures

3.1 Workflow Optimization

3.1.1 Protein Quantification of Fractionated Serum

3.1.1.1 Centrifugal Ultrafiltration

Three serially diluted serum aliquots were prepared: one containing 250 μ L of whole serum, one containing 100 μ L of serum and 150 μ L of triethylammonium bicarbonate (TEAB), and another containing 50 μ L of serum and 200 μ L of TEAB (0.5M). Each aliquot was placed in a Vivaspin® 500 Polyethersulfone, 300 kDa (Sartorius) MWCO filter and filtered by centrifugation (room temperature; 14 100 x g; 20min.) two times, with sample resuspension between centrifugations. The resulting filtrate was placed in an Amicon® Ultra 3K device (MWCO of 3 kDa), filtrated by two centrifugations under the same conditions, and stored in 1.5 mL Eppendorf tubes at 4°C. The retentate (resulting from filtration in 300 kDa MWCO filters) was washed by adding 500 μ L of TEAB (0.5M) and centrifuging two times under the same conditions, being subsequently collected to a new 1.5 mL Eppendorf tube and stored at 4°C. The retentates resulting from filtration using the 3 kDa MWCO filters were discarded.

3.1.1.2 Bicinchoninic acid assay quantification

A volume of 6 μ L of each fraction (stored filtrate, LMW fraction, and retentate, HMW fraction) was diluted 1:5 in Phosphate Buffer Saline (PBS) for a final volume of 30 μ L. Protein quantification by bicinchoninic acid assay was performed, following manufacturer indications and using bovine serum albumin as standard. After the reaction took place, absorbance at 562 nm was read, the standard curve was plotted, and protein quantification of each sample fraction was attained. Results for this protocol are presented in section 7.1.

3.1.2 Low Molecular Weight Fractionation

3.1.2.1 Internal Standard Protein: Fractionation

Briefly, 2 μ g of the recombinant protein Green Fluorescent Protein-Maltose Binding Protein (GFP-MBP) tryptic digest was spiked in 250 μ L of unfractionated serum and 250 μ L of TEAB (0.5M). The resulting samples were placed in an Amicon® Ultra 3K device (MWCO of 3 kDa) and filtered by two centrifugation steps (room temperature; 14,100 x

g; 20min.), followed by peptide clean-up of the resulting LMW fractions and subsequent MS/MS analysis. Results for this protocol are presented in section 7.2.

3.1.2.2 Internal Standard Protein: Single VS Double Digestion

Eight unfractionated serum aliquots of 5 μ L each and eight aliquots of a GFP-MBP (5 μ g) solution were formed. Followed by the addition of 10 μ L of buffer containing ammonium bicarbonate (50 mM) and urea (6M) and 1.5 μ L of DTT (110 mM) to each replicate. All aliquots were then sonicated using a sonicator with cuphorn (VibraCell 750 watt-Sonics®) (5 min pulse duration, at 1 second intervals, and with 45% amplitude). Aliquots were then incubated with 1 μ L of methyl methanethiosulfonate (MMTS) (200 mM) for 10 min. at room temperature. Then 5 μ L of the same buffer were added to stop the alkylation reaction. Four aliquots from each condition were then digested with trypsin alone and the remaining aliquots from each condition were first digested with lysyl endopeptidase (Lys-C) (Roche) and then with trypsin. In Lys-C digestion, 20 μ L and 1 μ L of a Lys-C [1 μ g/ μ L] solution were added to serum and GFP-MBP aliquots, respectively, and incubated for 6h at 37°C. In tryptic digestion, 60 μ L of TEAB (0.5 M) and 20 μ L of porcine trypsin (0.1 μ g/ μ L) were added to serum aliquots. Conversely, for tryptic digestion of GFP-MBP aliquots, 80 μ L of TEAB (0.5M) and 1 μ L of porcine trypsin (0.1 μ g/ μ L) were added. For both serum and GFP-MBP aliquot tryptic digestion, aliquots were incubated overnight (about 16h) at 37°C. After digestion, (single or double) 2 μ L of 98% formic acid (v/v) were added to each aliquot. Aliquots were then dried in a vacuum concentrator [Concentrator Plus (Eppendorf®)] and stored at 4°C, until subsequent peptide clean-up and MS/MS analysis. Results for this protocol are presented in section 7.3.

3.1.2.3 Internal Standard Protein: Different MWCO Filters

Six microliters of a GFP-MBP (0.5 μ g/ μ L) tryptic digest solution were added to six 250 μ L whole serum aliquots. Three different MWCO filters with two replicates each were used for fractionation, Amicon® Ultra 3K device (MWCO of 3 kDa), Vivaspin 500® Polyethersulfone, 5 kDa (Sartorius), and Amicon Ultra 10K device (MWCO 10 kDa). One of each type of MWCO filter was washed by adding 500 μ L of TEAB (0.5M) and the remaining three MWCO filters were washed by adding 500 μ L of 32% acetic acid (v/v) (172), both washing steps occurred through centrifugation (4°C; 14,100 \times g; 5min.). The TEAB and acetic acid in the MWCO filter tubes were discarded. The GFP-MBP spiked serum aliquots were placed in each filter tube, as well as either 250 μ L of TEAB (0.5M) or

250 μL of 32% acetic acid (v/v), in accordance to which of the later was used in the filter tubes during the aforementioned washing procedure. Two centrifugation steps followed (4°C ; $14,100 \times g$; 10 min.), with further addition of TEAB (0.5M) and 32% acetic acid (v/v) (500 μL each, in accordance to filter washing) between centrifugation steps. The resulting retentates were stored at -20°C and the resulting filtrates were dried in a vacuum concentrator [Concentrator Plus (Eppendorf®)]. Dried filtrates were stored at 4°C , until subsequent peptide clean-up and MS/MS analysis. Results for this protocol are presented in section 7.4.

3.1.3 HMW Fractionation

3.1.3.1 Internal Standard Protein

In order to assess which candidate would be the best HMW internal standard protein, 5 μg of equine ferritin and 5 μg of bovine thyroglobulin were digested with both trypsin and Lys-C identically to what is described for GFP-MBP double digestion in section 3.1.2.2.

3.2 Differential Proteomics of AD and PD Samples

3.2.1 Samples

In order to qualitatively and quantitatively assay serum proteins, 58 serum samples were taken from storage at -80°C and thawed on ice, comprising 3 cohorts: AD, PD, and Control. Aliquots of 200 μL were taken from each sample and each aliquot was spiked with 8 μg of equine ferritin. Additionally, five 750 μL sample pools were created (one for each cohort and each containing serum from all samples of that same cohort). To each pool, 30 μg of equine ferritin were added. All aliquots and pools were kept at -20°C until further processing.

3.2.2 High Molecular Weight Fractionations

Both individual aliquots and pools were filtrated using Vivaspin® 500 Polyethersulfone, 300 kDa (Sartorius). Cut-off filters were initially washed by adding 500 μL of PBS 1 \times concentrated and followed by centrifugation (4°C ; $14,500 \times g$; 5 min.). PBS was then discarded and 82.5 μL of either sample aliquot or pool were added, along with an additional 200 μL of PBS 1 \times , with further centrifugation (4°C ; $14,500 \times g$; 20 min.). Another 200 μL of PBS 1 \times were added and the centrifugation was repeated under the same conditions. The resulting filtrate was saved in 1.5 mL Eppendorf tubes and stored at -20°C .

The resulting retentate was collected to a 500 μ L LoBind Eppendorf tube and stored at -20°C.

Note that, while the filtration workflow occurred only once for sample aliquots, 5 replicates were elaborated for each pool, 1 for IDA analysis and the remainder for SWATH-MS. Also, in order to assume the ultrafiltration process as complete, a maximum threshold of 50 μ L of retentate was considered. Therefore, in some cases, a third centrifugation procedure was required (under the same conditions as the previous two).

3.2.3 Protein Precipitation

The retentates were then precipitated with ice-cold acetone. In accordance with a maximum volume of 50 μ L for each retentate and following an acetone-to-sample proportion of 9:1 (173), 450 μ L of ice-cold acetone were added to each retentate and incubated at -20°C overnight. Precipitated retentates were then centrifuged (4°C; 20,000 \times g; 10 min.) and the supernatant was collected. A volume of 450 μ L of ice-cold acetone were added once more to each retentate and the pellets were resuspended, followed by incubation at -20°C for at least 1 hour. Samples were then centrifuged, under the same conditions, and a second supernatant was collected. The precipitated retentates were dried using a vacuum concentrator [Concentrator Plus (Eppendorf®)] and stored at -20°C.

3.2.4 Solubilization, Denaturation, and Alkylation

The HMW samples were thawed at room temperature after retrieval from -20 °C storage and a volume of 30 μ L of a solution containing 2% SDS (v/v) and 1 M of Urea were added to each retentate, with resuspension (as described above) and vortexing until solubilization was apparent. Samples were then subjected to two sonication steps using a sonicator with cuphorn (VibraCell 750 watt-Sonics®), with ice in the cuphorn at all times (2 min. pulse duration, at 1 second intervals, and with 40% amplitude). Afterward, 6 μ L of Laemmli Sample Buffer 6 \times concentrated were added [0.35M Tris-HCl, pH 6.8 with 0.4% SDS (v/v), 30% glycerol (v/v), 10% SDS (w/v), 9.3% DTT (w/v) and 0.01% bromophenol blue (w/v)], with a 30 min. incubation at 4°C. Then, 1 μ L of iodoacetamide (IAA) (1.2M) was added, with incubation at 4°C for 20 min.

3.2.5 Short GeLC (174)

Precast Bio-Rad Gels were used to electrophoretically separate solubilized serum protein samples. These were retrieved from storage at 4°C as they need to be at room temperature. The 4-20% Mini-PROTEAN® TGX™ Precast Gels (Bio-Rad) were mounted in the appropriate assembly. The entire volume of sample aliquots and pools (about 37 µL) was loaded therein, immediately after IAA incubation, and resolved at 110V until the sample front was about 4 cm from the end of the gel, using a Mini-PROTEAN® Tetra Electrophoresis System (Bio-Rad). Whenever applicable, empty lanes were loaded with a similar volume of Laemmli Sample Buffer 1× concentrated. In-gel protein visualization was accomplished after gel staining with Colloidal Coomassie Blue G-250 (Thermo Scientific) and 50 mL of a staining solution bearing 10% ammonium sulfate (w/v), 20% methanol (v/v), and 11.7% (v/v) of 85% orthophosphoric acid (v/v), all under mild shaking and for at least 1h. This creates some background, which was de-stained by shaking the gel in a generous amount of Milli-Q Water overnight. De-stained gels were stored at 4°C when not processed immediately after de-staining.

3.2.6 Gel Processing

3.2.6.1 Lane Cutting and De-staining

The 96-MW plate wells were filled with 600 µL of a de-staining solution containing ammonium bicarbonate (50mM) and 30% acetonitrile (v/v). Using a scalpel blade, each sample containing the gel lane was divided into four equally sized sections, which were further sliced into smaller fragments. These fragments were then transferred, in a pre-defined order, into 96-MW plate wells previously filled with the aforementioned de-staining solution (each one of the four sections of a given lane was placed in a separate well, with gel fragments originating from the same section put into the same well) (175). Fragment loaded plates were then shaken in a thermomixer (Comfort, Eppendorf®) (25°C; 900 rpm; 15 min.). The de-staining solution was then discarded and 600 µL of ultra-pure LCMS water were added to each well, for further shaking under the same conditions. This de-staining/hydration cycle was repeated until most gel fragments in any given plate appeared discolored. Gel fragments were then dried in a vacuum concentrator [Concentrator Plus (Eppendorf®)] (60°C; Aq; 1h30min.).

3.2.6.2 In-Gel Digestion

The protein digestion was performed by adding 75 μL of a porcine trypsin (Roche) solution (0.01 mg/mL and 10 mM ammonium bicarbonate) to each well, covering all gel fragments. Trypsin laden plates were then incubated at 4°C for 15 min. Then, 75 μL of an ammonium bicarbonate solution (10 mM) were added to each well, and the respective plates were stored at room temperature for 16h.

3.2.6.3 Peptide Extraction

After the tryptic digestion time ended, the solution covering the gel fragments (containing trypsin and some peptides) was transferred into new LoBind Eppendorf tubes. In the case of SWATH samples, the four fractions were combined into a single tube while the fractions from the IDA samples were maintained in separate tubes). The peptide extraction then followed by sequentially adding 100 μL of three solutions containing a constant amount of formic acid [1%(v/v)], but progressively more concentrated in acetonitrile [30%(v/v), 50%(v/v), and 98%(v/v)], with plate shaking after each 100 μL increment using a thermomixer (Comfort, Eppendorf®) (25°C; 1050 rpm; 15 min.). After each shaking procedure, the remaining solution, enveloping gel fragments, was collected into the respective LoBind Eppendorf tubes (the same ones, as mentioned before) in a similar fashion to what was done for the trypsin solution collected after digestion, i.e. SWATH samples pooled together and IDA samples kept separate. The resulting peptide extract was then dried in a vacuum concentrator [Concentrator Plus (Eppendorf®)] and stored at 4°C.

3.2.7 Peptide Clean-Up

Dried peptide extracts were resuspended in 100 μL of a solution containing 2% acetonitrile (v/v) and 1% formic acid (v/v). Resuspended peptide extracts were then desalted using C18 OMIX tips according to the following procedure: (1) 200 μL of a solution containing 50% acetonitrile (v/v) were added to the tip and discarded; (2) 300 μL of a solution containing 2% acetonitrile (v/v) and 1% formic acid (v/v) were added to the tip and discarded; (3) the resuspended peptide extract was added to the tip, collected to the original LoBind Eppendorf tube, and added again, for a total of five times passing through the column; (4) 100 μL of a solution containing 2% acetonitrile (v/v) and 1% formic acid (v/v) were added to the tip and the resulting “rinse” was kept in a new Eppendorf

tube (and stored at 4°C); (5) 400 µL of a solution containing 70% acetonitrile (v/v) and 0.1% formic acid (v/v) was added to the tip and the resulting eluate was saved in a new 500 µL LoBind Eppendorf tube. Peptide extract eluates were then dried in a vacuum concentrator [Concentrator Plus (Eppendorf®)] and immediately resuspended in 30 µL of a solution containing 2% acetonitrile (v/v) and 0.1% formic acid (v/v). The resulting sample was then sonicated using a sonicator with cuphorn (VibraCell 750 watt-Sonics®) (5 min. pulse duration, at 1 second intervals, and with 40% amplitude), centrifuged (room temperature; 14,100 × g; 5 min.), and the resulting supernatant was loaded into the appropriate vials (compatible with automated injection) for subsequent separation by LC and MS/MS analysis.

3.3 SWATH Acquisition and Data Analysis

Samples were analyzed on a Triple TOF™ 5600 System (AB Sciex®) in two phases: IDA of the pooled samples and, SWATH (Sequential Windowed data-independent Acquisition of the Total High-resolution Mass Spectra) acquisition of each individual sample. Peptides were resolved by liquid chromatography (NanoLC™ 425 System, Eksigent®) on a MicroLC column ChromXP™ C18CL (300 µm ID × 15 cm length, 3 µm particles, 120 Å pore size, Eksigent®) at 5 µL/min with a multistep gradient: 0-2 min linear gradient from 2 % to 5 % mobile phase B; 2-50 min linear gradient from 5 % to 28 % B; and 50-51 min linear gradient from 28% to 35% B. Mobile phase A corresponding to 0.1 %FA with 5% DMSO, and mobile phase B to 0.1 % FA and 5% DMSO in ACN. Peptides were eluted into the mass spectrometer using an electrospray ionization source (DuoSpray™ Source, ABSciex®) with a 25 µm internal diameter (ID) hybrid PEEKsil/stainless steel emitter (ABSciex®).

The IDA experiments were performed for each pooled fraction. The mass spectrometer was set to scanning full spectra (350-1250 m/z) for 250ms, followed by up to 100 MS/MS scans (100–1500 m/z from a dynamic accumulation time – minimum 30 ms for precursor above the intensity threshold of 1000 – in order to maintain a cycle time of 3.298 s). Candidate ions with a charge state between +2 and +5 and counts above a minimum threshold of 10 counts per second were isolated for fragmentation and one MS/MS spectrum was collected before adding those ions to the exclusion list for 25 seconds (mass spectrometer operated by Analyst® TF 1.7, ABSciex®). The rolling collision was used with a collision energy spread of 5.

For SWATH-MS based experiments, the mass spectrometer was operated in a looped product ion mode (176) and the same chromatographic conditions used as in the IDA run described above. A set of 60 windows (Table 3.1) of variable width (containing 1 m/z for the window overlap) was constructed covering the precursor mass range of 350-1250 m/z. A 250 ms survey scan (350-1500 m/z) was acquired at the beginning of each cycle for instrument calibration and SWATH-MS/MS spectra were collected from 100–1500 m/z for 50 ms resulting in a cycle time of 3.304 s from the precursors ranging from 350 to 1250 m/z. The collision energy for each window was determined according to the calculation for a charge +2 ion centered upon the window with variable collision energy spread (CES) according with the window.

TABLE 3.1 – SWATH-MS METHOD.

	m/z range	Width (Da)	CES
Window 1	349.5-379.8	30.3	5
Window 2	378.8-401.1	22.3	5
Window 3	400.1-416.6	16.5	5
Window 4	415.6-430.4	14.8	5
Window 5	429.4-441.9	12.5	5
Window 6	440.9-452.3	11.4	5
Window 7	451.3-462	10.7	5
Window 8	461-470.7	9.7	5
Window 9	469.7-479.9	10.2	5
Window 10	478.9-488.5	9.6	5
Window 11	487.5-497.1	9.6	5
Window 12	496.1-505.2	9.1	5
Window 13	504.2-513.8	9.6	5
Window 14	512.8-522.4	9.6	5
Window 15	521.4-531	9.6	5
Window 16	530-539.7	9.7	5
Window 17	538.7-547.7	9	5
Window 18	546.7-556.4	9.7	5
Window 19	555.4-565	9.6	5
Window 20	564-573.6	9.6	5
Window 21	572.6-581.7	9.1	5
Window 22	580.7-589.7	9	5
Window 23	588.7-598.3	9.6	5
Window 24	597.3-605.8	8.5	5
Window 25	604.8-613.9	9.1	5
Window 26	612.9-621.9	9	5
Window 27	620.9-630	9.1	5
Window 28	629-637.4	8.4	5

Window 29	636.4-644.3	7.9	5
Window 30	643.3-651.2	7.9	5
Window 31	650.2-658.1	7.9	5
Window 32	657.1-664.5	7.4	5
Window 33	663.5-671.4	7.9	5
Window 34	670.4-677.7	7.3	5
Window 35	676.7-685.2	8.5	5
Window 36	684.2-692.6	8.4	5
Window 37	691.6-700.1	8.5	5
Window 38	699.1-708.2	9.1	5
Window 39	707.2-717.4	10.2	5
Window 40	716.4-727.1	10.7	5
Window 41	726.1-739.2	13.1	5
Window 42	738.2-752.4	14.2	5
Window 43	751.4-766.2	14.8	5
Window 44	765.2-780.6	15.4	5
Window 45	779.6-795.6	16	5
Window 46	794.6-810.5	15.9	8
Window 47	809.5-826	16.5	8
Window 48	825-841.6	16.6	8
Window 49	840.6-858.2	17.6	8
Window 50	857.2-876.6	19.4	8
Window 51	875.6-897.3	21.7	8
Window 52	896.3-919.2	22.9	8
Window 53	918.2-941.6	23.4	8
Window 54	940.6-962.9	22.3	8
Window 55	961.9-980.1	18.2	8
Window 56	979.1-998.5	19.4	8
Window 57	997.5-1019.8	22.3	10
Window 58	1018.8-1047.4	28.6	10
Window 59	1046.4-1116.4	70	10
Window 60	1115.4-1249.8	134.4	10
Window 61	609.7-613.7	4	5

A specific library of precursor masses and fragment ions was created by combining all files from the IDA experiments, and used for subsequent SWATH processing. Libraries were obtained using ProteinPilot™ software (v5.1, ABSciex®), using the following parameters: i) search against a database composed by the UniProt reviewed human database, and the sequences of the horse ferritin light and heavy chains (IS); ii) iodoacetamide alkylated cysteines as fixed modification; iii) trypsin as digestion type. An independent False Discovery Rate (FDR) analysis using the target-decoy approach provided with Protein Pilot software was used to assess the quality of the identifications and positive

identifications were considered when identified proteins and peptides reached a 5% local FDR (177, 178).

Data processing was performed using SWATH™ processing plug-in for PeakView™ (v2.0.01, AB Sciex®) (179). After retention time adjustment using a combination of IS and endogenous peptides, up to 15 peptides, with up to 5 fragments each, were chosen per protein, and quantitation was attempted for all proteins in library file that were identified from ProteinPilot™ searches.

Peptides' confidence threshold was determined based on an FDR analysis using the target-decoy approach and those that met the 1% FDR threshold in at least six of the biological replicates, and with at least 3 transitions were retained. Peak areas of the target fragment ions (transitions) of the retained peptides were extracted across the experiments using an extracted-ion chromatogram (XIC) window of 5 minutes with 100 ppm XIC width.

The levels of the proteins were estimated by summing all the transitions from all the peptides for a given protein that met the criteria described above (an adaptation of (180)) and normalized to the internal standard (181).

3.4 Bioinformatics Tools

ProteinPilot software (v5.1, ABSciex®), was used for protein identification from MS/MS data.

PeakView™ (v2.0.01, ABSciex®), was used for identification and comparison between samples.

BioVenn was used to generate Venn diagram, with the inputs being the list of UniProt accession numbers corresponding to the desired proteins. (<http://www.biovenn.nl/>)

PANTHER, Protein Analysis Through Evolutionary Relationships, was used to classify proteins (and their genes) according to class, molecular function, biological process, cellular component, and pathways. (<http://www.pantherdb.org>)

RStudio Software (v. 1.1.463) was used as a tool for data analysis, visualization, and performance of statistical tests.

3.5 Ethics Committee Approval

This study was approved by the Ethics Committee of the Faculty of Medicine of the University of Coimbra and by the Ethics Committee of the Coimbra University Hospital Center to ensure the protection of the rights, safety and welfare of all patients or other participants included and to ensure public proof of such protection. Additionally, informed consent was obtained for all study participants.

4. Results and Discussion

The present section contains results from a poster publication entitled: *A different perspective of circulatory biomarker discovery in neurodegenerative diseases: combined use of alternative proteomics analyses to create a comprehensive “proteomics signature of the blood”*. It was elaborated during the production of this document and is to be presented in the 18th Human Proteome Organization World Congress - HUPO 2019, 15th-19th September - Adelaide, Australia. The authors are Sandra I. Anjo, Rafael Silva, Miguel Rosado, Inês Baldeiras, Alexandre Mendonça, Cristina Januário, Isabel Santana, Ana Verdelho, Diana Santos, Andreia Gomes, Miguel Castelo-Branco, Bruno Manadas.

4.1 Patient Information

The present exploratory analysis used 58 serum samples comprising 3 cohorts: 22 diagnosed AD patients, 24 diagnosed PD patients, and 12 healthy controls (with no signs of development of neurological disorders). Table 4.1 shows the distribution of the collected serum samples regarding the cohort, age, and gender. All samples were accounted for except for one originating from a PD patient, for which there is no information concerning age and gender. Nonetheless, this did not exclude the analysis of this sample.

Table 4.1 Sample distribution regarding cohort, age, and gender. Each cohort was divided by gender and age group, as being younger than 65 years of age (<65 y) or older than 65 years of age (>65 y). In one sample, only the cohort could be determined (“PD – Undetermined”). y, years.

Cohort Age	AD		PD			Control	
	Male	Female	Male	Female	Undetermined	Male	Female
<65 y	4	4	6	9	-	2	2
>65 y	5	9	4	4	-	1	7
Mean ± SD (y)	68.36 ± 8.19		59.96 ± 10.51		-	67.5 ± 7.15	
Total	9	13	10	13	1	3	9
	22		23			12	

4.2 Protein Identification Library

IDA mass spectrometry analysis of the HMW fraction of each serum pooled samples from each cohort, i.e. a PD pool, an AD pool, and a control pool, resulted in the “HMW protein library”. This was further used for the protein quantification in isolated samples by

SWATH-MS. All pools contained an equal volume of the HMW fraction from the respective serum samples, in order to have a “HMW protein library” representative of all cohorts.

A total of 244 proteins were identified and their distribution (according to the respective annotated mass) is illustrated in Figure 4.1, showing a clear overrepresentation of proteins well below 300 kDa. About 93% (227 out of 244) of all identified proteins fall under 150 kDa, which according to the “1.5-2 rule” (157) (and since a 300 kDa MWCO filter was used for serum fractionation) indicates that non-denatured serum filtration may not be the most adequate method to fractionate samples if clear separation by molecular weight is the final goal. However, another possible explanation for this overrepresentation of non-HMW proteins may be the presence of highly complexed protein assemblies, possibly involving abundant protein-carriers in serum, like albumin (157) (also identified in the protein library). Considering that several circulatory proteins have this “carrier” role, it is therefore an expected result, as fractionation took place under non-denaturing conditions.

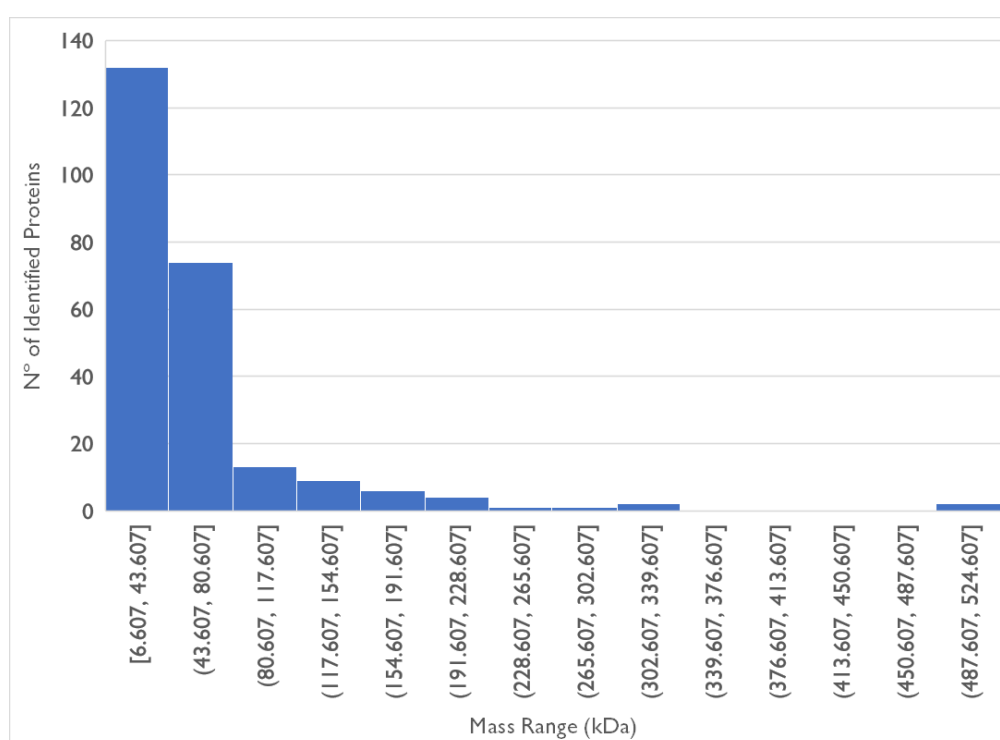


Figure 4.1 Mass distribution of all 244 proteins identified in the IDA library of HMW serum fraction samples.

To further explore this assumption, identifications from this library were compared with those obtained from another IDA protein library, generated from a pool of unfractionated serum samples. Note that the latter samples are not included in the original 58 serum samples and are instead from blood from volunteers. This comparison demonstrated a

profound overlap in identifications between the two IDA protein libraries, as shown in Figure 4.2. Nevertheless, it is evident that HMW serum fractionation yielded a more comprehensive identification profile, with a large number of proteins (73) identified solely in fractionated samples.

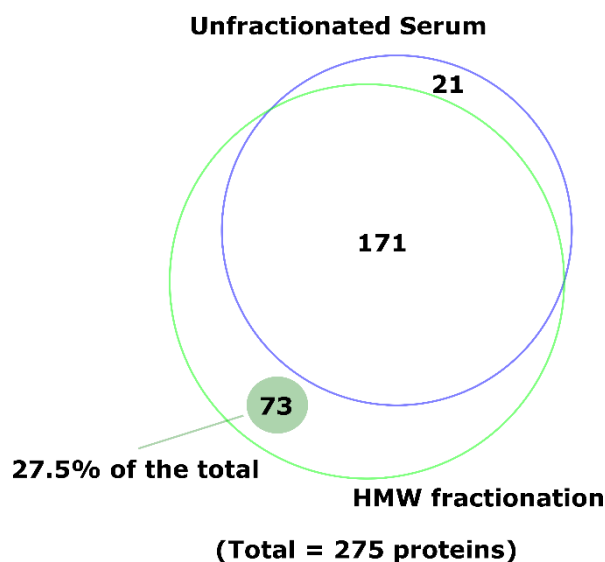


Figure 4.2 Venn diagram illustrating the overlap between identified proteins in fractionated serum (HMW) and unfractionated serum. Results show a great overlap between identifications in the fractionated and unfractionated serum IDA libraries. Yet, fractionated serum allows for a more wide-ranging identification profile, yielding both more total (244 versus 192) and exclusive (73 versus 21) protein identifications than unfractionated serum. Image generated from BioVenn (<http://www.biovenn.nl/>) and later adapted using Inkscape.

While using such a stringent MWCO filter (300 kDa) and in accordance with the aforementioned “1.5-2 rule” rule, one would expect that these 73 proteins (identified only in fractionated samples) to mostly be of HMW, particularly above 150 kDa. But upon plotting the mass distribution of these HMW fractionation-exclusive proteins (Figure 4.3), a clear tendency for the overrepresentation of proteins with a lower molecular weight is observed, much like what was seen for the entirety of the HMW protein library. In fact, only 6 of these proteins have a mass over 150 kDa and more than half (37 out of 73) are under 25 kDa. These results corroborate the assumption that complex protein assemblies in serum can be enriched through HMW fractionation under non-denaturing conditions. The protein list with the respective masses are presented in section 7.5, Figure S10.

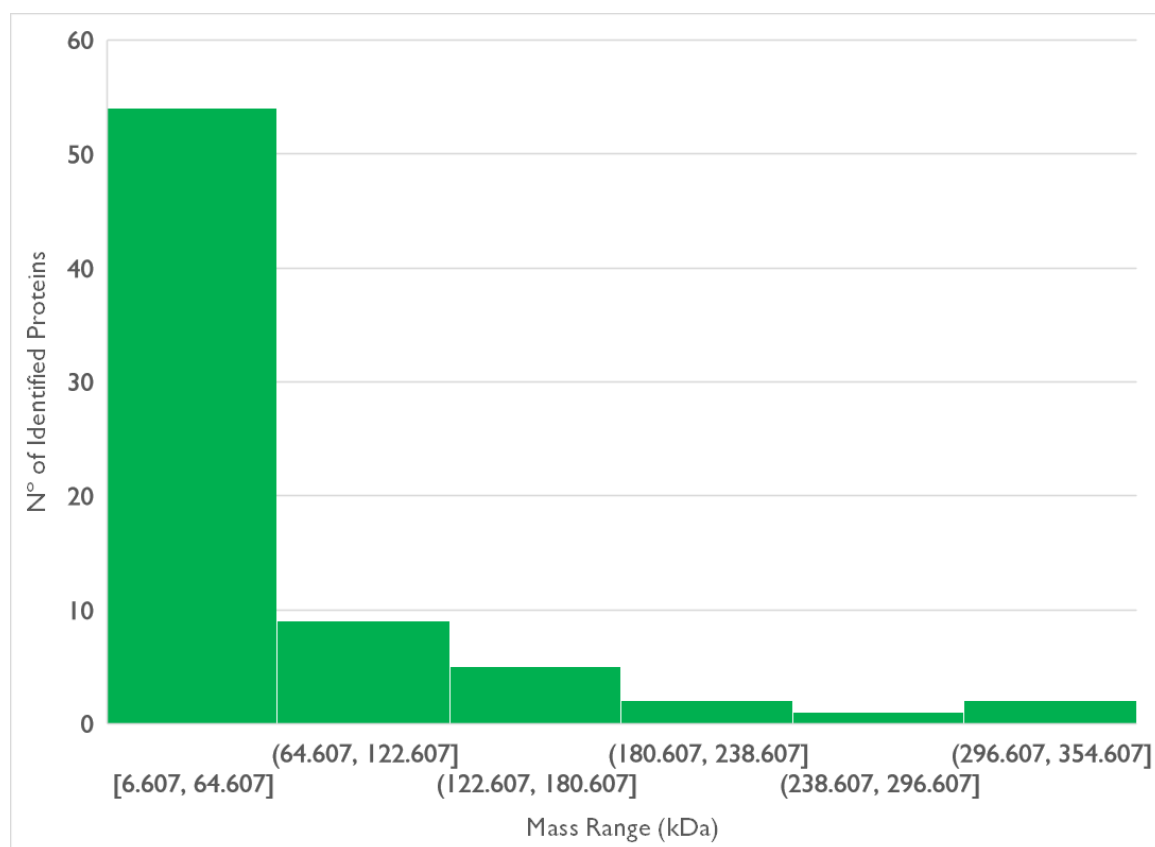


Figure 4.3 Mass distribution of 73 proteins identified exclusively in the library of HMW serum fraction samples.

To further characterize the HMW protein library, all 244 proteins were analyzed using a Gene Ontology software (PANTHER Classification System) in order to extract information about identified proteins, concerning the involved pathways, biological processes, cellular components, and molecular functions, but also to ascertain protein class information.

Regarding associated molecular functions (Figure 4.4), binding (41.4%), catalytic activity (28.5%), and molecular function regulation (19.9%) were the most abundantly matched to the queried proteins. Across these three functions, serine protease inhibitors appeared to be more represented.

In the case of associated biological processes (Figure 4.5), none of the utmost represented categories dominated over others, with the majority being somewhat equally represented (ranging from 11.7% and 24.2%), namely (and in ascending order of representation) localization, biological regulation, metabolic processes, stimulus responses, immune system processes, and cellular processes.

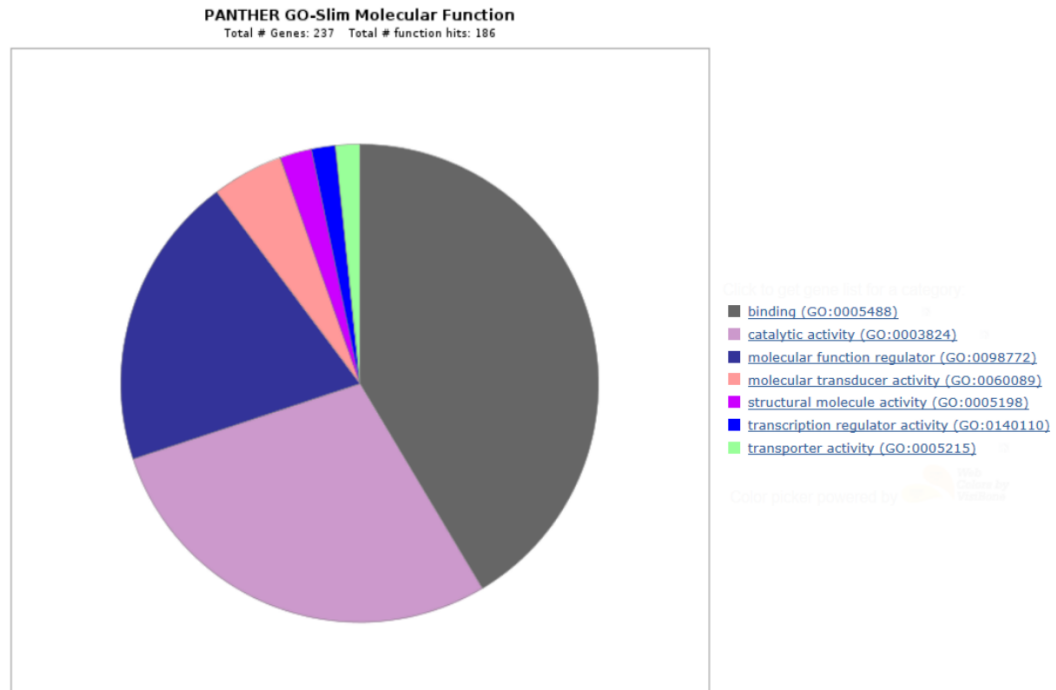


Figure 4.4 Pie chart of molecular functions associated with all proteins identified in the HMW protein library. Generated using PANTHER Gene List Analysis tool.

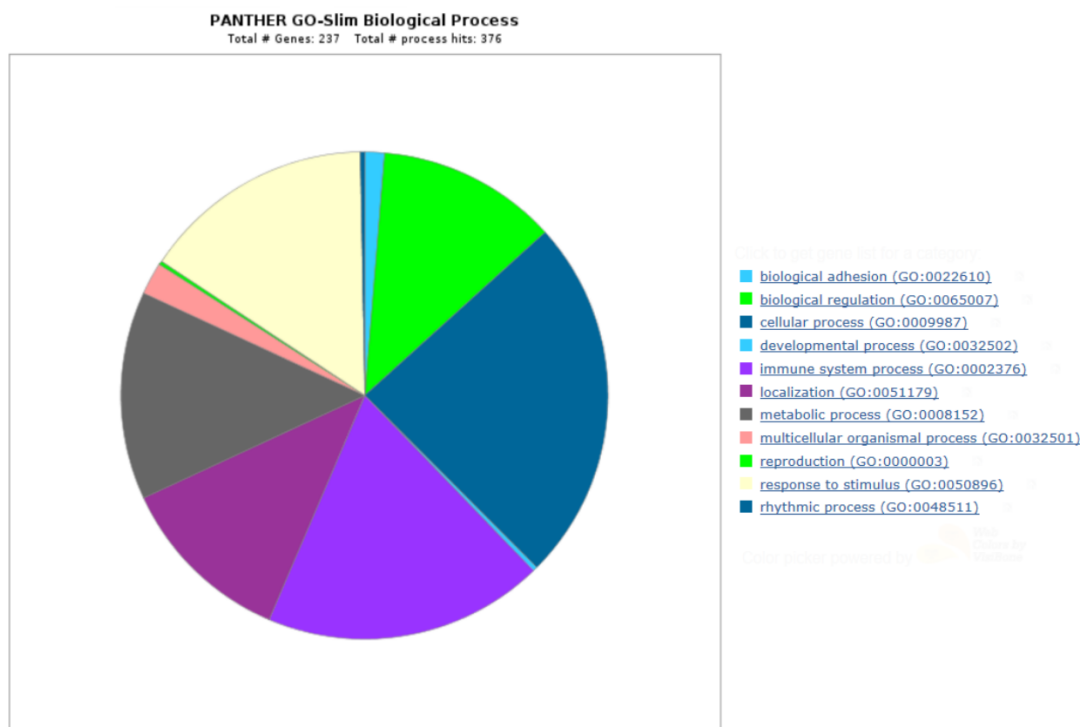


Figure 4.5 Pie chart of biological processes associated with all proteins identified in the HMW protein library. Generated using PANTHER Gene List Analysis tool.

As for cellular components relative to protein identifications in the HMW protein library (Figure 4.6), the majority were respective to the extracellular region (47.5%), followed by cell components (21.6%), protein-containing complexes (15.3%), and membrane components (11.8%). In all these categories, immunoglobulins were the most abundantly found proteins.

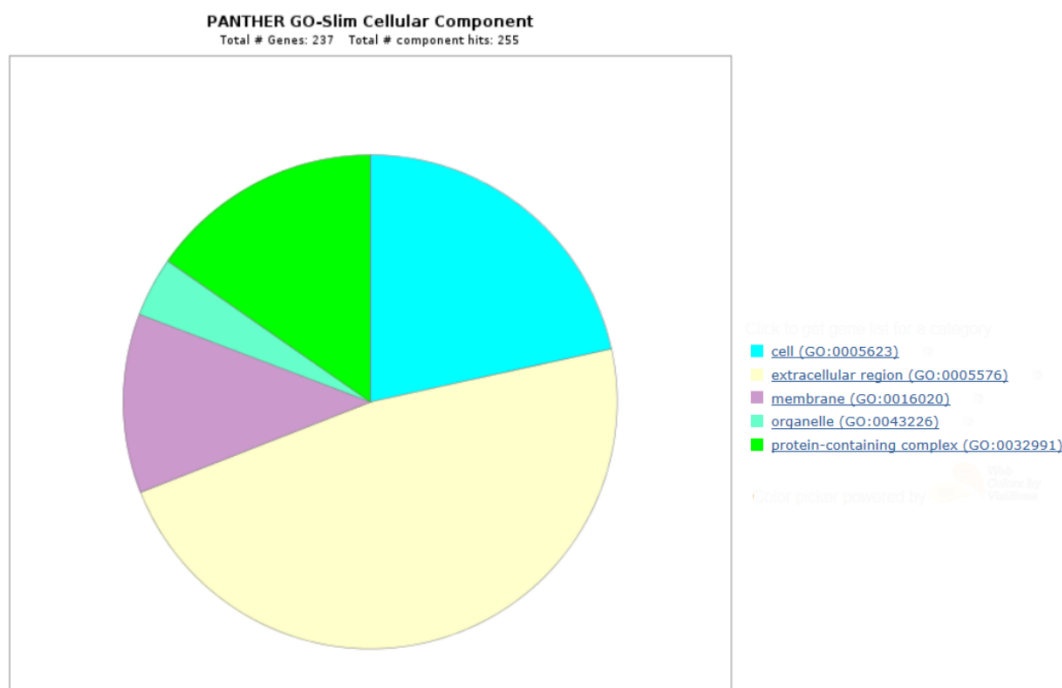


Figure 4.6 Pie chart of cellular components associated with all proteins identified in the HMW protein library. Generated using PANTHER Gene List Analysis tool.

Coherently with this finding, defense/immunity proteins (27.3%) were the most copious protein class, in which immunoglobulins dominated once more, followed by enzyme modulators (21.1%) and hydrolases (14.9%), as shown in Figure 4.7. Signaling molecules (7.5%), transfer/carrier proteins (6.8%), and transporters (5%) were modestly represented. Cumulatively, the latter three may have influenced the observed trend of LMW proteins in the HMW fraction of serum samples, which led to the previously mentioned assumption that protein complexes are responsible for the overrepresentation of LMW proteins in the fractionated serum samples.

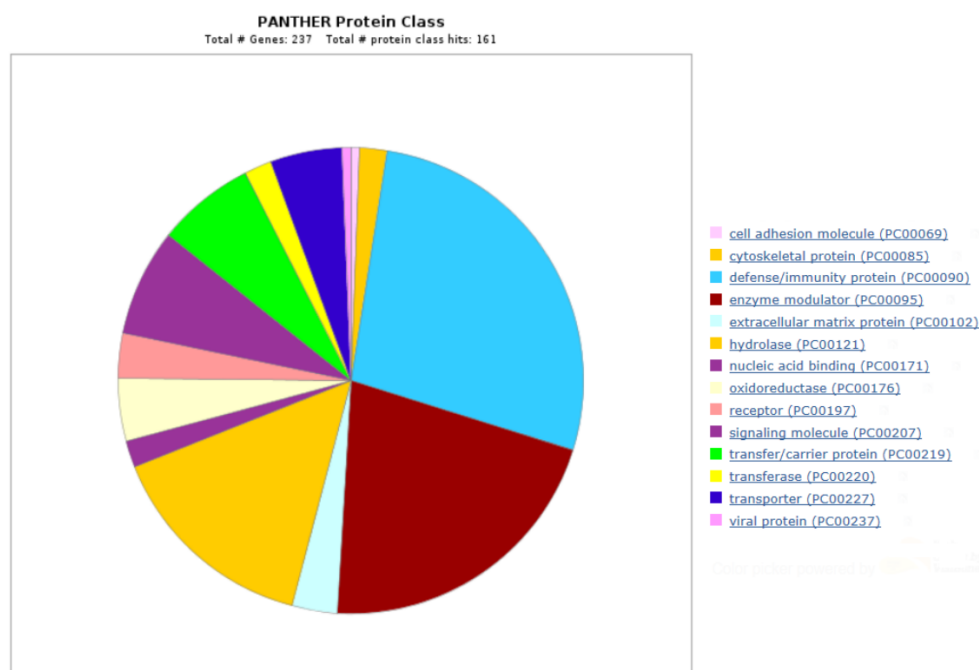


Figure 4.7 Pie chart of protein classes associated with all proteins identified in the HMW protein library. Generated using PANTHER Gene List Analysis tool.

Finally, for PANTHER pathways associated with the HMW protein library identifications (Figure 4.8), blood coagulation (34%), plasminogen activating cascade (10%), and chemokine and cytokine signaling-mediated inflammation (8%) were overwhelmingly profuse. Interestingly, there was a minor representation of the AD-presenilin pathway (2%), albeit with only one match (actin, cytoplasmic 2).

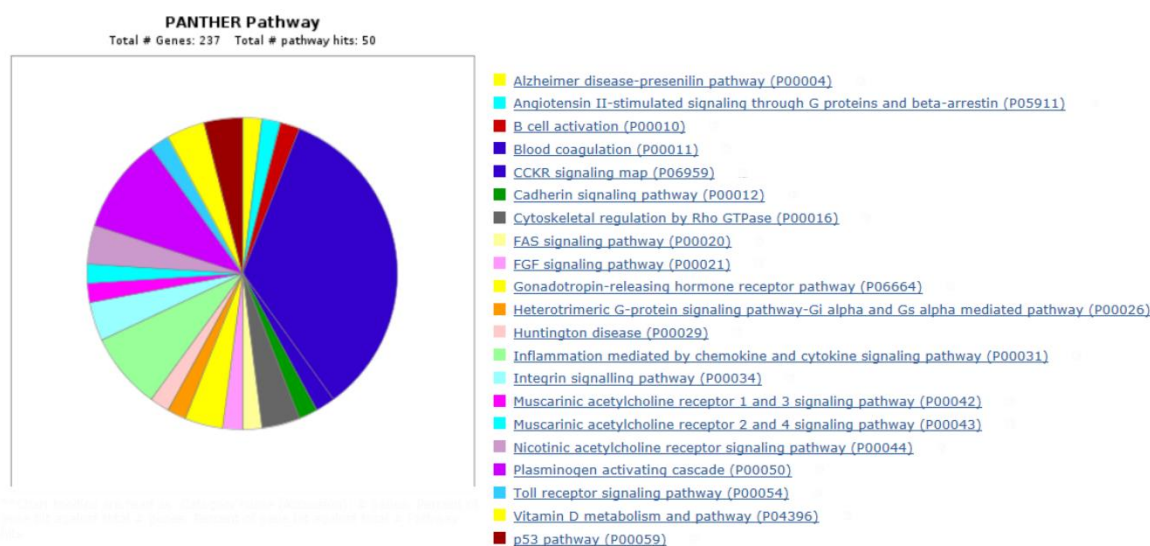


Figure 4.8 Pie chart of pathways associated with all proteins identified in the HMW protein library. Generated using PANTHER Gene List Analysis tool.

4.3 Differential Proteomics Analysis

SWATH-MS analysis of the HMW fraction of serum samples across all cohorts resulted in the relative quantification of 186 proteins. The quantification data were normalized by internal standard protein, ferritin in this case, for which only the light chain could be accounted for and quantified. These 186 proteins resulted from filtering the original SWATH file so that, to be considered for the rest of the analysis, proteins had to be identified in the HMW protein library (IDA) with a False Discovery Rate (FDR) inferior to 1%, have a relative quantification value while being present in at least 6 samples from the same cohort, and have at least 1 peptide (with at least 3 transitions) per quantified protein. The number of peptides used in the relative quantification of the 186 proteins is illustrated in Figure 4.9.

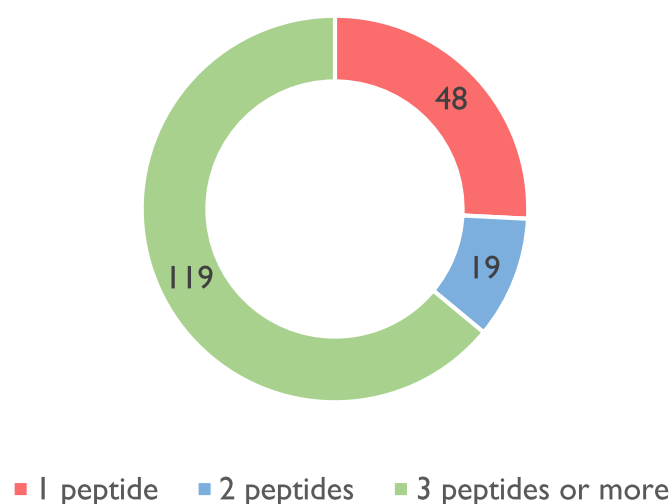


Figure 4.9 Number of quantified proteins using 1, 2, 3 or more peptides. For a total of 186 quantified proteins, about 63.9% were based on 3 peptides or more.

Before trying to find statistically significant proteins between cohorts, the sample distribution must be known, so in order to ascertain the normality of distribution of SWATH samples, Q-Q plots were elaborated for every sample. As can be observed in Figures 4.10, 4.11, and 4.12, SWATH data of the samples do not follow a normal distribution and so, for statistical analysis, non-parametric tests present the best alternative to find statistically significant proteins between cohorts.

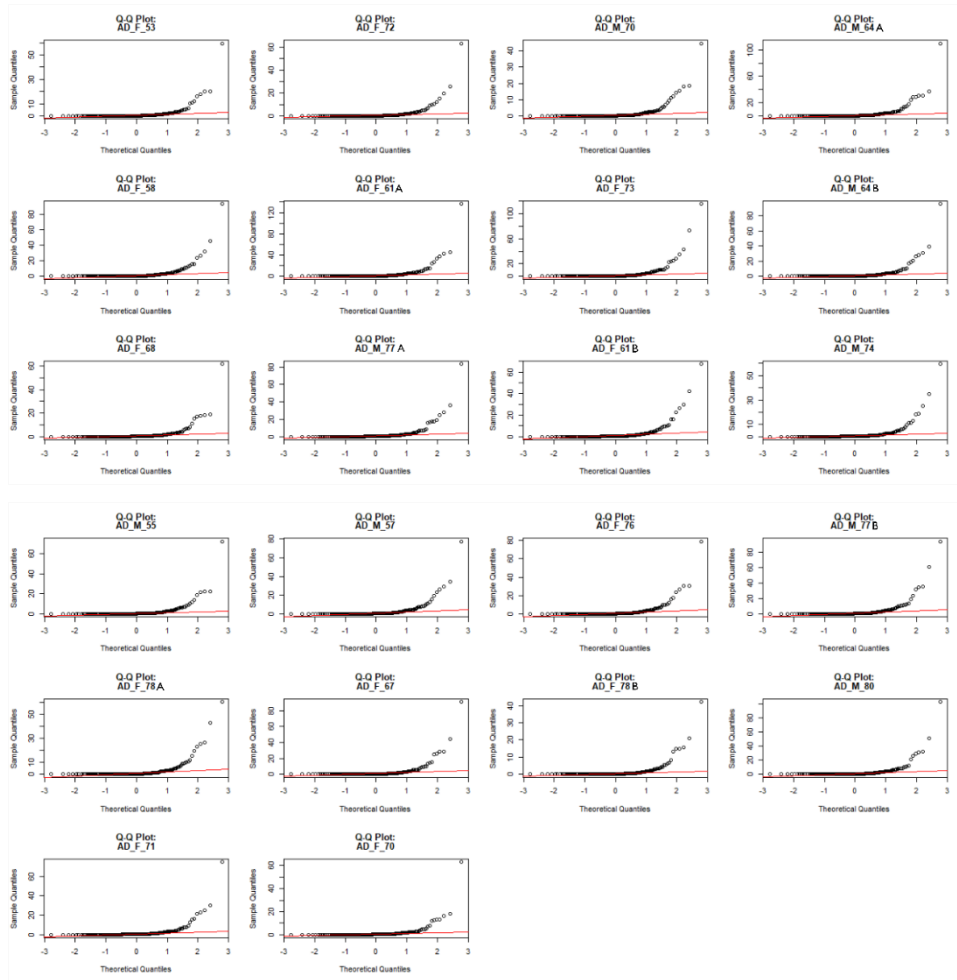


Figure 4.10 Individual Q-Q plots for all samples from the AD cohort. Red lines represent normal distribution. Generated using R-Studio.

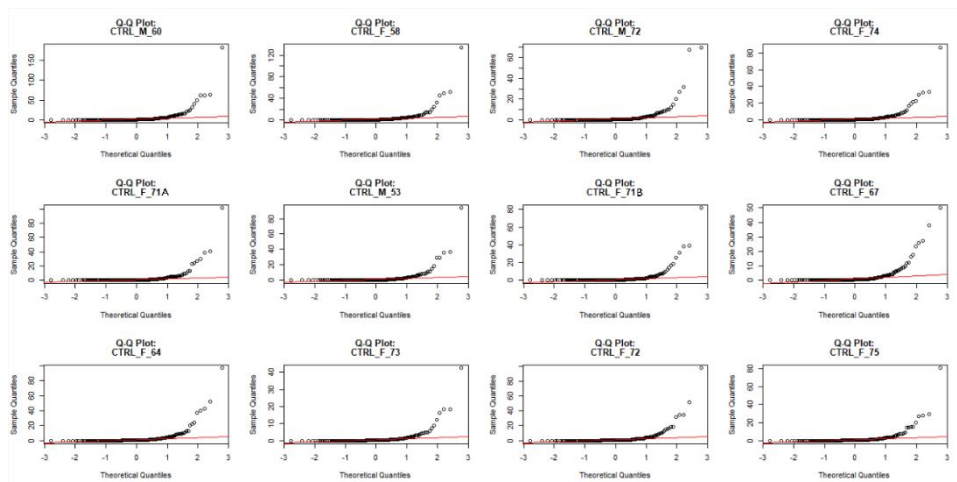


Figure 4.11 Individual Q-Q plots for all samples from the control cohort. Red lines represent normal distribution. Generated using R-Studio.

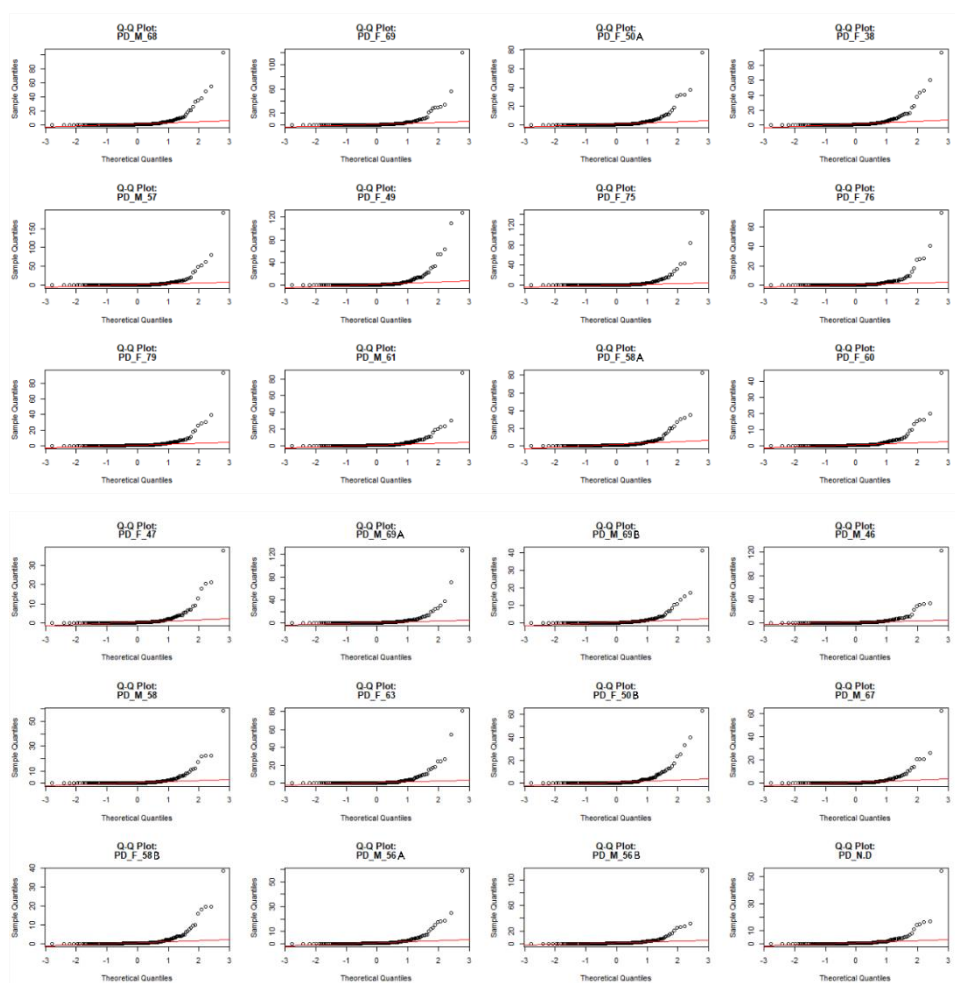


Figure 4.12 Individual Q-Q plots for all samples from the PD cohort. Red lines represent normal distribution. Generated using R-Studio.

To have a first glance of which (and how many) proteins are significantly altered between cohorts, a Kruskal-Wallis test was performed, comparing all three cohorts simultaneously. Because this test only points out that statistical significance exists in at least one cohort comparison for that protein and since this comparison was a three-way comparison, to establish in which exact sample pairs this significance is observed, a Dunn's test was elaborated (using only the output samples from the Kruskal-Wallis test). This resulted in the observation of 39 proteins (from a total of 186 quantified), whose alteration between discriminate cohort pairs was considered as statistically significant (Figure 4.13).

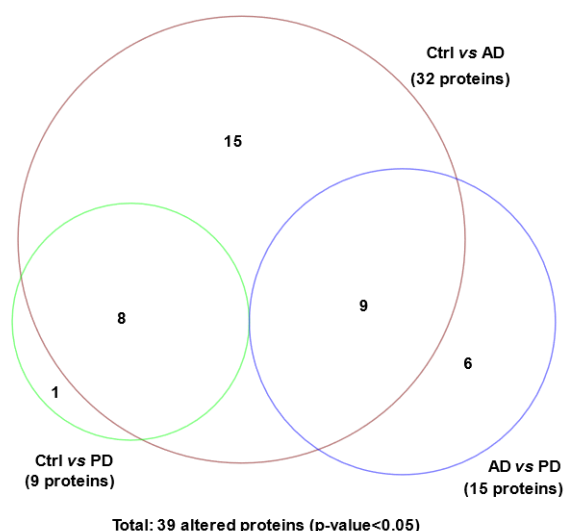


Figure 4.13 Venn diagram illustrating proteins from the HMW fraction of serum samples which are significantly altered between cohorts. The diagram represents a subset of all quantified proteins that have p-value below 0.05 according to Dunn's test. Image generated from BioVenn (<http://www.biovenn.nl/>) and later adapted using Inkscape.

Surprisingly, only one of these proteins has a mass above 100 kDa. Keeping in mind these proteins are being quantified and identified in the HMW fraction of serum, above 300 kDa, it could very well be that their significance between cohorts has its roots on their overrepresentation in this fraction, potentially due to the formation of protein complexes.

To further inspect the discriminant power of these 39 statistically significant proteins, an arbitrary fold change cut-off was applied to select for proteins with a fold change above 1.5 and below 0.66, as is shown in Figures 4.14, 4.15, and 4.16.

Consequently, a total of 14 proteins were found to be both statistically significant and either over-represented or under-represented in at least one of these cohort comparisons. Most referred to the AD vs control juxtaposition (11 proteins), followed by AD vs PD (6 proteins), and PD vs control (4 proteins). In all cases, under-represented proteins are no less than half of all flagged proteins. Alpha-2-antiplasmin, immunoglobulin heavy variable 4-28, and APOE were all found to have a fold change under 0.66, exclusively in the AD vs control differentiation.

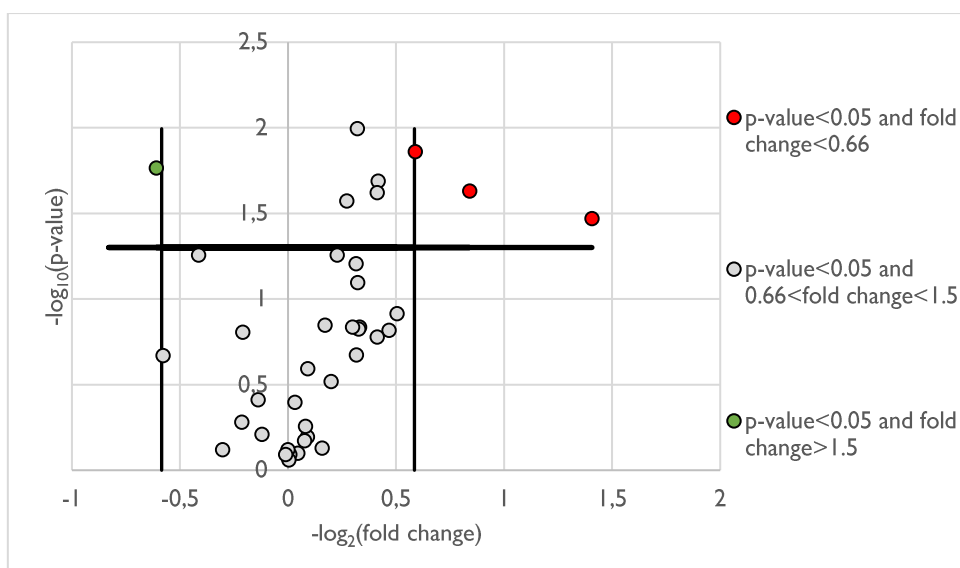


Figure 4.14 Volcano plot illustrating proteins from the HMW fraction of serum samples which are significantly altered between the PD and control cohorts while having at least 1.5 or below 0.66 fold change. Dots above the horizontal line represent proteins that are statistically significant between cohorts according to Dunn's test. Green dots represent statistically significant protein with fold change above 1.5 and red dots represent statistically significant protein with fold change below 0.66.

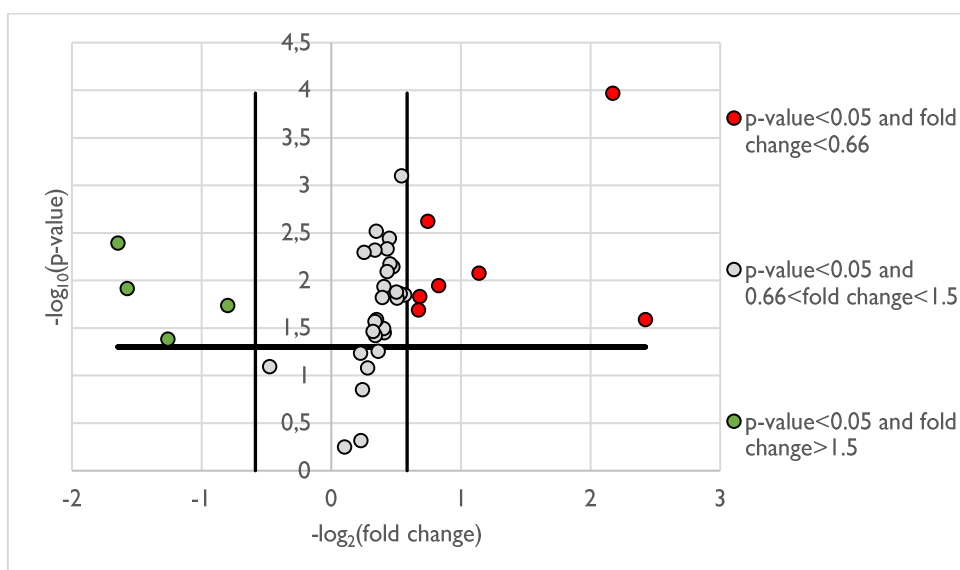


Figure 4.15 Volcano plot illustrating proteins from the HMW fraction of serum samples which are significantly altered between the AD and control cohorts while having at least 1.5 or below 0.66 fold change. Dots above the horizontal line represent proteins that are statistically significant between cohorts according to Dunn's test. Green dots represent statistically significant protein with fold change above 1.5 and red dots represent statistically significant protein with fold change below 0.66.

Interestingly, three proteins had a somewhat similar trend fold change in both the control vs AD comparison and the control vs PD comparison (Serum amyloid A-I protein, in

upfolded proteins and SRR I-like protein and Apolipoprotein A-II, in downfolded proteins), as can be observed in Table 4.2.

Table 4.2 Fold change of 3 proteins between disease and control cohorts with similar change trend

Protein	Fold Change AD vs control	Fold Change PD vs control
Apolipoprotein A-II	0.45	0.56
Serum amyloid A-1 protein	1.74	1.78
SRR1-like protein	0.22	0.38

This observation of significant protein alterations between healthy and diseased subjects should be further investigated, as it could present a source of potential markers of neurodegeneration (common amongst AD and PD). Additionally, SRR1-like protein also had a fold change under 0.66 in the AD vs PD comparison, making it the only protein flagged in all of them.

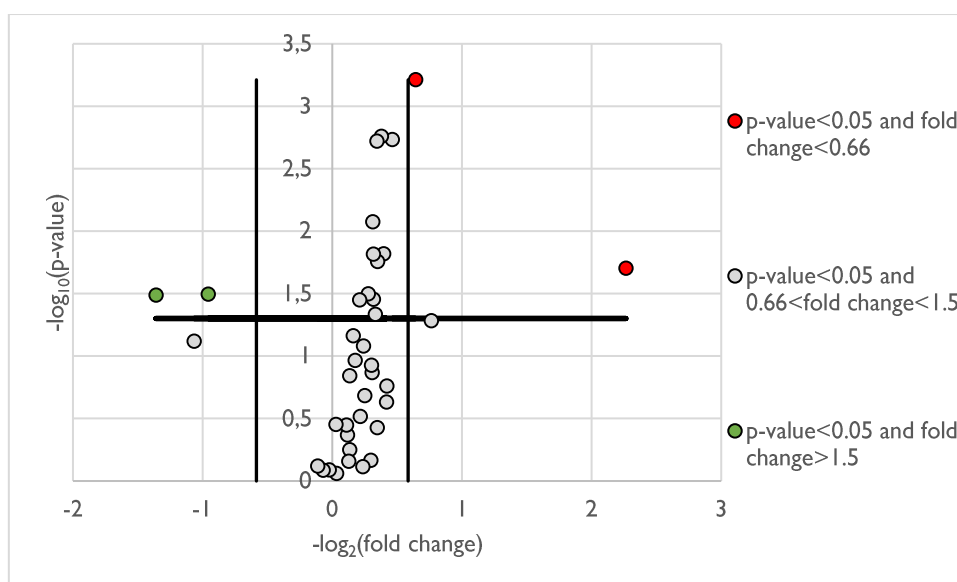


Figure 4.16 Volcano plot illustrating proteins from the HMW fraction of serum samples which are significantly altered between the AD and PD cohorts while having at least 1.5 or below 0.66 fold change. Dots above the horizontal line represent proteins that are statistically significant between cohorts according to Dunn's test. Green dots represent statistically significant protein with fold change above 1.5 and red dots represent statistically significant protein with fold change below 0.66.

4.4 Cohort Discrimination Using Altered Proteins

In an effort to discover potentially altered proteins that may serve as possible biomarker candidates of NDs discussed herein, the final aim of identifying and quantifying proteins from the HMW fraction of serum samples was to explore possibilities that might help differentiate between disease conditions and, ideally, between healthy controls and AD and/or PD cohorts.

An initial attempt to elaborate this, using Principal Component Analysis (PCA), failed at properly separating cohorts upon comparing all 186 quantified proteins, as seen in Figure 4.17, or all 39 statistically significant proteins, as seen in Figure 4.18.



Figure 4.17 PCA analysis of the HMW fraction of serum samples using relative quantification of 186 proteins. Analysis was done using autoscaling. Red dots represent AD samples, blue dots PD samples, and green dots control samples. Sample labels are designated as “cohort”_”gender”_”age”. Generated using R-Studio.

To circumvent this challenge, Partial Least Squares Discriminant Analysis (PLS-DA) encompassing all three cohorts was applied to the quantification data of the 39 statistically significant proteins (Figure 4.19 B). This did not yield fruitful results, but repeating the analysis with selection of proteins of interest using the Variable Importance for Projection (VIP) table (Table 4.2), another PLS-DA output which indicates the loading weights for each component and the variability of the response explained by the respective component (182), led to a very slight improvement in cohort separation using only 17 proteins (Figure 4.19 A), mainly regarding the PD and control cohorts.



Figure 4.18 PCA analysis of the HMW fraction of serum samples using relative quantification of 39 statistically significant proteins. Analysis was done using autoscaling. Red dots represent AD samples, blue dots PD samples, and green dots control samples. Sample labels are designated as “cohort”_”gender”_”age”. Selected proteins are statistically significant between cohorts with p-value below 0.05, according to Dunn’s test. Generated using R-Studio.

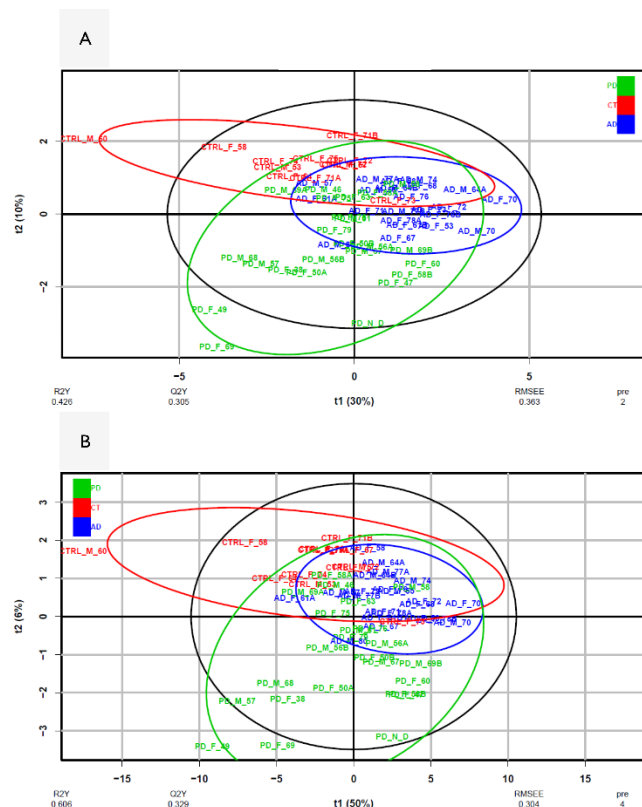


Figure 4.19 PLS-DA analysis of the HMW fraction of serum samples using relative quantification of 39 statistically significant proteins (B) and those selected with VIP values (A). Selected proteins are statistically significant between cohorts with p -value < 0.05, according to Dunn's test. Y is the character factor vector with description of sample class membership according to previous patients' medical diagnosis (whether being Controls or having Alzheimer's/Parkinson's Disease). R2Y represents the fraction of the variation of the Y variables explained by the model, Q2Y represents the fraction of the variation of the Y variables predicted by the model. RMSEE, Root Mean Squared Error of Estimation. Generated using R-Studio.

Table 4.2 Proteins Selected for Second PLS-DA and Respective VIP Values

Accession Number	VIP
P06310	1.68
P35527	1.65
Q9UH36	1.64
P02654	1.39
P01611	1.29
P02743	1.20
P32119	1.19
P0DJ18	1.18
P01709	1.16
Q96KN2	1.15
P68871	1.15
P00915	1.14
P05543	1.12
P02652	1.10
P01009	1.05
P02775	1.04
P05452	1.04

Using the flagged proteins from previous data analysis (Figures 4.14, 4.15, and 4.16), PLS-DA was used for tentative differentiation between the respective cohorts. AD cohort vs control cohort (Figure 4.20 A) showed the most distinctive sample separation profile, with an increased performance as compared to the remaining discriminant analysis (highest Q2Y value). In the case of PD versus control (Figure 4.20 B) there was significant overlap between cohorts, not unlike what was observed for PLS-DA in figure 4.19. although some separation can be visualized. PLS-DA of AD vs PD (Figure 4.20 C) presented the worst performance (lowest Q2Y value) with a clear and overwhelming overlap between plotted samples.

Finally, to try and extract some biological significance from these altered proteins, they were searched in the literature, namely in PubMed. The outcome is in the form of three different tables (Tables S10, S11, and S12), found in section 7.5, each briefly describing the potential relationship between disease and respective proteins.

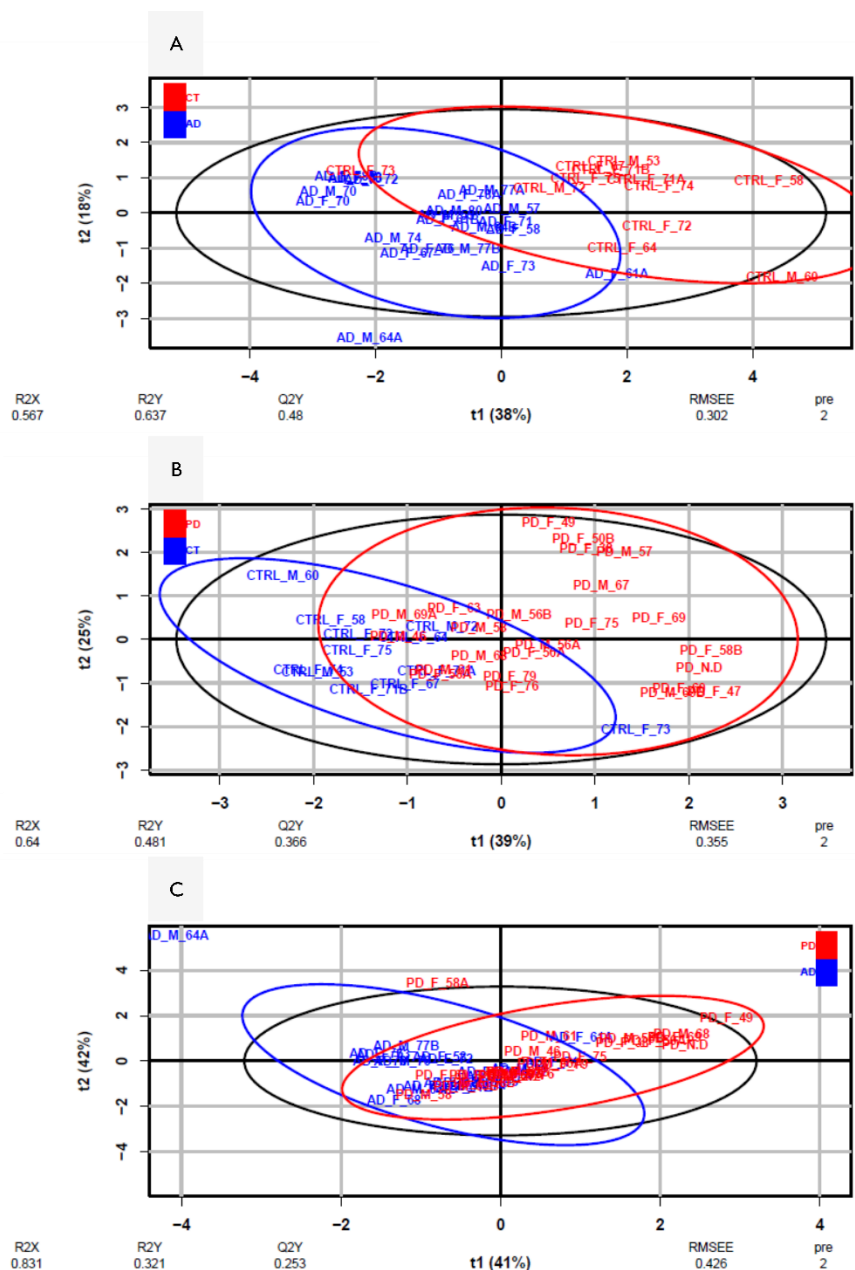


Figure 4.20 PLS-DA analysis of the HMW fraction of serum samples using relative quantification of 11 (A), 5 (B), and 4 (C) statistically significant proteins with fold change above 1.5 or below 0.66. Proteins were chosen from 14 statistically significant and altered proteins for discrimination of AD vs control (A), PD vs control (B), and AD vs PD (C). Selected proteins are statistically significant between the designated cohorts with p -value < 0.05 , according to Dunn's test. Y is the character factor vector with description of sample class membership according to previous patients' medical diagnosis (whether being Controls or having Alzheimer's/Parkinson's Disease). R2Y represents the fraction of the variation of the Y variables explained by the model, Q2Y represents the fraction of the variation of the Y variables predicted by the model. RMSEE, Root Mean Squared Error of Estimation. Generated using R-Studio.

5. General Conclusions

Although some sample separation was achieved and some statistically significant proteins were identified, definitive conclusions as to their potential use as biomarkers of the discussed NDs leaves some space for improvement.

First and foremost, a bibliographic convention and literature review must be elaborated in order to ascertain already documented connections of these proteins to both AD and PD, especially pertaining to their presence in the systemic circulation, far from what is usually the focus of ND-related studies, the brain. Acquiring this knowledge is then of utmost importance for the contextualization of the finding contained herein.

Additionally, validation of these results with larger cohorts and preferably blind samples to confirm these observations must transpire. This procedure will benefit greatly from the use of orthogonal and complementary techniques for protein identification, quantification, and visualization, such as Western Blot analysis of fractionated serum samples.

However, with the interesting finding of LMW proteins with statistical significance and considerable fold changes in HMW serum fractions, analysis of the remainder fraction (below 300 kDa) is also paramount to determine the origin of these quantified protein alterations. If the latter are, for instance, a consequence of overall increases and/or decreases in expression levels, analysis of both fractions should yield similar results (and the same can be said of analysis under denaturing conditions). Conversely, if these proteins are being more abundantly (and unexpectedly) found in HMW fractions, due to the formation of otherwise unobservable increased complexing with each other (or other proteins like protein carriers), then these results should not be reproducible in the opposite (<300 kDa) fraction or by using Western Blot, since this would mean that absolute protein levels are being fairly conserved.

All in all, having a disease-related context of the observed findings, validating them, and testing the latter hypothesis, will definitively create robust foundations on which future ND biomarker discovery-driven research will stand.

6. References

1. ANDERSON, R. M., et al. - Why do so many clinical trials of therapies for Alzheimer's disease fail? *Lancet*. Vol. 390. n.º 10110 (2017). p. 2327-2329. ISSN: 0140-6736
2. DUGGER, B. N.; DICKSON, D. W. - Pathology of Neurodegenerative Diseases. *Cold Spring Harb Perspect Biol*. Vol. 9. n.º 7 (2017). Disponível em WWW: <<https://www.ncbi.nlm.nih.gov/pubmed/28062563>>. ISSN: 1943-0264 (Electronic)
1943-0264 (Linking)
3. LIN, M. T.; BEAL, M. F. - Mitochondrial dysfunction and oxidative stress in neurodegenerative diseases. *Nature*. Vol. 443. n.º 7113 (2006). p. 787-95. ISSN: 0028-0836
4. SOTO, C.; PRITZKOW, S. - Protein misfolding, aggregation, and conformational strains in neurodegenerative diseases. *Nat Neurosci*. Vol. 21. n.º 10 (2018). p. 1332-1340. Disponível em WWW: <<https://www.ncbi.nlm.nih.gov/pubmed/30250260>>. ISSN: 1546-1726 (Electronic)
1097-6256 (Linking)
5. MASTERS, C. L., et al. - Alzheimer's disease. *Nat Rev Dis Primers*. Vol. 1. (2015). p. 15056. Disponível em WWW: <<https://www.ncbi.nlm.nih.gov/pubmed/27188934>>. ISSN: 2056-676X (Electronic)
2056-676X (Linking)
6. LICKER, Virginie; BURKHARD, Pierre R. - Proteomics as a new paradigm to tackle Parkinson's disease research challenges. *Translational Proteomics*. Vol. 4-5. (2014). p. 1-17. ISSN: 22129626
7. NUSSBAUM, R. L.; ELLIS, C. E. - Alzheimer's disease and Parkinson's disease. *N Engl J Med*. Vol. 348. n.º 14 (2003). p. 1356-64. ISSN: 0028-4793
8. MOTA, Bruno; HERCULANO-HOUZEL, Suzana - All brains are made of this: a fundamental building block of brain matter with matching neuronal and glial masses. *Frontiers in Neuroanatomy*. Vol. 8. n.º 127 (2014). Disponível em WWW: <<https://www.frontiersin.org/article/10.3389/fnana.2014.00127>>. ISSN: 1662-5129
9. JUCKER, M.; WALKER, L. C. - Propagation and spread of pathogenic protein assemblies in neurodegenerative diseases. *Nat Neurosci*. Vol. 21. n.º 10 (2018). p. 1341-1349. Disponível em WWW: <<https://www.ncbi.nlm.nih.gov/pubmed/30258241>>. ISSN: 1546-1726 (Electronic)
1097-6256 (Linking)
10. MALKUS, K. A.; TSIKA, E.; ISCHIROPOULOS, H. - Oxidative modifications, mitochondrial dysfunction, and impaired protein degradation in Parkinson's disease: how neurons are lost in the Bermuda triangle. *Mol Neurodegener*. Vol. 4. (2009). p. 24. Disponível em WWW: <<https://www.ncbi.nlm.nih.gov/pubmed/19500376>>. ISSN: 1750-1326 (Electronic)

1750-1326 (Linking)

11. FISCHER, H. - File:Glial Cell Types.png. 2013. ISBN/ISSN:
12. SERRANO-POZO, Alberto, et al. - Neuropathological alterations in Alzheimer disease. *Cold Spring Harbor perspectives in medicine*. Vol. 1. n.º 1 (2011). p. a006189-a006189. Disponível em WWW: <<https://www.ncbi.nlm.nih.gov/pubmed/22229116>

<<https://www.ncbi.nlm.nih.gov/pmc/articles/PMC3234452/>>. ISSN: 2157-1422

13. WYSS-CORAY, T. - Ageing, neurodegeneration and brain rejuvenation. *Nature*. Vol. 539. n.º 7628 (2016). p. 180-186. Disponível em WWW: <<https://www.ncbi.nlm.nih.gov/pubmed/27830812>>. ISSN: 1476-4687 (Electronic)

0028-0836 (Linking)

14. HO, J. Y.; HENDI, A. S. - Recent trends in life expectancy across high income countries: retrospective observational study. *Bmj*. Vol. 362. (2018). p. k2562. ISSN: 0959-8138
15. DILUCA, M.; OLESEN, J. - The cost of brain diseases: a burden or a challenge? *Neuron*. Vol. 82. n.º 6 (2014). p. 1205-8. ISSN: 0896-6273
16. OLESEN, J., et al. - The economic cost of brain disorders in Europe. *Eur J Neurol*. Vol. 19. n.º 1 (2012). p. 155-62. ISSN: 1351-5101
17. PATTERSON, Christina - World Alzheimer Report 2018 The state of the art of dementia research: New frontiers. Alzheimer's Disease International (ADI), 2018. ISBN/ISSN:
18. BANERJEE, Rebecca; BEAL, M. Flint; THOMAS, Bobby - Autophagy in neurodegenerative disorders: pathogenic roles and therapeutic implications. *Trends in neurosciences*. Vol. 33. n.º 12 (2010). p. 541-549. Disponível em WWW: <<https://www.ncbi.nlm.nih.gov/pubmed/20947179>

<<https://www.ncbi.nlm.nih.gov/pmc/articles/PMC2981680/>>. ISSN: 1878-108X

0166-2236

19. DOS SANTOS PICANCO, L. C., et al. - Alzheimer's Disease: A Review from the Pathophysiology to Diagnosis, New Perspectives for Pharmacological Treatment. *Curr Med Chem*. Vol. 25. n.º 26 (2018). p. 3141-3159. Disponível em WWW: <<https://www.ncbi.nlm.nih.gov/pubmed/30191777>>. ISSN: 1875-533X (Electronic)

0929-8673 (Linking)

20. DU, X.; WANG, X.; GENG, M. - Alzheimer's disease hypothesis and related therapies. *Transl Neurodegener*. Vol. 7. (2018). p. 2. Disponível em WWW: <<https://www.ncbi.nlm.nih.gov/pubmed/29423193>>. ISSN: 2047-9158 (Print)

2047-9158 (Linking)

21. KUMAR, A.; SINGH, A.; EKAVALI - A review on Alzheimer's disease pathophysiology and its management: an update. *Pharmacol Rep.* Vol. 67. n.º 2 (2015). p. 195-203. Disponível em WWW: <<https://www.ncbi.nlm.nih.gov/pubmed/25712639>>. ISSN: 1734-1140 (Print)

1734-1140 (Linking)

22. WANG, J., et al. - A systemic view of Alzheimer disease - insights from amyloid-beta metabolism beyond the brain. *Nat Rev Neurol.* Vol. 13. n.º 10 (2017). p. 612-623. Disponível em WWW: <<https://www.ncbi.nlm.nih.gov/pubmed/28960209>>. ISSN: 1759-4766 (Electronic)

1759-4758 (Linking)

23. PETERSEN, R. C., et al. - Mild cognitive impairment: a concept in evolution. *J Intern Med.* Vol. 275. n.º 3 (2014). p. 214-28. ISSN: 0954-6820
24. CARLYLE, B. C.; TROMBETTA, B. A.; ARNOLD, S. E. - Proteomic Approaches for the Discovery of Biofluid Biomarkers of Neurodegenerative Dementias. *Proteomes.* Vol. 6. n.º 3 (2018). Disponível em WWW: <<https://www.ncbi.nlm.nih.gov/pubmed/30200280>>. ISSN: 2227-7382 (Print)

2227-7382 (Linking)

25. BOGDANOVIC, Nenad - The Challenges of Diagnosis in Alzheimer's Disease. *US Neurology.* Vol. 14. n.º 1 (2018). p. 15. ISSN: 1758-4000
26. ALZHEIMER, A., et al. - An English translation of Alzheimer's 1907 paper, "Über eine eigenartige Erkrankung der Hirnrinde". *Clin Anat.* Vol. 8. n.º 6 (1995). p. 429-31. ISSN: 0897-3806 (Print)

0897-3806

27. HIPPIUS, H.; NEUNDORFER, G. - The discovery of Alzheimer's disease. *Dialogues Clin Neurosci.* Vol. 5. n.º 1 (2003). p. 101-8. ISSN: 1294-8322 (Print)

1294-8322

28. MOLLER, H. J.; GRAEBER, M. B. - The case described by Alois Alzheimer in 1911. Historical and conceptual perspectives based on the clinical record and neurohistological sections. *Eur Arch Psychiatry Clin Neurosci.* Vol. 248. n.º 3 (1998). p. 111-22. ISSN: 0940-1334 (Print)

0940-1334

29. FEIGIN, Valery L., et al. - Global, regional, and national burden of neurological disorders, 1990–2016: a systematic analysis for the Global Burden of Disease Study 2016. *The Lancet Neurology.* Vol. 18. n.º 5 (2019). p. 459-480. Consult. em 2019/06/13. Disponível em WWW: <[https://doi.org/10.1016/S1474-4422\(18\)30499-X](https://doi.org/10.1016/S1474-4422(18)30499-X)>. ISSN: 1474-4422

30. HARMAN, D. - Alzheimer's disease: A hypothesis on pathogenesis. *Journal of the American Aging Association*. Vol. 23. n.º 3 (2000). p. 147-161. Disponível em WWW: <<https://www.ncbi.nlm.nih.gov/pubmed/23604855>
<https://www.ncbi.nlm.nih.gov/pmc/articles/PMC3455602/>>. ISSN: 2152-4041
31. MUSIEK, E. S.; HOLTZMAN, D. M. - Three dimensions of the amyloid hypothesis: time, space and 'wingmen'. *Nat Neurosci*. Vol. 18. n.º 6 (2015). p. 800-6. ISSN: 1097-6256
32. LI, Hongmei, et al. - Amyloid, tau, pathogen infection and antimicrobial protection in Alzheimer's disease –conformist, nonconformist, and realistic prospects for AD pathogenesis. *Translational Neurodegeneration*. Vol. 7. n.º 1 (2018). p. 34. Disponível em WWW: <<https://doi.org/10.1186/s40035-018-0139-3>>. ISSN: 2047-9158
33. KAMETANI, Fuyuki; HASEGAWA, Masato - Reconsideration of Amyloid Hypothesis and Tau Hypothesis in Alzheimer's Disease. *Frontiers in neuroscience*. Vol. 12. (2018). p. 25-25. Disponível em WWW: <<https://www.ncbi.nlm.nih.gov/pubmed/29440986>
<https://www.ncbi.nlm.nih.gov/pmc/articles/PMC5797629/>>. ISSN: 1662-4548
1662-453X
34. REITZ, Christiane - Alzheimer's disease and the amyloid cascade hypothesis: a critical review. *International journal of Alzheimer's disease*. Vol. 2012. (2012). p. 369808-369808. Disponível em WWW: <<https://www.ncbi.nlm.nih.gov/pubmed/22506132>
<https://www.ncbi.nlm.nih.gov/pmc/articles/PMC3313573/>>. ISSN: 2090-0252
2090-8024
35. HARDY, J. A.; HIGGINS, G. A. - Alzheimer's disease: the amyloid cascade hypothesis. *Science*. Vol. 256. n.º 5054 (1992). p. 184-5. ISSN: 0036-8075 (Print)
0036-8075
36. SHANKAR, G. M.; WALSH, D. M. - Alzheimer's disease: synaptic dysfunction and Abeta. *Mol Neurodegener*. Vol. 4. (2009). p. 48. Disponível em WWW: <<https://www.ncbi.nlm.nih.gov/pubmed/19930651>>. ISSN: 1750-1326 (Electronic)
1750-1326 (Linking)
37. BRAAK, H.; BRAAK, E. - Neuropathological staging of Alzheimer-related changes. *Acta Neuropathol*. Vol. 82. n.º 4 (1991). p. 239-59. ISSN: 0001-6322 (Print)
0001-6322
38. HAASS, C., et al. - Trafficking and proteolytic processing of APP. *Cold Spring Harb Perspect Med*. Vol. 2. n.º 5 (2012). p. a006270. ISSN: 2157-1422

39. BREDESEN, D. E. - Neurodegeneration in Alzheimer's disease: caspases and synaptic element interdependence. *Mol Neurodegener.* Vol. 4. (2009). p. 27. Disponível em WWW: <<https://www.ncbi.nlm.nih.gov/pubmed/19558683>>. ISSN: 1750-1326 (Electronic)

1750-1326 (Linking)

40. THAL, Dietmar R., et al. - Phases of A β -deposition in the human brain and its relevance for the development of AD. *Neurology.* Vol. 58. n.º 12 (2002). p. 1791-1800. Disponível em WWW: <<https://n.neurology.org/content/neurology/58/12/1791.full.pdf>>. ISSN:
41. KUHN, P. H., et al. - ADAM10 is the physiologically relevant, constitutive alpha-secretase of the amyloid precursor protein in primary neurons. *Embo j.* Vol. 29. n.º 17 (2010). p. 3020-32. ISSN: 0261-4189
42. STEINER, H.; FLUHRER, R.; HAASS, C. - Intramembrane proteolysis by gamma-secretase. *J Biol Chem.* Vol. 283. n.º 44 (2008). p. 29627-31. ISSN: 0021-9258 (Print)

0021-9258

43. YAMADA, M. - Cerebral amyloid angiopathy: emerging concepts. *J Stroke.* Vol. 17. n.º 1 (2015). p. 17-30. ISSN: 2287-6391 (Print)

2287-6391

44. BARGHORN, Stefan; DAVIES, Peter; MANDELKOW, Eckhard - Tau Paired Helical Filaments from Alzheimer's Disease Brain and Assembled in Vitro Are Based on β -Structure in the Core Domain. *Biochemistry.* Vol. 43. n.º 6 (2004). p. 1694-1703. Disponível em WWW: <<https://doi.org/10.1021/bi0357006>>. ISSN: 0006-2960
45. FITZPATRICK, Anthony W. P., et al. - Cryo-EM structures of tau filaments from Alzheimer's disease. *Nature.* Vol. 547. (2017). p. 185. Disponível em WWW: <<https://doi.org/10.1038/nature23002>>. ISSN:
46. GENDRON, T. F.; PETRUCELLI, L. - The role of tau in neurodegeneration. *Mol Neurodegener.* Vol. 4. (2009). p. 13. Disponível em WWW: <<https://www.ncbi.nlm.nih.gov/pubmed/19284597>>. ISSN: 1750-1326 (Electronic)

1750-1326 (Linking)

47. MARAMBAUD, P.; DRESES-WERRINGLOER, U.; VINGTDEUX, V. - Calcium signaling in neurodegeneration. *Mol Neurodegener.* Vol. 4. (2009). p. 20. Disponível em WWW: <<https://www.ncbi.nlm.nih.gov/pubmed/19419557>>. ISSN: 1750-1326 (Electronic)

1750-1326 (Linking)

48. MUKHIN, V. N.; PAVLOV, K. I.; KLIMENKO, V. M. - Mechanisms of Neuron Loss in Alzheimer's Disease. *Neuroscience and Behavioral Physiology.* Vol. 47. n.º 5

- (2017). p. 508-516. Disponível em WWW: <<https://doi.org/10.1007/s11055-017-0427-x>>. ISSN: 1573-899X
49. INGELSSON, M., et al. - Early Abeta accumulation and progressive synaptic loss, gliosis, and tangle formation in AD brain. *Neurology*. Vol. 62. n.º 6 (2004). p. 925-31. ISSN: 0028-3878
50. SERRANO-POZO, A., et al. - Reactive glia not only associates with plaques but also parallels tangles in Alzheimer's disease. *Am J Pathol*. Vol. 179. n.º 3 (2011). p. 1373-84. ISSN: 0002-9440
51. HENEKA, M. T., et al. - Neuroinflammation in Alzheimer's disease. *Lancet Neurol*. Vol. 14. n.º 4 (2015). p. 388-405. ISSN: 1474-4422
52. OSBORN, L. M., et al. - Astroglia: An integral player in the pathogenesis of Alzheimer's disease. *Prog Neurobiol*. Vol. 144. (2016). p. 121-41. ISSN: 0301-0082
53. PEKNY, Milos; PEKNA, Marcela - Reactive gliosis in the pathogenesis of CNS diseases. *Biochimica et Biophysica Acta (BBA) - Molecular Basis of Disease*. Vol. 1862. n.º 3 (2016). p. 483-491. Disponível em WWW: <<http://www.sciencedirect.com/science/article/pii/S0925443915003531>>. ISSN: 0925-4439
54. KRAFT, A. W., et al. - Attenuating astrocyte activation accelerates plaque pathogenesis in APP/PS1 mice. *FASEB J*. Vol. 27. n.º 1 (2013). p. 187-98. ISSN: 0892-6638
55. FUNK, K. E.; MRAK, R. E.; KURET, J. - Granulovacuolar degeneration (GVD) bodies of Alzheimer's disease (AD) resemble late-stage autophagic organelles. *Neuropathol Appl Neurobiol*. Vol. 37. n.º 3 (2011). p. 295-306. ISSN: 0305-1846
56. KURDI, M.; CHIN, E.; ANG, L. C. - Granulovacuolar Degeneration in Hippocampus of Neurodegenerative Diseases: Quantitative Study. *J Neurodegener Dis*. Vol. 2016. (2016). p. 6163186. ISSN: 2090-858X (Print)
2090-8601
57. SPEARS, W., et al. - Hirano bodies differentially modulate cell death induced by tau and the amyloid precursor protein intracellular domain. *BMC Neurosci*. Vol. 15. (2014). p. 74. ISSN: 1471-2202
58. CHIROMA, Samaila Musa, et al. - Inflammation in Alzheimer's disease: A friend or foe? *Biomedical Research and Therapy*. Vol. 5. n.º 8 (2018). p. 2552-2564. Consult. em 2019/07/02. Disponível em WWW: <<https://app.dimensions.ai/details/publication/pub.1106278738>>
<<http://www.bmrat.org/index.php/BMRAT/article/download/464/916>>. ISSN:
59. CHECHIK, Gal; MEILIJSON, Isaac; RUPPIN, Eytan - Synaptic Pruning in Development: A Computational Account. *Neural Computation*. Vol. 10. n.º 7 (1998). p. 1759-1777. Disponível em WWW: <<https://www.mitpressjournals.org/doi/abs/10.1162/089976698300017124>>. ISSN:

60. ALZHEIMER, A. - Über eigenartige Krankheitsfälle des späteren Alters:(On certain peculiar diseases of old age. *History of Psychiatry*. Vol. 2. n.º 5 (1991). p. 74-101. Disponível em WWW: <<https://journals.sagepub.com/doi/abs/10.1177/0957154X9100200506>>. ISSN: 0353-5053
61. PADURARIU, M., et al. - The oxidative stress hypothesis in Alzheimer's disease. *Psychiatr Danub*. Vol. 25. n.º 4 (2013). p. 401-9. ISSN: 0353-5053 (Print)
- 0353-5053
62. MARKESBERY, W. R. - Oxidative stress hypothesis in Alzheimer's disease. *Free Radic Biol Med*. Vol. 23. n.º 1 (1997). p. 134-47. ISSN: 0891-5849 (Print)
- 0891-5849
63. HUANG, W. J.; ZHANG, X.; CHEN, W. W. - Role of oxidative stress in Alzheimer's disease. *Biomed Rep*. Vol. 4. n.º 5 (2016). p. 519-522. ISSN: 2049-9434 (Print)
- 2049-9434
64. PRATICÒ, Domenico - Oxidative stress hypothesis in Alzheimer's disease: a reappraisal. *Trends in Pharmacological Sciences*. Vol. 29. n.º 12 (2008). p. 609-615. Disponível em WWW: <<http://www.sciencedirect.com/science/article/pii/S0165614708002071>>. ISSN: 0165-6147
65. SWERDLOW, Russell H. - Mitochondria and Mitochondrial Cascades in Alzheimer's Disease. *Journal of Alzheimer's disease : JAD*. Vol. 62. n.º 3 (2018). p. 1403-1416. Disponível em WWW: <<https://www.ncbi.nlm.nih.gov/pubmed/29036828>>. ISSN: 1875-8908
- <https://www.ncbi.nlm.nih.gov/pmc/articles/PMC5869994/>>. ISSN: 1875-8908
- 1387-2877
66. CARDOSO, S. M., et al. - Functional mitochondria are required for amyloid beta-mediated neurotoxicity. *Faseb j*. Vol. 15. n.º 8 (2001). p. 1439-41. ISSN: 0892-6638 (Print)
- 0892-6638
67. KHAN, S. M., et al. - Alzheimer's disease cybrids replicate beta-amyloid abnormalities through cell death pathways. *Ann Neurol*. Vol. 48. n.º 2 (2000). p. 148-55. ISSN: 0364-5134 (Print)
- 0364-5134
68. RIDGE, Perry G.; KAUWE, John S. K. - Mitochondria and Alzheimer's Disease: the Role of Mitochondrial Genetic Variation. *Current Genetic Medicine Reports*. Vol. 6. n.º 1 (2018). p. 1-10. Disponível em WWW: <<https://doi.org/10.1007/s40142-018-0132-2>>. ISSN: 2167-4876

69. KOWALSKI, Karol; MULAK, Agata - Brain-Gut-Microbiota Axis in Alzheimer's Disease. *Journal of neurogastroenterology and motility*. Vol. 25. n.º 1 (2019). p. 48-60. Disponível em WWW: <<https://www.ncbi.nlm.nih.gov/pubmed/30646475>
<https://www.ncbi.nlm.nih.gov/pmc/articles/PMC6326209/>>. ISSN: 2093-0879
2093-0887
70. FUNDERBURK, Sarah F.; MARCELLINO, Bridget K.; YUE, Zhenyu - Cell "self-eating" (autophagy) mechanism in Alzheimer's disease. *The Mount Sinai journal of medicine, New York*. Vol. 77. n.º 1 (2010). p. 59-68. Disponível em WWW: <<https://www.ncbi.nlm.nih.gov/pubmed/20101724>
<https://www.ncbi.nlm.nih.gov/pmc/articles/PMC2835623/>>. ISSN: 1931-7581
0027-2507
71. KARABIYIK, Cansu; LEE, Min Jae; RUBINSZTEIN, David C. - Autophagy impairment in Parkinson's disease. *Essays In Biochemistry*. Vol. 61. n.º 6 (2017). p. 711-720. Disponível em WWW: <<http://essays.biochemistry.org/content/ppebio/61/6/711.full.pdf>>. ISSN:
72. LYNCH-DAY, Melinda A., et al. - The role of autophagy in Parkinson's disease. *Cold Spring Harbor perspectives in medicine*. Vol. 2. n.º 4 (2012). p. a009357-a009357. Disponível em WWW: <<https://www.ncbi.nlm.nih.gov/pubmed/22474616>
<https://www.ncbi.nlm.nih.gov/pmc/articles/PMC3312403/>>. ISSN: 2157-1422
73. NILSSON, Per; SAIDO, Takaomi C. - Dual roles for autophagy: degradation and secretion of Alzheimer's disease A β peptide. *BioEssays : news and reviews in molecular, cellular and developmental biology*. Vol. 36. n.º 6 (2014). p. 570-578. Disponível em WWW: <<https://www.ncbi.nlm.nih.gov/pubmed/24711225>
<https://www.ncbi.nlm.nih.gov/pmc/articles/PMC4316186/>>. ISSN: 1521-1878
0265-9247
74. UDDIN, Md Sahab, et al. - Autophagy and Alzheimer's Disease: From Molecular Mechanisms to Therapeutic Implications. *Frontiers in aging neuroscience*. Vol. 10. (2018). p. 04-04. Disponível em WWW: <<https://www.ncbi.nlm.nih.gov/pubmed/29441009>
<https://www.ncbi.nlm.nih.gov/pmc/articles/PMC5797541/>>. ISSN: 1663-4365
75. NILSSON, P., et al. - Abeta secretion and plaque formation depend on autophagy. *Cell Rep*. Vol. 5. n.º 1 (2013). p. 61-9. ISSN:
76. DORSEY, E. Ray, et al. - Global, regional, and national burden of Parkinson's disease, 1990–2016: a systematic analysis for the Global Burden of Disease Study 2016. *The Lancet Neurology*. Vol. 17. n.º 11 (2018). p. 939-953. Consult. em 2019/07/18. Disponível em WWW: <[https://doi.org/10.1016/S1474-4422\(18\)30295-3](https://doi.org/10.1016/S1474-4422(18)30295-3)>. ISSN: 1474-4422

77. PARKINSON, J. - An essay on the shaking palsy. 1817. *J Neuropsychiatry Clin Neurosci*. Vol. 14. n.º 2 (2002). p. 223-36; discussion 222. ISSN: 0895-0172 (Print)
0895-0172
78. GOETZ, Christopher G. - The history of Parkinson's disease: early clinical descriptions and neurological therapies. *Cold Spring Harbor perspectives in medicine*. Vol. 1. n.º 1 (2011). p. a008862-a008862. Disponível em WWW: <<https://www.ncbi.nlm.nih.gov/pubmed/22229124>>
<<https://www.ncbi.nlm.nih.gov/pmc/articles/PMC3234454/>>. ISSN: 2157-1422
79. ANTONY, P. M., et al. - The hallmarks of Parkinson's disease. *Febs j*. Vol. 280. n.º 23 (2013). p. 5981-93. ISSN: 1742-464x
80. LASTRES-BECKER, Isabel - Role of the Transcription Factor Nrf2 in Parkinson's Disease: New Insights. *Journal of Alzheimer's Disease & Parkinsonism*. Vol. 07. (2017). ISSN:
81. POEWE, Werner, et al. - Parkinson disease. *Nature Reviews Disease Primers*. Vol. 3. (2017). p. 17013. Disponível em WWW: <<https://doi.org/10.1038/nrdp.2017.13>>. ISSN:
82. RADHAKRISHNAN, D. M.; GOYAL, V. - Parkinson's disease: A review. *Neurol India*. Vol. 66. n.º Supplement (2018). p. S26-s35. ISSN: 0028-3886 (Print)
0028-3886
83. ROCCA, Walter A. - The burden of Parkinson's disease: a worldwide perspective. *The Lancet Neurology*. Vol. 17. n.º 11 (2018). p. 928-929. Consult. em 2019/07/18. Disponível em WWW: <[https://doi.org/10.1016/S1474-4422\(18\)30355-7](https://doi.org/10.1016/S1474-4422(18)30355-7)>. ISSN: 1474-4422
84. LIX, L. M., et al. - Socioeconomic variations in the prevalence and incidence of Parkinson's disease: a population-based analysis. *J Epidemiol Community Health*. Vol. 64. n.º 4 (2010). p. 335-40. ISSN: 0143-005x
85. LANGSTON, J. W.; BALLARD, P. A., Jr. - Parkinson's disease in a chemist working with 1-methyl-4-phenyl-1,2,5,6-tetrahydropyridine. *N Engl J Med*. Vol. 309. n.º 5 (1983). p. 310. ISSN: 0028-4793 (Print)
0028-4793
86. MOSTAFALOU, S.; ABDOLLAHI, M. - The link of organophosphorus pesticides with neurodegenerative and neurodevelopmental diseases based on evidence and mechanisms. *Toxicology*. Vol. 409. (2018). p. 44-52. ISSN: 0300-483x
87. RICHARDSON, Jason R., et al. - Elevated serum pesticide levels and risk of Parkinson disease. *Archives of neurology*. Vol. 66. n.º 7 (2009). p. 870-875. Disponível em WWW: <<https://www.ncbi.nlm.nih.gov/pubmed/19597089>>
<<https://www.ncbi.nlm.nih.gov/pmc/articles/PMC3383784/>>. ISSN: 1538-3687

0003-9942

88. WIRDEFELDT, K., et al. - Epidemiology and etiology of Parkinson's disease: a review of the evidence. *Eur J Epidemiol.* Vol. 26 Suppl 1. (2011). p. S1-58. ISSN: 0393-2990
89. RABEY, J. M.; KORCZYN, A. D. - The Hoehn and Yahr Rating Scale for Parkinson's Disease. Berlin, Heidelberg: Springer Berlin Heidelberg, 1995. ISBN/ISSN: 978-3-642-78914-4
90. BRAAK, H., et al. - Staging of brain pathology related to sporadic Parkinson's disease. *Neurobiol Aging.* Vol. 24. n.º 2 (2003). p. 197-211. ISSN: 0197-4580 (Print)

0197-4580

91. HOEHN, M. M.; YAHR, M. D. - Parkinsonism: onset, progression and mortality. *Neurology.* Vol. 17. n.º 5 (1967). p. 427-42. ISSN: 0028-3878 (Print)

0028-3878

92. COOKSON, M. R. - alpha-Synuclein and neuronal cell death. *Mol Neurodegener.* Vol. 4. (2009). p. 9. Disponível em WWW: <<https://www.ncbi.nlm.nih.gov/pubmed/19193223>>. ISSN: 1750-1326 (Electronic)

1750-1326 (Linking)

93. TURRENS, J. F. - Mitochondrial formation of reactive oxygen species. *J Physiol.* Vol. 552. n.º Pt 2 (2003). p. 335-44. ISSN: 0022-3751 (Print)

0022-3751

94. ORHAN, H., et al. - Evaluation of a multi-parameter biomarker set for oxidative damage in man: increased urinary excretion of lipid, protein and DNA oxidation products after one hour of exercise. *Free Radic Res.* Vol. 38. n.º 12 (2004). p. 1269-79. ISSN: 1071-5762 (Print)

1029-2470

95. BOSCO, Daryl A., et al. - Elevated levels of oxidized cholesterol metabolites in Lewy body disease brains accelerate α -synuclein fibrilization. *Nature Chemical Biology.* Vol. 2. n.º 5 (2006). p. 249-253. Disponível em WWW: <<https://doi.org/10.1038/nchembio782>>. ISSN: 1552-4469
96. NAKABEPPU, Yusaku, et al. - Oxidative damage in nucleic acids and Parkinson's disease. *Journal of Neuroscience Research.* Vol. 85. n.º 5 (2007). p. 919-934. Disponível em WWW: <<https://onlinelibrary.wiley.com/doi/abs/10.1002/jnr.21191>>. ISSN: 0360-4012
97. BRUNDIN, Patrik; MELKI, Ronald - Prying into the Prion Hypothesis for Parkinson's Disease. *The Journal of Neuroscience.* Vol. 37. n.º 41 (2017). p. 9808-9818. Disponível em WWW: <<https://www.jneurosci.org/content/jneuro/37/41/9808.full.pdf>>. ISSN:

98. OLANOW, C. Warren; PRUSINER, Stanley B. - Is Parkinson's disease a prion disorder? *Proceedings of the National Academy of Sciences of the United States of America*. Vol. 106. n.º 31 (2009). p. 12571-12572. Disponível em WWW: <<https://www.ncbi.nlm.nih.gov/pubmed/19666621>

<https://www.ncbi.nlm.nih.gov/pmc/articles/PMC2722298/>>. ISSN: 1091-6490

0027-8424

99. HAWKES, C. H.; DEL TREDICI, K.; BRAAK, H. - Parkinson's disease: a dual-hit hypothesis. *Neuropathol Appl Neurobiol*. Vol. 33. n.º 6 (2007). p. 599-614. ISSN: 0305-1846 (Print)

0305-1846

100. HAWKES, C. H.; DEL TREDICI, K.; BRAAK, H. - Parkinson's disease: the dual hit theory revisited. *Ann N Y Acad Sci*. Vol. 1170. (2009). p. 615-22. ISSN: 0077-8923

101. PEREZ-PARDO, Paula, et al. - The gut-brain axis in Parkinson's disease: Possibilities for food-based therapies. *European Journal of Pharmacology*. Vol. 817. (2017). p. 86-95. Disponível em WWW: <<http://www.sciencedirect.com/science/article/pii/S0014299917303734>>. ISSN: 0014-2999

102. RIETDIJK, Carmen D., et al. - Exploring Braak's Hypothesis of Parkinson's Disease. *Frontiers in neurology*. Vol. 8. (2017). p. 37-37. Disponível em WWW: <<https://www.ncbi.nlm.nih.gov/pubmed/28243222>

<https://www.ncbi.nlm.nih.gov/pmc/articles/PMC5304413/>>. ISSN: 1664-2295

103. DOTY, R. L.; MARCUS, A.; LEE, W. W. - Development of the 12-item Cross-Cultural Smell Identification Test (CC-SIT). *Laryngoscope*. Vol. 106. n.º 3 Pt 1 (1996). p. 353-6. ISSN: 0023-852X (Print)

0023-852x

104. VISANJI, Naomi P., et al. - The prion hypothesis in Parkinson's disease: Braak to the future. *Acta neuropathologica communications*. Vol. 1. (2013). p. 2-2. Disponível em WWW: <<https://www.ncbi.nlm.nih.gov/pubmed/24252164>

<https://www.ncbi.nlm.nih.gov/pmc/articles/PMC3776210/>>. ISSN: 2051-5960

105. CALIFF, Robert M. - Biomarker definitions and their applications. *Experimental biology and medicine (Maywood, N.J.)*. Vol. 243. n.º 3 (2018). p. 213-221. Disponível em WWW: <<https://www.ncbi.nlm.nih.gov/pubmed/29405771>

<https://www.ncbi.nlm.nih.gov/pmc/articles/PMC5813875/>>. ISSN: 1535-3699

1535-3702

106. MARTINS-DE-SOUZA, D. - Is the word 'biomarker' being properly used by proteomics research in neuroscience? *Eur Arch Psychiatry Clin Neurosci*. Vol. 260.

n.º 7 (2010). p. 561-2. Disponível em WWW:
<<https://www.ncbi.nlm.nih.gov/pubmed/20155362>>. ISSN: 1433-8491 (Electronic)

0940-1334 (Linking)

107. BEACH, T. G. - A Review of Biomarkers for Neurodegenerative Disease: Will They Swing Us Across the Valley? *Neurol Ther.* Vol. 6. n.º Suppl 1 (2017). p. 5-13. Disponível em WWW: <<https://www.ncbi.nlm.nih.gov/pubmed/28733961>>. ISSN: 2193-8253 (Print)

2193-6536 (Linking)

108. ARONSON, J. K. - Biomarkers and surrogate endpoints. *British journal of clinical pharmacology.* Vol. 59. n.º 5 (2005). p. 491-494. Disponível em WWW: <<https://www.ncbi.nlm.nih.gov/pubmed/15842546>

<https://www.ncbi.nlm.nih.gov/pmc/articles/PMC1884846/>>. ISSN: 0306-5251

1365-2125

109. HAMPEL, H., et al. - Blood-based biomarkers for Alzheimer disease: mapping the road to the clinic. *Nat Rev Neurol.* Vol. 14. n.º 11 (2018). p. 639-652. Disponível em WWW: <<https://www.ncbi.nlm.nih.gov/pubmed/30297701>>. ISSN: 1759-4766 (Electronic)

1759-4758 (Linking)

110. BLENNOW, Kaj; ZETTERBERG, Henrik; FAGAN, Anne M. - Fluid biomarkers in Alzheimer disease. *Cold Spring Harbor perspectives in medicine.* Vol. 2. n.º 9 (2012). p. a006221-a006221. Disponível em WWW: <<https://www.ncbi.nlm.nih.gov/pubmed/22951438>

<https://www.ncbi.nlm.nih.gov/pmc/articles/PMC3426814/>>. ISSN: 2157-1422

111. LEWCZUK, Piotr, et al. - Cerebrospinal fluid and blood biomarkers for neurodegenerative dementias: An update of the Consensus of the Task Force on Biological Markers in Psychiatry of the World Federation of Societies of Biological Psychiatry. *The world journal of biological psychiatry : the official journal of the World Federation of Societies of Biological Psychiatry.* Vol. 19. n.º 4 (2018). p. 244-328. Disponível em WWW: <<https://www.ncbi.nlm.nih.gov/pubmed/29076399>

<https://www.ncbi.nlm.nih.gov/pmc/articles/PMC5916324/>>. ISSN: 1814-1412

1562-2975

112. SHI, L., et al. - A Decade of Blood Biomarkers for Alzheimer's Disease Research: An Evolving Field, Improving Study Designs, and the Challenge of Replication. *J Alzheimers Dis.* Vol. 62. n.º 3 (2018). p. 1181-1198. Disponível em WWW: <<https://www.ncbi.nlm.nih.gov/pubmed/29562526>>. ISSN: 1875-8908 (Electronic)

1387-2877 (Linking)

113. LASHLEY, T., et al. - Molecular biomarkers of Alzheimer's disease: progress and prospects. *Dis Model Mech.* Vol. 11. n.º 5 (2018). Disponível em WWW: <<https://www.ncbi.nlm.nih.gov/pubmed/29739861>>. ISSN: 1754-8411 (Electronic)

1754-8403 (Linking)

114. COVA, Ilaria; PRIORI, Alberto - Diagnostic biomarkers for Parkinson's disease at a glance: where are we? *Journal of neural transmission (Vienna, Austria : 1996).* Vol. 125. n.º 10 (2018). p. 1417-1432. Disponível em WWW: <<https://www.ncbi.nlm.nih.gov/pubmed/30145631>

<https://www.ncbi.nlm.nih.gov/pmc/articles/PMC6132920/>>. ISSN: 1435-1463

0300-9564

115. JOACHIM, C. L.; MORI, H.; SELKOE, D. J. - Amyloid beta-protein deposition in tissues other than brain in Alzheimer's disease. *Nature.* Vol. 341. n.º 6239 (1989). p. 226-30. ISSN: 0028-0836 (Print)

0028-0836

116. HYE, A., et al. - Proteome-based plasma biomarkers for Alzheimer's disease. *Brain.* Vol. 129. n.º Pt 11 (2006). p. 3042-50. ISSN: 0006-8950

117. GUNTERT, A., et al. - Plasma gelsolin is decreased and correlates with rate of decline in Alzheimer's disease. *J Alzheimers Dis.* Vol. 21. n.º 2 (2010). p. 585-96. ISSN: 1387-2877

118. HAKOBYAN, S., et al. - Complement Biomarkers as Predictors of Disease Progression in Alzheimer's Disease. *J Alzheimers Dis.* Vol. 54. n.º 2 (2016). p. 707-16. ISSN: 1387-2877

119. THAMBISETTY, Madhav, et al. - Association of plasma clusterin concentration with severity, pathology, and progression in Alzheimer disease. *Archives of general psychiatry.* Vol. 67. n.º 7 (2010). p. 739-748. Disponível em WWW: <<https://www.ncbi.nlm.nih.gov/pubmed/20603455>

<https://www.ncbi.nlm.nih.gov/pmc/articles/PMC3111021/>>. ISSN: 1538-3636

0003-990X

120. NEERGAARD, J. S., et al. - Two novel blood-based biomarker candidates measuring degradation of tau are associated with dementia: A prospective study. *PLoS One.* Vol. 13. n.º 4 (2018). p. e0194802. Disponível em WWW: <<https://www.ncbi.nlm.nih.gov/pubmed/29641555>>. ISSN: 1932-6203 (Electronic)

1932-6203 (Linking)

121. CHAKRABARTI, Sasanka, et al. - Serum biomarkers of Alzheimer's disease: Utility in differential diagnosis and implications in pathogenesis. *Alzheimer's & Dementia.* Vol. 8. n.º 4 (2012). p. P110. ISSN: 15525260

122. ZABEL, M., et al. - Assessing candidate serum biomarkers for Alzheimer's disease: a longitudinal study. *J Alzheimers Dis.* Vol. 30. n.º 2 (2012). p. 311-21. ISSN: 1387-2877
123. BA, F.; MARTIN, W. R. - Dopamine transporter imaging as a diagnostic tool for parkinsonism and related disorders in clinical practice. *Parkinsonism Relat Disord.* Vol. 21. n.º 2 (2015). p. 87-94. ISSN: 1353-8020
124. BROOKS, David J.; PAVESE, Nicola - Imaging biomarkers in Parkinson's disease. *Progress in Neurobiology.* Vol. 95. n.º 4 (2011). p. 614-628. Disponível em WWW: <<http://www.sciencedirect.com/science/article/pii/S0301008211001547>>. ISSN: 0301-0082
125. CHAHINE, Lana M., et al. - Feasibility and Safety of Multicenter Tissue and Biofluid Sampling for α -Synuclein in Parkinson's Disease: The Systemic Synuclein Sampling Study (S4). *Journal of Parkinson's disease.* Vol. 8. n.º 4 (2018). p. 517-527. Disponível em WWW: <<https://www.ncbi.nlm.nih.gov/pubmed/30248065>
<<https://www.ncbi.nlm.nih.gov/pmc/articles/PMC6226302/>>. ISSN: 1877-718X
1877-7171
126. LEHÉRICY, Stéphane, et al. - 7 tesla magnetic resonance imaging: A closer look at substantia nigra anatomy in Parkinson's disease. *Movement Disorders.* Vol. 29. n.º 13 (2014). p. 1574-1581. Disponível em WWW: <<https://onlinelibrary.wiley.com/doi/abs/10.1002/mds.26043>>. ISSN: 0885-3185
127. VISANJI, N. P., et al. - The Systemic Synuclein Sampling Study: toward a biomarker for Parkinson's disease. *Biomark Med.* Vol. 11. n.º 4 (2017). p. 359-368. ISSN: 1752-0363
128. LEE, John M., et al. - The Search for a Peripheral Biopsy Indicator of α -Synuclein Pathology for Parkinson Disease. *Journal of Neuropathology & Experimental Neurology.* Vol. 76. n.º 1 (2017). p. 2-15. Consult. em 9/1/2019. Disponível em WWW: <<https://doi.org/10.1093/jnen/nlw103>>. ISSN: 0022-3069
129. YAZDANI, U., et al. - Blood biomarker for Parkinson disease: peptoids. *NPJ Parkinsons Dis.* Vol. 2. (2016). Disponível em WWW: <<https://www.ncbi.nlm.nih.gov/pubmed/27812535>>. ISSN: 2373-8057 (Print)
2373-8057 (Linking)
130. DEMARSHALL, Cassandra; SARKAR, Abhirup; NAGELE, Robert - Serum Autoantibodies as Biomarkers for Parkinson's Disease: Background and Utility. *AIMS Medical Science.* Vol. 2. (2015). p. 316-327. ISSN:
131. DUFEK, M., et al. - Serum inflammatory biomarkers in Parkinson's disease. *Parkinsonism Relat Disord.* Vol. 15. n.º 4 (2009). p. 318-20. Disponível em WWW: <<https://www.ncbi.nlm.nih.gov/pubmed/18672391>>. ISSN: 1873-5126 (Electronic)
1353-8020 (Linking)

132. ALBERIO, T., et al. - Parkinson's disease plasma biomarkers: an automated literature analysis followed by experimental validation. *J Proteomics*. Vol. 90. (2013). p. 107-14. Disponível em WWW: <<https://www.ncbi.nlm.nih.gov/pubmed/23385359>>. ISSN: 1876-7737 (Electronic)
- 1874-3919 (Linking)
133. WANG, Yu, et al. - Phosphorylated α -Synuclein in Parkinson's Disease. *Science Translational Medicine*. Vol. 4. n.º 121 (2012). p. 121ra20-121ra20. Disponível em WWW: <<https://stm.sciencemag.org/content/scitransmed/4/121/121ra20.full.pdf>>. ISSN:
134. PAN, C., et al. - Targeted discovery and validation of plasma biomarkers of Parkinson's disease. *J Proteome Res*. Vol. 13. n.º 11 (2014). p. 4535-45. Disponível em WWW: <<https://www.ncbi.nlm.nih.gov/pubmed/24853996>>. ISSN: 1535-3907 (Electronic)
- 1535-3893 (Linking)
135. CHAHINE, Lama M.; STERN, Matthew B.; CHEN-PLOTKIN, Alice - Blood-based biomarkers for Parkinson's disease. *Parkinsonism & Related Disorders*. Vol. 20. (2014). p. S99-S103. ISSN: 13538020
136. ROSADO, Miguel, et al. - Advances in Clinical Chemistry. Elsevier, 2019. Disponível em WWW: <<http://www.sciencedirect.com/science/article/pii/S0065242319300290>>. Cap. - Chapter Four - Advances in biomarker detection: Alternative approaches for blood-based biomarker detection. ISBN: 0065-2423
137. ANTORANZ, Asier, et al. - Mechanism-based biomarker discovery. *Drug Discovery Today*. Vol. 22. n.º 8 (2017). p. 1209-1215. Disponível em WWW: <<http://www.sciencedirect.com/science/article/pii/S1359644617301915>>. ISSN: 1359-6446
138. LEE, Joon Kyu; JEONG, Sangseom - Immediate Settlement of Ring Footings Resting on Inhomogeneous Finite Stratum. *Applied Sciences*. Vol. 8. n.º 2 (2018). p. 255. Disponível em WWW: <<https://www.mdpi.com/2076-3417/8/2/255>>. ISSN: 2076-3417
139. MENDY, Maimuna, et al. - Biospecimens and Biobanking in Global Health. *Clinics in Laboratory Medicine*. Vol. 38. n.º 1 (2018). p. 183-207. Disponível em WWW: <<http://www.sciencedirect.com/science/article/pii/S027227121730118X>>. ISSN: 0272-2712
140. ANJO, Sandra Isabel; SANTA, Cátia; MANADAS, Bruno - SWATH-MS as a tool for biomarker discovery: From basic research to clinical applications. *PROTEOMICS*. Vol. 17. n.º 3-4 (2017). p. 1600278. Disponível em WWW: <<https://onlinelibrary.wiley.com/doi/abs/10.1002/pmic.201600278>>. ISSN: 1615-9853
141. ANJO, Sandra I.; MANADAS, Bruno - A translational view of cells' secretome analysis - from untargeted proteomics to potential circulating biomarkers. *Biochimie*. Vol. 155. (2018). p. 37-49. Disponível em WWW:

<<http://www.sciencedirect.com/science/article/pii/S0300908418301305>>. ISSN: 0300-9084

142. MOHAMADKHANI, A.; POUSTCHI, H. - Repository of Human Blood Derivative Biospecimens in Biobank: Technical Implications. *Middle East J Dig Dis*. Vol. 7. n.º 2 (2015). p. 61-8. ISSN: 2008-5230 (Print)

2008-5230

143. SUBRAMANYAM, Meena; GOYAL, Jaya - Translational biomarkers: from discovery and development to clinical practice. *Drug Discovery Today: Technologies*. Vol. 21-22. (2016). p. 3-10. Disponível em WWW: <<http://www.sciencedirect.com/science/article/pii/S1740674916300324>>. ISSN: 1740-6749

144. THÉRY, Clotilde, et al. - Minimal information for studies of extracellular vesicles 2018 (MISEV2018): a position statement of the International Society for Extracellular Vesicles and update of the MISEV2014 guidelines. *Journal of Extracellular Vesicles*. Vol. 7. n.º 1 (2018). p. 1535750. Disponível em WWW: <<https://doi.org/10.1080/20013078.2018.1535750>>. ISSN: null

145. GEYER, Philipp E, et al. - Revisiting biomarker discovery by plasma proteomics. *Molecular Systems Biology*. Vol. 13. n.º 9 (2017). p. 942. Disponível em WWW: <<https://www.embopress.org/doi/abs/10.15252/msb.20156297>>. ISSN: 1744-4292

146. DE BOCK, Muriel, et al. - Challenges for biomarker discovery in body fluids using SELDI-TOF-MS. *Journal of biomedicine & biotechnology*. Vol. 2010. (2010). p. 906082-906082. Disponível em WWW: <<https://www.ncbi.nlm.nih.gov/pubmed/20029632>

<<https://www.ncbi.nlm.nih.gov/pmc/articles/PMC2793423/>>. ISSN: 1110-7251

1110-7243

147. DRUCKER, E.; KRAPPENBAUER, K. - Pitfalls and limitations in translation from biomarker discovery to clinical utility in predictive and personalised medicine. *Epma j*. Vol. 4. n.º 1 (2013). p. 7. ISSN: 1878-5077 (Print)

1878-5077

148. STASTNA, Miroslava; VAN EYK, Jennifer E. - Secreted proteins as a fundamental source for biomarker discovery. *PROTEOMICS*. Vol. 12. n.º 4-5 (2012). p. 722-735. Disponível em WWW: <<https://onlinelibrary.wiley.com/doi/abs/10.1002/pmic.201100346>>. ISSN: 1615-9853

149. AL-DAGHRI, Nasser M., et al. - Whole Serum 3D LC-nESI-FTMS Quantitative Proteomics Reveals Sexual Dimorphism in the Milieu Intérieur of Overweight and Obese Adults. *Journal of Proteome Research*. Vol. 13. n.º 11 (2014). p. 5094-5105. Disponível em WWW: <<https://doi.org/10.1021/pr5003406>>. ISSN: 1535-3893

150. LARKIN, S. E. T., et al. - Detection of candidate biomarkers of prostate cancer progression in serum: a depletion-free 3D LC/MS quantitative proteomics pilot

- study. *British Journal Of Cancer*. Vol. 115. (2016). p. 1078. Disponível em WWW: <<https://doi.org/10.1038/bjc.2016.291>>. ISSN:
151. JIA, Lulu, et al. - An Attempt to Understand Kidney's Protein Handling Function by Comparing Plasma and Urine Proteomes. *PLOS ONE*. Vol. 4. n.º 4 (2009). p. e5146. Disponível em WWW: <<https://doi.org/10.1371/journal.pone.0005146>>. ISSN:
152. MOLINA, Henrik, et al. - A Proteomic Analysis of Human Hemodialysis Fluid. *Molecular & Cellular Proteomics*. Vol. 4. n.º 5 (2005). p. 637-650. Disponível em WWW: <<https://www.mcponline.org/content/mcprot/4/5/637.full.pdf>>. ISSN:
153. BIOSA, Grazia, et al. - Comparison of blood serum peptide enrichment methods by Tricine SDS-PAGE and mass spectrometry. *Journal of Proteomics*. Vol. 75. n.º 1 (2011). p. 93-99. Disponível em WWW: <<http://www.sciencedirect.com/science/article/pii/S187439191100282X>>. ISSN: 1874-3919
154. CAPRIOTTI, Anna Laura, et al. - Comparison of three different enrichment strategies for serum low molecular weight protein identification using shotgun proteomics approach. *Analytica Chimica Acta*. Vol. 740. (2012). p. 58-65. Disponível em WWW: <<http://www.sciencedirect.com/science/article/pii/S0003267012009014>>. ISSN: 0003-2670
155. KAWASHIMA, Yusuke, et al. - High-Yield Peptide-Extraction Method for the Discovery of Subnanomolar Biomarkers from Small Serum Samples. *Journal of Proteome Research*. Vol. 9. n.º 4 (2010). p. 1694-1705. Disponível em WWW: <<https://doi.org/10.1021/pr9008018>>. ISSN: 1535-3893
156. GREENING, David W.; SIMPSON, Richard J. - A centrifugal ultrafiltration strategy for isolating the low-molecular weight ($\leq 25K$) component of human plasma proteome. *Journal of Proteomics*. Vol. 73. n.º 3 (2010). p. 637-648. Disponível em WWW: <<http://www.sciencedirect.com/science/article/pii/S1874391909002644>>. ISSN: 1874-3919
157. GREENING, David W.; SIMPSON, Richard J. - Serum/Plasma Proteomics: Methods and Protocols. Totowa, NJ: Humana Press, 2011. Disponível em WWW: <https://doi.org/10.1007/978-1-61779-068-3_6>. Cap. - Low-Molecular Weight Plasma Proteome Analysis Using Centrifugal Ultrafiltration. ISBN: 978-1-61779-068-3
158. TULIPANI, Sara, et al. - Comparative Analysis of Sample Preparation Methods To Handle the Complexity of the Blood Fluid Metabolome: When Less Is More. *Analytical Chemistry*. Vol. 85. n.º 1 (2013). p. 341-348. Disponível em WWW: <<https://doi.org/10.1021/ac302919t>>. ISSN: 0003-2700
159. BONNIER, Franck, et al. - Screening the low molecular weight fraction of human serum using ATR-IR spectroscopy. *Journal of Biophotonics*. Vol. 9. n.º 10 (2016). p. 1085-1097. Disponível em WWW:

<<https://onlinelibrary.wiley.com/doi/abs/10.1002/jbio.201600015>>. ISSN: 1864-063X

160. HU, Lianghai; YE, Mingliang; ZOU, Hanfa - Recent advances in mass spectrometry-based peptidome analysis. *Expert Review of Proteomics*. Vol. 6. n.º 4 (2009). p. 433-447. Disponível em WWW: <<https://doi.org/10.1586/epr.09.55>>. ISSN: 1478-9450

161. WEI, X.; LI, L. - Mass spectrometry-based proteomics and peptidomics for biomarker discovery in neurodegenerative diseases. *Int J Clin Exp Pathol*. Vol. 2. n.º 2 (2009). p. 132-48. Disponível em WWW: <<https://www.ncbi.nlm.nih.gov/pubmed/19079648>>. ISSN: 1936-2625 (Electronic)

1936-2625 (Linking)

162. AEBERSOLD, R.; MANN, M. - Mass-spectrometric exploration of proteome structure and function. *Nature*. Vol. 537. n.º 7620 (2016). p. 347-55. ISSN: 0028-0836

163. GROSS, Jürgen H. - Mass spectrometry : a textbook. 2018. ISBN: 9783319853857 3319853856

164. ANJO, S. I.; SANTA, C.; MANADAS, B. - SWATH-MS as a tool for biomarker discovery: From basic research to clinical applications. *Proteomics*. Vol. 17. n.º 3-4 (2017). Disponível em WWW: <<https://www.ncbi.nlm.nih.gov/pubmed/28127880>>. ISSN: 1615-9861 (Electronic)

1615-9853 (Linking)

165. QIAN, W. J., et al. - Probability-based evaluation of peptide and protein identifications from tandem mass spectrometry and SEQUEST analysis: the human proteome. *J Proteome Res*. Vol. 4. n.º 1 (2005). p. 53-62. ISSN: 1535-3893 (Print)

1535-3893

166. GEDELA, Srinubabu; MEDICHERLA, Narasimha Rao - Chromatographic Techniques for the Separation of Peptides: Application to Proteomics. *Chromatographia*. Vol. 65. n.º 9 (2007). p. 511-518. Disponível em WWW: <<https://doi.org/10.1365/s10337-007-0215-9>>. ISSN: 1612-1112

167. BODZON-KULAKOWSKA, Anna, et al. - Methods for samples preparation in proteomic research. *Journal of Chromatography B*. Vol. 849. n.º 1 (2007). p. 1-31. Disponível em WWW: <<http://www.sciencedirect.com/science/article/pii/S1570023206008555>>. ISSN: 1570-0232

168. KINTER, Michael; SHERMAN, Nicholas E. - Protein sequencing and identification using tandem mass spectrometry. New York: Wiley-Interscience, 2000. ISBN: 0471322490 9780471322498

169. DOERR, Allison - DIA mass spectrometry. *Nature Methods*. Vol. 12. (2014). p. 35. Disponível em WWW: <<https://doi.org/10.1038/nmeth.3234>>. ISSN:

170. GILLET, L. C., et al. - Targeted data extraction of the MS/MS spectra generated by data-independent acquisition: a new concept for consistent and accurate proteome analysis. *Mol Cell Proteomics*. Vol. 11. n.º 6 (2012). p. O111 016717. Disponível em WWW: <<https://www.ncbi.nlm.nih.gov/pubmed/22261725>>. ISSN: 1535-9484 (Electronic)

1535-9476 (Linking)

171. ZHANG, Y., et al. - The Use of Variable Q1 Isolation Windows Improves Selectivity in LC-SWATH-MS Acquisition. *J Proteome Res*. Vol. 14. n.º 10 (2015). p. 4359-71. ISSN: 1535-3893

172. ALETTI, F., et al. - Peptidomic Analysis of Rat Plasma: Proteolysis in Hemorrhagic Shock. *Shock*. Vol. 45. n.º 5 (2016). p. 540-54. ISSN: 1073-2322

173. ALSHAMMARI, Thamir M., et al. - Comparison of different serum sample extraction methods and their suitability for mass spectrometry analysis. *Saudi Pharmaceutical Journal*. Vol. 23. n.º 6 (2015). p. 689-697. Disponível em WWW: <<http://www.sciencedirect.com/science/article/pii/S1319016415000365>>. ISSN: 1319-0164

174. ANJO, S. I.; SANTA, C.; MANADAS, B. - Short GeLC-SWATH: a fast and reliable quantitative approach for proteomic screenings. *Proteomics*. Vol. 15. n.º 4 (2015). p. 757-62. ISSN: 1615-9853

175. ANJO, Sandra, et al. - 2017. - Neuroproteomics Using Short GeLC-SWATH: From the Evaluation of Proteome Changes to the Clarification of Protein Function. ISBN: 978-1-4939-7118-3

176. GILLET, Ludovic C, et al. - Targeted data extraction of the MS/MS spectra generated by data-independent acquisition: a new concept for consistent and accurate proteome analysis. *Molecular & Cellular Proteomics*. Vol. 11. n.º 6 (2012). ISSN: 1535-9476

177. TANG, W. H.; SHILOV, I. V.; SEYMOUR, S. L. - Nonlinear fitting method for determining local false discovery rates from decoy database searches. *J Proteome Res*. Vol. 7. n.º 9 (2008). p. 3661-7. Disponível em WWW: <<http://www.ncbi.nlm.nih.gov/pubmed/18700793>>. ISSN: 1535-3893 (Print)

1535-3893 (Linking)

178. SENNELS, L.; BUKOWSKI-WILLS, J. C.; RAPPILBER, J. - Improved results in proteomics by use of local and peptide-class specific false discovery rates. *BMC Bioinformatics*. Vol. 10. (2009). p. 179. Disponível em WWW: <<http://www.ncbi.nlm.nih.gov/pubmed/19523214>>. ISSN: 1471-2105 (Electronic)

1471-2105 (Linking)

179. LAMBERT, Jean-Philippe, et al. - Mapping differential interactomes by affinity purification coupled with data-independent mass spectrometry acquisition. *Nature methods*. (2013). ISSN: 1548-7091

180. COLLINS, Ben C, et al. - Quantifying protein interaction dynamics by SWATH mass spectrometry: application to the 14-3-3 system. *Nature methods*. (2013). ISSN: 1548-7091
181. ANJO, Sandra Isabel, et al. - Use of recombinant proteins as a simple and robust normalization method for untargeted proteomics screening: exhaustive performance assessment. *Talanta*. Vol. 205. (2019). p. 120163. ISSN: 0039-9140
182. THEVENOT, E. A., et al. - Analysis of the Human Adult Urinary Metabolome Variations with Age, Body Mass Index, and Gender by Implementing a Comprehensive Workflow for Univariate and OPLS Statistical Analyses. *J Proteome Res*. Vol. 14. n.º 8 (2015). p. 3322-35. ISSN: 1535-3893
183. DEMING, Y., et al. - A potential endophenotype for Alzheimer's disease: cerebrospinal fluid clusterin. *Neurobiol Aging*. Vol. 37. (2016). p. 208.e1-208.e9. ISSN: 0197-4580
184. RUTHIRAKUHAN, M., et al. - Biomarkers of agitation and aggression in Alzheimer's disease: A systematic review. *Alzheimers Dement*. Vol. 14. n.º 10 (2018). p. 1344-1376. ISSN: 1552-5260
185. HSU, J. L., et al. - The clinical significance of plasma clusterin and Abeta in the longitudinal follow-up of patients with Alzheimer's disease. *Alzheimers Res Ther*. Vol. 9. n.º 1 (2017). p. 91. ISSN:
186. FOSTER, E. M., et al. - Clusterin in Alzheimer's Disease: Mechanisms, Genetics, and Lessons From Other Pathologies. *Front Neurosci*. Vol. 13. (2019). p. 164. ISSN: 1662-4548 (Print)
- 1662-453x
187. LI, X., et al. - Clusterin in Alzheimer's disease: a player in the biological behavior of amyloid-beta. *Neurosci Bull*. Vol. 30. n.º 1 (2014). p. 162-8. ISSN: 1995-8218
188. MINERS, J. S.; CLARKE, P.; LOVE, S. - Clusterin levels are increased in Alzheimer's disease and influence the regional distribution of Abeta. *Brain Pathol*. Vol. 27. n.º 3 (2017). p. 305-313. ISSN: 1015-6305
189. JONGBLOED, W., et al. - Clusterin Levels in Plasma Predict Cognitive Decline and Progression to Alzheimer's Disease. *J Alzheimers Dis*. Vol. 46. n.º 4 (2015). p. 1103-10. ISSN: 1387-2877
190. WEINSTEIN, G., et al. - Plasma clusterin levels and risk of dementia, Alzheimer's disease, and stroke. *Alzheimers Dement (Amst)*. Vol. 3. (2016). p. 103-9. ISSN: 2352-8729 (Print)
191. YU, J. T.; TAN, L.; HARDY, J. - Apolipoprotein E in Alzheimer's disease: an update. *Annu Rev Neurosci*. Vol. 37. (2014). p. 79-100. ISSN: 0147-006x
192. SHACKLETON, B.; CRAWFORD, F.; BACHMEIER, C. - Apolipoprotein E-mediated Modulation of ADAM10 in Alzheimer's Disease. *Curr Alzheimer Res*. Vol. 14. n.º 6 (2017). p. 578-585. ISSN: 1567-2050

193. JENDRESEN, C., et al. - The Alzheimer's disease risk factors apolipoprotein E and TREM2 are linked in a receptor signaling pathway. *J Neuroinflammation*. Vol. 14. n.º 1 (2017). p. 59. ISSN: 1742-2094
194. ALZATE, O., et al. - Differentially charged isoforms of apolipoprotein E from human blood are potential biomarkers of Alzheimer's disease. *Alzheimers Res Ther*. Vol. 6. n.º 4 (2014). p. 43. ISSN: 1758-9193 (Print)
195. RICHENS, J. L., et al. - Practical detection of a definitive biomarker panel for Alzheimer's disease; comparisons between matched plasma and cerebrospinal fluid. *Int J Mol Epidemiol Genet*. Vol. 5. n.º 2 (2014). p. 53-70. ISSN: 1948-1756 (Print)
- 1948-1756
196. MAHONEY-SANCHEZ, L., et al. - The Complex Role of Apolipoprotein E in Alzheimer's Disease: an Overview and Update. *J Mol Neurosci*. Vol. 60. n.º 3 (2016). p. 325-335. ISSN: 0895-8696
197. KIM, J., et al. - Apolipoprotein E in synaptic plasticity and Alzheimer's disease: potential cellular and molecular mechanisms. *Mol Cells*. Vol. 37. n.º 11 (2014). p. 767-76. ISSN: 1016-8478
198. XIE, L. K.; YANG, S. H. - Brain globins in physiology and pathology. *Med Gas Res*. Vol. 6. n.º 3 (2016). p. 154-163. ISSN: 2045-9912 (Print)
- 2045-9912
199. HUANG, Y., et al. - Elevation of the level and activity of acid ceramidase in Alzheimer's disease brain. *Eur J Neurosci*. Vol. 20. n.º 12 (2004). p. 3489-97. ISSN: 0953-816X (Print)
- 0953-816x
200. SHEN, L., et al. - Proteomics Analysis of Blood Serums from Alzheimer's Disease Patients Using iTRAQ Labeling Technology. *J Alzheimers Dis*. Vol. 56. n.º 1 (2017). p. 361-378. ISSN: 1387-2877
201. KHOONSARI, P. E., et al. - Improved Differential Diagnosis of Alzheimer's Disease by Integrating ELISA and Mass Spectrometry-Based Cerebrospinal Fluid Biomarkers. *J Alzheimers Dis*. Vol. 67. n.º 2 (2019). p. 639-651. ISSN: 1387-2877
202. DI DOMENICO, F., et al. - Oxidative signature of cerebrospinal fluid from mild cognitive impairment and Alzheimer disease patients. *Free Radic Biol Med*. Vol. 91. (2016). p. 1-9. ISSN: 0891-5849
203. KNEBL, J., et al. - Plasma lipids and cholesterol esterification in Alzheimer's disease. *Mech Ageing Dev*. Vol. 73. n.º 1 (1994). p. 69-77. ISSN: 0047-6374 (Print)

0047-6374

204. BENUSSI, L., et al. - The level of 24-Hydroxycholesteryl Esters is an Early Marker of Alzheimer's Disease. *J Alzheimers Dis*. Vol. 56. n.º 2 (2017). p. 825-833. ISSN: 1387-2877
205. HUANG, M., et al. - Pigment Epithelium-Derived Factor Plays a Role in Alzheimer's Disease by Negatively Regulating Abeta42. *Neurotherapeutics*. Vol. 15. n.º 3 (2018). p. 728-741. ISSN: 1878-7479
206. CUTLER, P., et al. - Proteomic identification and early validation of complement I inhibitor and pigment epithelium-derived factor: Two novel biomarkers of Alzheimer's disease in human plasma. *Proteomics Clin Appl*. Vol. 2. n.º 4 (2008). p. 467-77. ISSN: 1862-8346 (Print)

1862-8346

207. LLANO, D. A.; DEVANARAYAN, V.; SIMON, A. J. - Evaluation of plasma proteomic data for Alzheimer disease state classification and for the prediction of progression from mild cognitive impairment to Alzheimer disease. *Alzheimer Dis Assoc Disord*. Vol. 27. n.º 3 (2013). p. 233-43. ISSN: 0893-0341
208. MORSY, A.; TRIPPIER, P. C. - Amyloid-Binding Alcohol Dehydrogenase (ABAD) Inhibitors for the Treatment of Alzheimer's Disease. *J Med Chem*. Vol. 62. n.º 9 (2019). p. 4252-4264. ISSN: 0022-2623
209. AHMADINEJAD, F., et al. - Molecular Mechanisms behind Free Radical Scavengers Function against Oxidative Stress. *Antioxidants (Basel)*. Vol. 6. n.º 3 (2017). ISSN: 2076-3921 (Print)

2076-3921

210. ZAMOLODCHIKOV, D., et al. - Activation of the factor XII-driven contact system in Alzheimer's disease patient and mouse model plasma. *Proc Natl Acad Sci U S A*. Vol. 112. n.º 13 (2015). p. 4068-73. ISSN: 0027-8424
211. ASHBY, E. L.; LOVE, S.; KEHOE, P. G. - Assessment of activation of the plasma kallikrein-kinin system in frontal and temporal cortex in Alzheimer's disease and vascular dementia. *Neurobiol Aging*. Vol. 33. n.º 7 (2012). p. 1345-55. ISSN: 0197-4580
212. BAKER, S. K., et al. - Blood-derived plasminogen drives brain inflammation and plaque deposition in a mouse model of Alzheimer's disease. *Proc Natl Acad Sci U S A*. Vol. 115. n.º 41 (2018). p. E9687-e9696. ISSN: 0027-8424
213. WANG, E. S., et al. - Tetranectin and apolipoprotein A-I in cerebrospinal fluid as potential biomarkers for Parkinson's disease. *Acta Neurol Scand*. Vol. 122. n.º 5 (2010). p. 350-9. ISSN: 0001-6314
214. XIE, Q., et al. - Exogenous Tetranectin Protects Against 1-Methyl-4-Phenylpyridine-Induced Neurotoxicity by Inhibiting Apoptosis and Autophagy Through Ribosomal Protein S6 Kinase Beta-1. *World Neurosurg*. Vol. 122. (2019). p. e375-e382. ISSN: 1878-8750

215. ALBERIO, Tiziana, et al. - Parkinson's disease plasma biomarkers: An automated literature analysis followed by experimental validation. *Journal of Proteomics*. Vol. 90. (2013). p. 107-114. Disponível em WWW: <<http://www.sciencedirect.com/science/article/pii/S1874391913000559>>. ISSN: 1874-3919
216. HALBGEBAUER, S., et al. - Protein biomarkers in Parkinson's disease: Focus on cerebrospinal fluid markers and synaptic proteins. *Mov Disord*. Vol. 31. n.º 6 (2016). p. 848-60. ISSN: 0885-3185
217. ZHANG, J., et al. - CSF multianalyte profile distinguishes Alzheimer and Parkinson diseases. *Am J Clin Pathol*. Vol. 129. n.º 4 (2008). p. 526-9. ISSN: 0002-9173 (Print)
0002-9173
218. SCHWIERTZ, A., et al. - Fecal markers of intestinal inflammation and intestinal permeability are elevated in Parkinson's disease. *Parkinsonism Relat Disord*. Vol. 50. (2018). p. 104-107. ISSN: 1353-8020
219. PRENDECKI, M., et al. - Biothiols and oxidative stress markers and polymorphisms of TOMM40 and APOC1 genes in Alzheimer's disease patients. *Oncotarget*. Vol. 9. n.º 81 (2018). p. 35207-35225. ISSN: 1949-2553
220. ABDI, F., et al. - Detection of biomarkers with a multiplex quantitative proteomic platform in cerebrospinal fluid of patients with neurodegenerative disorders. *J Alzheimers Dis*. Vol. 9. n.º 3 (2006). p. 293-348. ISSN: 1387-2877 (Print)
1387-2877
221. CHEN, Han-Min; LIN, Ching-Yu; WANG, Vinchi - Amyloid P component as a plasma marker for Parkinson's disease identified by a proteomic approach. *Clinical Biochemistry*. Vol. 44. n.º 5 (2011). p. 377-385. Disponível em WWW: <<http://www.sciencedirect.com/science/article/pii/S0009912011000208>>. ISSN: 0009-9120
222. KITAMURA, Yuki, et al. - Plasma protein profiling for potential biomarkers in the early diagnosis of Alzheimer's disease. *Neurological Research*. Vol. 39. n.º 3 (2017). p. 231-238. Disponível em WWW: <<https://doi.org/10.1080/01616412.2017.1281195>>. ISSN: 0161-6412
223. ZÜRBIG, Petra; JAHN, Holger - Use of proteomic methods in the analysis of human body fluids in Alzheimer research. *ELECTROPHORESIS*. Vol. 33. n.º 24 (2012). p. 3617-3630. Consult. em 2019/09/13. Disponível em WWW: <<https://doi.org/10.1002/elps.201200360>>. ISSN: 0173-0835
224. FANG, Jianguo, et al. - S-nitrosylation of peroxiredoxin 2 promotes oxidative stress-induced neuronal cell death in Parkinson's disease. *Proceedings of the National Academy of Sciences*. Vol. 104. n.º 47 (2007). p. 18742. Disponível em WWW: <<http://www.pnas.org/content/104/47/18742.abstract>>. ISSN:
225. VRANOVÁ, Hana Přikrylová, et al. - Tau protein, beta-amyloid₁₋₄₂ and clusterin CSF levels in the differential diagnosis of Parkinsonian syndrome with dementia. *Journal of the Neurological*

Sciences. Vol. 343. n.º 1 (2014). p. 120-124. Consult. em 2019/09/13. Disponível em WWW: <<https://doi.org/10.1016/j.jns.2014.05.052>>. ISSN: 0022-510X

226. PŘIKRYLOVÁ VRANOVÁ, Hana, et al. - Clusterin CSF levels in differential diagnosis of neurodegenerative disorders. *Journal of the Neurological Sciences*. Vol. 361. (2016). p. 117-121. Consult. em 2019/09/13. Disponível em WWW: <<https://doi.org/10.1016/j.jns.2015.12.023>>. ISSN: 0022-510X

7. Supplementary Data

7.1 Protein Quantification Results of Fractionated Serum

After fractionation, all samples yielded a volume of about 20 μL , thus, concentrations are shown relative to this volume. Concentrations were determined according to a previously plotted standard calibration curve (Figure S1). Serum is highly enriched in proteins overall, but (as expected) the HMW fraction is dramatically more complex than the LMW fraction. This explains why no signal was obtained for the HMW whole serum fraction (III – 300 kDa), as shown in Figure S2. Still, one can estimate from the diluted II – 300 kDa sample signal that there are about 661.75 μg of protein in 20 μL of the HMW fraction of whole serum.

Since the LMW fraction of serum is less complex, there is no need for this estimation and according to the obtained result, one can conclude there are about 109.95 μg of protein in 20 μL of the LMW fraction of whole serum.

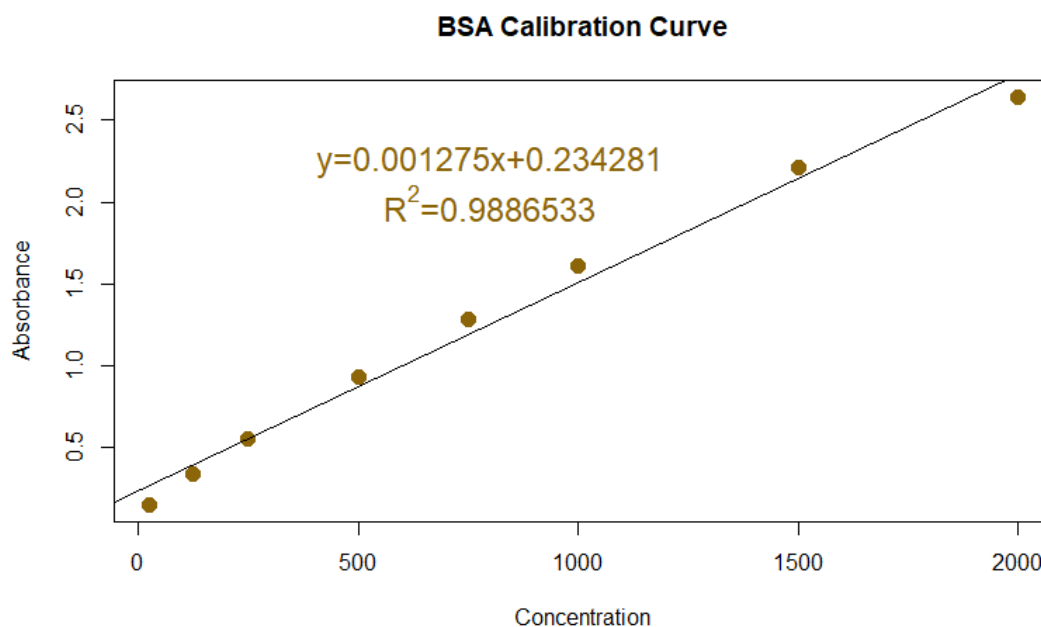


Figure S1 Standard Calibration Curve for Bicinchoninic Acid Assay of Fractionated Serum Samples. The BCA standard curve was obtained by plotting progressively larger concentration values of bovine serum albumin against their respective absorbances at 562 nm. The value of coefficient of determination is presented and indicates linearity, required for sample absolute quantification.

According to the LMW fraction results, serum dilution can benefit protein quantification through BCA assay, since the diluted samples show a higher concentration than that estimated through the LMW whole serum value (e.g. estimating the II – 3 kDa sample protein content [in 20 μ L] from the value obtained in the III – 3 kDa whole serum sample results in a value of 43.98 μ g when in fact the measured value is of 51.98 μ g of protein, indicating serum complexity might hinder protein quantification by this method).

Nonetheless, sample dilution should not be drastic, since it had the reverse effect on the HMW fraction (e.g. estimating the I – 300 kDa sample protein content [in 20 μ L] from the value obtained in the II – 300 kDa sample results in a value of 132.35 μ g when in fact the measured value is of 56.61 μ g of protein);

Therefore, one can conclude that the undiluted serum HMW fraction seems to be too complex to quantify through BCA assay, but an optimal dilution should be investigated. Additional attention should be given to the fact that the principle of quantification used in BCA assay is different from that of MS, hence, results might not be transposable.

Sample	Absorbance	ug/20uL
I-300kDa	0.956	56.61
II-300kDa	3.609	264.70
III-300kDa	N/A	N/A
I-3kDa	0.764	41.55
II-3kDa	0.897	51.98
III-3kDa	1.636	109.95
PBS	0.094	-11.00

Figure S2 Absolute Quantification Values of Diluted and Fractionated Serum Samples. Total protein concentrations were determined according to the standard calibration curve for an of 20 μ L of sample. Samples were diluted 1:5 in PBS before measuring absorbance at 562nm. Fractions above 300 kDa and below 3 kDa are indicated. I, 50 μ L of serum with 200 μ L of TEAB (0.5M). II, 100 μ L of serum with 150 μ L of TEAB (0.5M). III, 250 μ L of serum. PBS, phosphate buffer saline.

7.2 Identification of LMW Internal Standard Protein in Fractionated Serum and Buffer

Digested GFP can pass through the 3 kDa MWCO filter, as evidenced by its identification in the respective fraction (both mixed in buffer and spiked in serum) in the protein grouping results (Figure S3). Still, the unused score is much higher in the fraction above 3 kDa, indicating that a majority of digested GFP peptides do not pass through the membrane filter.

A similar observation can be made with respect to the sequence coverage results (Figure S4), high sequence coverage in the fraction above 3 kDa and low sequence coverage in the remaining fractions, below 3 kDa. This could be either due to inefficient digestion of GFP-MBP and/or because the MWCO filter is too stringent. Both these hypotheses are explored in further results.

Protein Group 1 - IS						
Proteins in Group						
N	Unused	Total	Accession #	Name	Species	
1	167.78	167.78	sp I00001 MALE_GFP	IS	GFP	

Protein Group 1 - IS						
Proteins in Group						
N	Unused	Total	Accession #	Name	Species	
1	46.36	46.36	sp I00001 MALE_GFP	IS	GFP	

Protein Group 2 - IS						
Proteins in Group						
N	Unused	Total	Accession #	Name	Species	
2	47.10	49.14	sp I00001 MALE_GFP	IS	GFP	

Figure S3 Protein Grouping Results for the fraction of digested GFP-MBP-spiked Serum and Buffer Samples above and below 3 kDa. Unused and total scores are presented for GFP. (A) refers to the fraction of a spiked buffer sample above 3 kDa. (B) refers to the fraction of spiked buffer sample below 3 kDa. (C) refers to the fraction of a spiked serum sample below 3 kDa. The buffer used was TEAB (0.5M). Results obtained from Protein Pilot software.

As can be observed in Figure S3, in the presence of serum, GFP jumps from n=1 to n=2, but since this is probably caused by abundant albumin fragments passing through the membrane filter and the GFP unused score is still high when compared to its total score, one can conclude that nor does serum hinder GFP's passage through the filter nor does it compromise its identification, at least with respect to protein grouping results.

When looking at the sequence coverage results (Figure S4) of both LMW fractions (buffer and serum "spike-in"), a decrease in confidence of some peptides and slight reduction in the number of identified peptides is observable in the serum sample as compared to the buffer sample. Nonetheless, both fractions show poor sequence coverage, indicating serum complexity might not be the main causative agent of this observation and further justifying the investigation of the aforementioned hypotheses.

A MKHHHHHPMKIEEGKLVIIWINGDKGYNGLAEVGKKFEKDTGKIKVTVEHPDKLEEKFPQVAATGDGPDIIFWAHDRF
GGYAQSGLLAEITPDKAFQDKLYPFTWDAVRYNGKLIAYPIAVEALSILIYKDLLPNPFTWEEIIPALDKELKAKGK
SALMFNLQEPYFTWPLIAADGGYAFKYENGYDIKDVGVNDAGAKAGLTFVLVDLIKHKHMNADTDYSIAEAAFNKGE
TAMTINGPWASNIDTSKVNYGVTVLPTFKGQPSKPFVGVLSAGINAASFNKELAKEFLENYLLTDEGLEAVNKDKP
LGAVALKSYEEELAKDFRIIATMENAQKGEIMPNI PQMSAFWYAVRTAVINAASGRQTVDEALKDAQTNSGSGSGSE
NLYFQGAMGKVSKEELFTGVVPII LVELDGDVNGHKFSVSGEGEGDATYGLTLKFICTTGKLPVWPPTLVTTFGYG
LQCFARYPDHMKQHDFFKSAMPEGYVQERTIFFKDDGNYKTRAEVKFEGDTLVNRIELKIDFKEDGNILGHKLEYN
YNSHNVIYIMADKQKNGIKVNFKIRHNIEDGVSQ LADHYQQNTPIGDGPVLLPDNHYLSTQSALS KDPNEKRDMVLL
EFVTAAGITLGMDELYK

B MKHHHHHPMKIEEGKLVIIWINGDKGYNGLAEVGKFEKDTGKIKVTVEHPDKLEEKFPQVAATGDGPDIIFWAHDRF
GGYAQSGLLAEITPDKAFQDKLYPFTWDAVRYNGKLIAYPIAVEALSILIYKDLLPNPFTWEEIIPALDKELKAKGK
SALMFNLQEPYFTWPLIAADGGYAFKYENGYDIKDVGVNDAGAKAGLTFVLVDLIKHKHMNADTDYSIAEAAFNKGE
TAMTINGPWASNIDTSKVNYGVTVLPTFKGQPSKPFVGVLSAGINAASFNKELAKEFLENYLLTDEGLEAVNKDKP
LGAVALKSYEEELAKDFRIIATMENAQKGEIMPNI PQMSAFWYAVRTAVINAASGRQTVDEALKDAQTNSGSGSGSE
NLYFQGAMGKVSKEELFTGVVPII LVELDGDVNGHKFSVSGEGEGDATYGLTLKFICTTGKLPVWPPTLVTTFGYG
LQCFARYPDHMKQHDFFKSAMPEGYVQERTIFFKDDGNYKTRAEVKFEGDTLVNRIELKIDFKEDGNILGHKLEYN
YNSHNVIYIMADKQKNGIKVNFKIRHNIEDGVSQ LADHYQQNTPIGDGPVLLPDNHYLSTQSALS KDPNEKRDMVLL
EFVTAAGITLGMDELYK

C MKHHHHHPMKIEEGKLVIIWINGDKGYNGLAEVGKFEKDTGKIKVTVEHPDKLEEKFPQVAATGDGPDIIFWAHDRF
GGYAQSGLLAEITPDKAFQDKLYPFTWDAVRYNGKLIAYPIAVEALSILIYKDLLPNPFTWEEIIPALDKELKAKGK
SALMFNLQEPYFTWPLIAADGGYAFKYENGYDIKDVGVNDAGAKAGLTFVLVDLIKHKHMNADTDYSIAEAAFNKGE
TAMTINGPWASNIDTSKVNYGVTVLPTFKGQPSKPFVGVLSAGINAASFNKELAKEFLENYLLTDEGLEAVNKDKP
LGAVALKSYEEELAKDFRIIATMENAQKGEIMPNI PQMSAFWYAVRTAVINAASGRQTVDEALKDAQTNSGSGSGSE
NLYFQGAMGKVSKEELFTGVVPII LVELDGDVNGHKFSVSGEGEGDATYGLTLKFICTTGKLPVWPPTLVTTFGYG
LQCFARYPDHMKQHDFFKSAMPEGYVQERTIFFKDDGNYKTRAEVKFEGDTLVNRIELKIDFKEDGNILGHKLEYN
YNSHNVIYIMADKQKNGIKVNFKIRHNIEDGVSQ LADHYQQNTPIGDGPVLLPDNHYLSTQSALS KDPNEKRDMVLL
EFVTAAGITLGMDELYK

Figure S4 Sequence Coverage Results for GFP in the fraction of digested GFP-MBP-spiked Serum and Buffer Samples above and below 3 kDa. Green, yellow, and red indicate peptide confidence equal or over 95%, below 95% and equal or over 50%, and under 50%, respectively. Grey represents peptides with no match. (A) refers to the fraction of a spiked buffer sample above 3 kDa. (B) refers to the fraction of spiked buffer sample below 3 kDa. (C) refers to the fraction of a spiked serum sample below 3 kDa. The buffer used was TEAB (0.5M). Results obtained from Protein Pilot software.

7.3 Single vs Double Digestion of LMW Internal Standard Protein

According to protein grouping (Figures S5 and S6) and sequence coverage (Figures S7 and S8) results, double digestion does in fact favor the identification of GFP-MBP, mainly due to enhancement of the unused score and a dramatic increase in sequence coverage in all replicates of double digestion.

Protein Group 3 - Green fluorescent protein OS=Aequorea victoria OX=6100 GN=GFP PE=1 SV=1						
Proteins in Group						
N	Unused	Total	Accessio...	Name	Species	
3	16.95	16.95	sp P4221...	Green fluorescent protein OS=Aequo...	AEQVI	

Protein Group 2 - Green fluorescent protein OS=Aequorea victoria OX=6100 GN=GFP PE=1 SV=1						
Proteins in Group						
N	Unused	Total	Accessio...	Name	Species	
2	28.96	28.96	sp P4221...	Green fluorescent protein OS=Aequo...	AEQVI	

Protein Group 3 - Green fluorescent protein OS=Aequorea victoria OX=6100 GN=GFP PE=1 SV=1						
Proteins in Group						
N	Unused	Total	Accessio...	Name	Species	
3	23.31	23.31	sp P4221...	Green fluorescent protein OS=Aequo...	AEQVI	

Protein Group 3 - Green fluorescent protein OS=Aequorea victoria OX=6100 GN=GFP PE=1 SV=1						
Proteins in Group						
N	Unused	Total	Accessio...	Name	Species	
3	18.37	18.37	sp P4221...	Green fluorescent protein OS=Aequo...	AEQVI	

Figure S5 Protein Grouping Results of GFP in 4 GFP-MBP Replicates Digested with Trypsin. Unused and total scores are presented for GFP. Results obtained from Protein Pilot software. Replicates are indicated A-D.

Protein Group 2 - Green fluorescent protein OS=Aequorea victoria OX=6100 GN=GFP PE=1 SV=1						
Proteins in Group						
N	Unused	Total	Accessio...	Name	Species	
2	31.44	31.44	sp P4221...	Green fluorescent protein OS=Aequo...	AEQVI	

Protein Group 2 - Green fluorescent protein OS=Aequorea victoria OX=6100 GN=GFP PE=1 SV=1						
Proteins in Group						
N	Unused	Total	Accessio...	Name	Species	
2	47.83	47.83	sp P4221...	Green fluorescent protein OS=Aequo...	AEQVI	

Protein Group 2 - Green fluorescent protein OS=Aequorea victoria OX=6100 GN=GFP PE=1 SV=1						
Proteins in Group						
N	Unused	Total	Accessio...	Name	Species	
2	60.15	60.15	sp P4221...	Green fluorescent protein OS=Aequo...	AEQVI	

Protein Group 2 - Green fluorescent protein OS=Aequorea victoria OX=6100 GN=GFP PE=1 SV=1						
Proteins in Group						
N	Unused	Total	Accessio...	Name	Species	
2	45.14	45.14	sp P4221...	Green fluorescent protein OS=Aequo...	AEQVI	

Figure S6 Protein Grouping Results of GFP in 4 GFP-MBP Replicates Digested with Trypsin and LysC. Unused and total scores are presented for GFP. Results obtained from Protein Pilot software. Replicates are indicated A-D.



Figure S7 Sequence Coverage Results of GFP in 4 GFP-MBP Replicates Digested with Trypsin. Green, yellow, and red indicate peptide confidence equal or over 95%, below 95% and equal or over 50%, and under 50%, respectively. Grey represents peptides with no match. Replicates are indicated A-D. Results obtained from Protein Pilot software.



Figure S8 Sequence Coverage Results of GFP in 4 GFP-MBP Replicates Digested with Trypsin and LysC. Green, yellow, and red indicate peptide confidence equal or over 95%, below 95% and equal or over 50%, and under 50%, respectively. Grey represents peptides with no match. Replicates are indicated A-D. Results obtained from Protein Pilot software.

Regarding Figure S9, although there is an increase in missed cleavages, there is also an increase (to a greater extent) in identified peptides with confidence over 95%, leading to the reduced value of “Missed Cleavages/Peptide (95%) Ratio”. If similar situations are

observed in arbitrarily chosen serum proteins, it should be safe to conclude that digestion with both Trypsin and LysC enhances digestion efficiency, when compared to digestion with Trypsin alone, thereby (potentially) increasing the number of peptides identified with confidence over 95% and consequently augmenting the confidence of the respectively identified proteins.

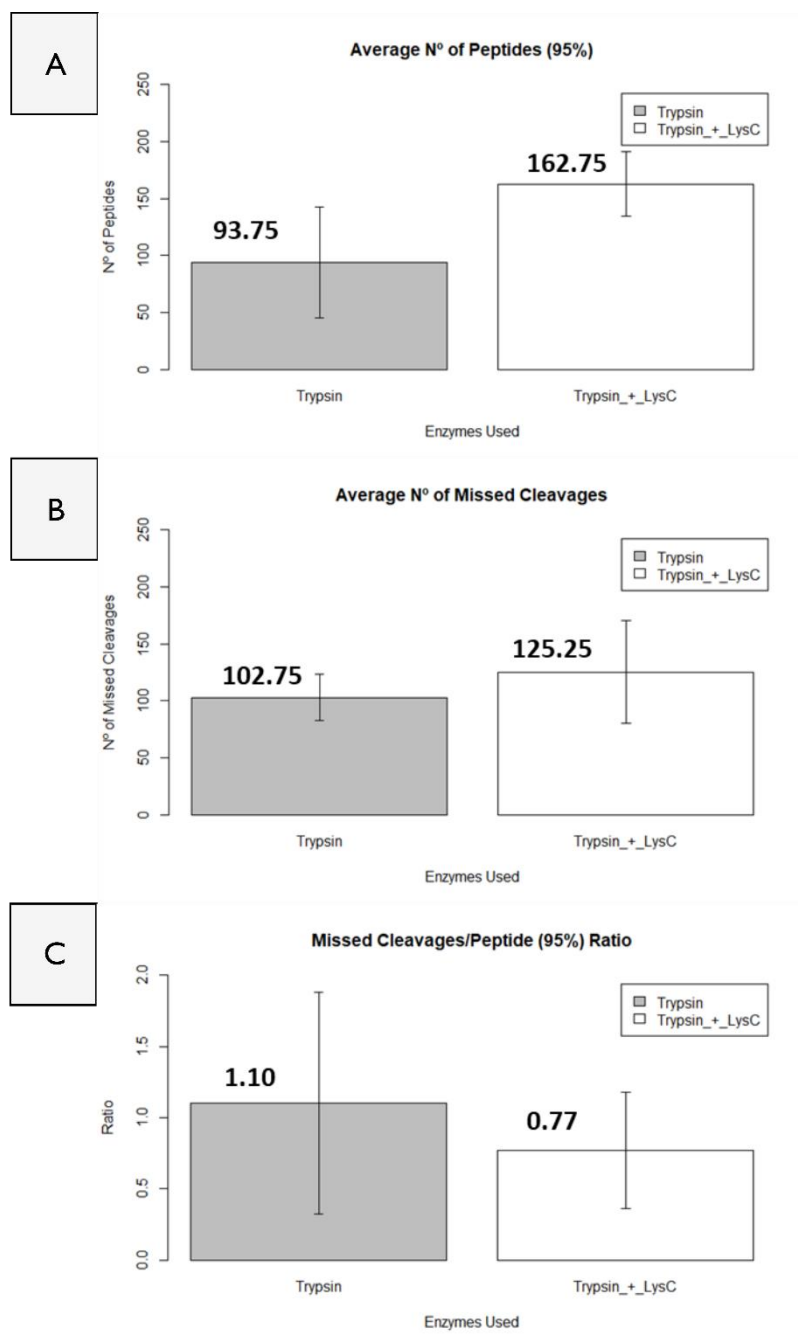


Figure S9 GFP Peptides Confidently Identified, Average Number of Missed Cleavages, and the Ratio Thereof. Grey depicts values for tryptic digestion. White depicts values for tryptic digestion followed by digestion with LysC. (A) refers to the number of peptides identified with confidence over 95%. (B) refers to the total number of missed cleavage sites. (C) refers to the ratio of B/A. Error bars depict standard deviation.

7.4 Low Molecular Weight Protein Identifications Using Different MWCO Filters

As a last attempt to optimize LMW fractionation of serum, different low MWCO filters using either 32% acetic acid (v/v) or TEAB (0.5M) did not reveal many protein identifications, as can be seen in the following tables (Table S3-S8). Assuming only proteins with a local FDR of 5% or less are confidently identified, this experiment may not be the most adequate for fractionation of serum samples, since at best it led to the identification of 33 proteins, using TEAB and the least exclusive MWCO filter, and at worst, resulted in no proteins being confidently identified, in the case of serum fractionation using acetic acid and 5 kDa MWCO filters. Hence, the search for biomarkers in this serum fraction was abandoned, so that all efforts could be directed at optimizing the HMW fractionation protocol.

Table S3 Number of Identified Proteins Using TEAB (0.5M) and a 3 kDa MWCO Filter.

Critical FDR	Local FDR	Global FDR	Global FDR from Fit
1.0%	20	20	21
5.0%	21	20	21
10.0%	21	21	21

Table S4 Number of Identified Proteins Using 32% acetic acid (v/v) and a 3 kDa a MWCO Filter.

Critical FDR	Local FDR	Global FDR	Global FDR from Fit
1.0%	13	12	13
5.0%	13	12	13
10.0%	13	12	15

Table S5 Number of Identified Proteins Using TEAB (0.5M) and a 5 kDa MWCO Filter.

Critical FDR	Local FDR	Global FDR	Global FDR from Fit
1.0%	9	8	9
5.0%	9	8	9
10.0%	9	8	11

Table S6 Number of Identified Proteins Using 32% acetic acid (v/v) and a 5 kDa a MWCO Filter.

Critical FDR	Local FDR	Global FDR	Global FDR from Fit
--------------	-----------	------------	---------------------

1.0%	0	15	15
5.0%	0	15	15
10.0%	0	15	15

Table S7 Number of Identified Proteins Using TEAB (0.5M) and a 10 kDa MWCO Filter.

Critical FDR	Local FDR	<i>Global FDR</i>	Global FDR from Fit
1.0%	33	32	33
5.0%	33	32	33
10.0%	33	34	34

Table S8 Number of Identified Proteins Using 32% acetic acid (v/v) and a 10 kDa a MWCO Filter.

Critical FDR	Local FDR	<i>Global FDR</i>	Global FDR from Fit
1.0%	7	6	7
5.0%	7	6	7
10.0%	7		8

7.5 Additional Tables

Table S9 Proteins Identified Exclusively in the “HMW Protein Library”

Protein names	Accession number	Mass
Putative uncharacterized protein PRO2289	Q9P1D8	6 607
Apolipoprotein C-II	P02655	11 284
Dermcidin	P81605	11 284
Platelet factor 4 variant	P10720	11 553
Immunoglobulin lambda variable 3-19	P01714	12 042
Immunoglobulin lambda variable 3-10	A0A075B6K4	12 441
Immunoglobulin lambda variable 7-46	A0A075B6I9	12 468
Immunoglobulin lambda variable 1-36	A0A0B4J1U3	12 478
Immunoglobulin kappa variable 1-13	P0DP09	12 569
Immunoglobulin heavy variable 3-23	P01764	12 582
Immunoglobulin heavy variable 1-69D	A0A0B4J2H0	12 660
Immunoglobulin kappa variable 1-27	A0A075B6S5	12 712
Immunoglobulin heavy variable 1-18	A0A0C4DH31	12 820
Immunoglobulin heavy variable 3-9	P01782	12 945
Immunoglobulin heavy variable 1-3	A0A0C4DH29	13 008
Immunoglobulin heavy variable 4-38-2	P0DP08	13 016
Immunoglobulin lambda variable 9-49	A0A0B4J1Y8	13 024
Immunoglobulin heavy variable 2-5	P01817	13 231
Serum amyloid A-2 protein	P0DJ19	13 527
Serum amyloid A-1 protein	P0DJ18	13 532
Apolipoprotein C-IV	P55056	14 553
Ubiquitin-60S ribosomal protein L40	P62987	14 728
Cystatin-C	P01034	15 799
Hemoglobin subunit delta	P02042	16 055
Hemoglobin subunit gamma-2	P69892	16 126
Hemoglobin subunit gamma-1	P69891	16 140
Interleukin-36 alpha	Q9UHA7	17 684
Immunoglobulin J chain	P01591	18 099
Cathelicidin antimicrobial peptide	P49913	19 301
Ferritin light chain	P02791	19 978
Calcium and integrin-binding family member 2	O75838	21 644
Peroxiredoxin-2	P32119	21 892
Ras-related protein Rab-7b	Q96AH8	22 511
Peroxiredoxin-6	P30041	25 035
C-reactive protein	P02741	25 039
C4b-binding protein beta chain	P20851	28 357
Carbonic anhydrase 1	P00915	28 870
Carbonic anhydrase 2	P00918	29 246
Complement factor H-related protein 2	P36980	30 651
Insulin-like growth factor-binding protein 3	P17936	31 674
Olfactory receptor 7G3	Q8NG95	34 439
Voltage-dependent calcium channel gamma-4 subunit	Q9UBN1	36 579
SRR1-like protein	Q9UH36	38 573
LRP2-binding protein	Q9P2M1	39 780
Monocyte differentiation antigen CD14	P08571	40 076
Serpin B10	P48595	45 403
Actin-like protein 7A	Q9Y615	48 644
Protein Z-dependent protease inhibitor	Q9UK55	50 707
Coagulation factor IX	P00740	51 778
Lipopolysaccharide-binding protein	P18428	53 384
WD repeat-containing protein 13	Q9H1Z4	53 696
Phospholipid transfer protein	P55058	54 739
Preylcysteine oxidase 1	Q9UHG3	56 640
Beta-Ala-His dipeptidase	Q96KN2	56 706
Serine/threonine-protein phosphatase 2A 65 kDa regulatory subunit A alpha isoform	P30153	65 309
PiggyBac transposable element-derived protein 4	Q96DM1	67 004
Cholinesterase	P06276	68 418
Transforming growth factor-beta-induced protein ig-h3	Q15582	74 681
Thrombospondin-type laminin G domain and EAR repeat-containing protein	Q8WU66	74 924
Arachidonate 15-lipoxygenase B	O15296	75 857
Rhopilin-2	Q8IUC4	76 993
Glycogen phosphorylase, muscle form	P11217	97 092
Acyl-CoA dehydrogenase family member 10	Q6JQN1	118 834
Phospholipid-transporting ATPase IG	Q8NB49	129 477
von Willebrand factor A domain-containing protein 3A	A6NCI4	134 020
PAN2-PAN3 deadenylation complex catalytic subunit PAN2	Q504Q3	135 368
Protein diaphanous homolog 1	O60610	141 347
Leucine-rich repeat-containing protein 9	Q6ZRR7	166 911
NEDD4-binding protein 2	Q86UW6	198 801
Nuclear receptor coactivator 6	Q14686	219 145
Centrosome-associated protein CEP250	Q9BV73	281 137
von Willebrand factor	P04275	309 265
Protein furry homolog	Q5TBA9	338 875

Table S10 Statistically altered proteins in CT vs AD comparison (Dunn's Test) that appeared related to Alzheimer's Disease*		
Protein Accession Number (UniProt)	Protein's name	Brief description of the potential relationship as explained in the found articles
P10909	Clusterin (CLU)	<ul style="list-style-type: none"> - CLU may have a role in influencing the immune system changes observed in AD (183) - Association with agitation, a typical neuropsychiatric symptom of AD (184, 185) - Possible link of CLU action with alterations of Aβ aggregation/clearance, as well as working as mediator of its toxicity. (186-188) - Possible link between CLU and altered cognitive and memory function, as well as altered brain function.(185, 186) - Elevated plasma CLU levels in MCI may reflect an increased risk for the progression of AD, and consequent cognitive decline. May serve as a prognostic marker for AD and increased risk of dementia. (185, 189, 190)
P02649	Apolipoprotein E (Apo-E)	<ul style="list-style-type: none"> - Major genetic risk factor for late onset AD cases (191-193) - Might be useful in genotyping AD diagnosis, risk assessment, prevention and treatment response. (191, 194-196) - Studies demonstrated that Apo-E might lead to synaptic deficits and impairment in LTP, memory and cognition, classic symptoms of AD. (197) - Its modulation of ADAM10 activity may influence the enhance Aβ levels in the brain of AD subjects carrying the APOE4 allele. (192)
P68871	Hemoglobin subunit beta (Beta-globin)	<ul style="list-style-type: none"> - Studies suggest Beta-globulin to regulate neurological disorders, thus providing insights on initiation and progression of AD. (198) - Might be related to acid ceramidase, which <i>per se</i> might play a role in controlling neuronal apoptosis and signaling pathways suggested to be involved in the molecular mechanism of AD. (199)

P02775	Platelet basic protein (PBP)	<ul style="list-style-type: none"> - Differential expression of PBP was detected in the serums of AD patients compared with healthy controls. Might serve as potential biomarkers for AD diagnosis.(200)
P04217	Alpha-1B-glycoprotein	<ul style="list-style-type: none"> - Might serve as a potential biomarker for distinguish AD and MCI/AD healthy controls, but also to differentiate between patients with fronto-temporal dementia and non-dementia controls. (201, 202)
P04180	Phosphatidylcholine-sterol acyltransferase	<ul style="list-style-type: none"> - Might be particularly altered in AD.(203) - Might have a role in AD onset/progression, thus targeting its metabolism might be a strategy to prevent AD associated cognitive decline. (204)
P36955	Pigment epithelium-derived factor (PEDF)	<ul style="list-style-type: none"> - PEDF negatively regulates Aβ42. PEDF deficiency with ageing might play a crucial role in the development of AD.(205) - PEDF was shown to be down-regulated in plasma from AD patients. (206)
P02652	Apolipoprotein A-II (Apo-AII)	<ul style="list-style-type: none"> - As part of a larger panel of analytes may provide a way to differentiate AD form healthy controls. It might also provide mechanistic insights to the etiology of AD, although it cannot predict MCI to AD conversion. (207)
P32119	Peroxiredoxin-2	<ul style="list-style-type: none"> - Is implied in the interaction between Aβ and amyloid-binding alcohol dehydrogenase, which may be a novel therapeutic target for AD.(208) - Involved in the apoptosis inhibition in cells treated with 3-methyl-1-phenyl-2-pyrazolin-5-one (Edaravone), a free radical detoxifier frequently used in acute ischemic stroke. (209)
P03952	Plasma kallikrein	<ul style="list-style-type: none"> - Increased activity in AD patients plasma.(210, 211)
P08697	Alpha-2-antiplasmin (A2AP)	<ul style="list-style-type: none"> - This study showed that an increase in plasmin activity through A2AP antisense oligonucleotide treatment exacerbated the brain's immune response and plaque deposition.(212)

*The articles cited above were obtained after a Pubmed search conducted on 12-09-2019, using keywords as follows: “protein name” + “Alzheimer’s Disease”.

Table S1 I Statistically altered proteins in CT vs PD comparison (Dunn’s Test) that appeared related to Parkinson’s Disease*		
Protein Accession Number (UniProt)	Protein’s name	Brief description of the potential relationship as explained in the found articles
P05452	Tetranectin (TN)	<ul style="list-style-type: none"> - TN might serve as a potential biomarker for PD, but further validation is required. (213) - TN might have a neuroprotective role by attenuating MPP⁺-induced neurotoxicity, ROS levels, apoptosis, and autophagy.(214)
P0DJ18	Serum amyloid A-I protein (SAA)	<ul style="list-style-type: none"> - Potential plasma biomarker for PD.(215) - Found to be differentially expressed in several studies regarding PD biomarker discovery. (216)
P02652	Apolipoprotein A-II (Apo-AII)	<ul style="list-style-type: none"> - Part of multi-protein biomarker panel capable of distinguishing patients with probable PD from healthy controls. (217)
P01009	Alpha-1-antitrypsin	<ul style="list-style-type: none"> - Might be part of a potential group of PD biomarkers, and further studies are required in order to evaluate the possibility to also be used to discriminate PD subgroups and to monitor the effect of interventions in PD. (218)
P35542	Serum amyloid A-4 protein	<ul style="list-style-type: none"> - Was shown to be increased in some PD patients. (131)

*The articles cited above were obtained after a Pubmed search conducted on 12-09-2019, using keywords as follows: “protein name” + “Parkinson’s Disease”.

Table S12 Statistically altered proteins in AD vs PD comparison (Dunn's Test) that appeared related to both Alzheimer and Parkinson's Disease*

Protein Assession Number (UniProt)	Protein's name	Brief description of the potential relationship as explained in the found articles
P02654	Apolipoprotein C-I (Apo-CI)	- Apo-CI isomorphisms may be an independent risk factor for AD developing, at least. (219)
P04180	Phosphatidylcholine-sterol acyltransferase	- Altered levels of this protein in AD patients when compared to PD and Dementia with Lewy Bodies (BLB). (220)
P01709	Immunoglobulin lambda variable 2-8	- Might have implications in AD pathogenesis. (220)
P02743	Serum amyloid P-component (SAP)	- Might be a good plasma biomarker for PD. (221)
P01042	Kininogen- I	- Altered in AD patients when compared to controls. (222)
Q96KN2	Beta-Ala-His dipeptidase	- Reduced levels of expression in AD patients, while appearing stable in MCI patients. (201) - Could be a potential biomarker for AD. (223)
P32119	Peroxiredoxin-2	- Might be of importance for the development of new therapeutic approaches for sporadic PD and other neurodegenerative disorders associated with nitrosative/oxidative stress. (224)

P10909	Clusterin	<ul style="list-style-type: none">- Might be involved in PD pathogenesis, with increased levels in this pathology when compared to AD. (225, 226)- Clusterin measured on CSF might serve as a potential marker for differentiation between patients with Dementia associated with Parkinson Disease from patients with Dementia with Lewy Bodies. (226)
--------	-----------	--

*The articles cited above were obtained after a Pubmed search conducted on 12-09-2019, using keywords as follows: “protein name” + “Alzheimer’s Disease” + “Parkinson’s Disease”.